UNIVERSITY OF SOUTHAMPTON

FACULTY OF ENGINEERING, SCIENCE AND MATHEMATICS
School of Civil Engineering and the Environment

Microbial Generation of Highly Magnetic Iron Sulphide for Heavy Metal Recovery

By

Merissa S Marius

A thesis submitted
for the fulfilment of degree of
Doctor of Philosophy

June 2006

UNIVERSITY OF SOUTHAMPTON

ABSTRACT

FACULTY OF ENGINEERING, SCIENCE AND MATHEMATICS

SCHOOL OF CIVIL ENGINEERING AND THE ENVIRONMENT

Doctor of Philosophy

MICROBIAL GENERATION OF HIGHLY MAGNETIC IRON SULPHIDE FOR HEAVY METAL RECOVERY

by Merissa S Marius

Biosorption of heavy metals using microbial biomass sorbents has been extensively studied in the laboratory with the view to eventual commercial application. Microbially produced iron sulphide biosorbents are known to have a high affinity for heavy metals and magnetic properties which have the potential for use in biomagnetic separation processes. However, unwillingness to change from conventional methods, combined with the poor economic viability of the biomass separation has stalled commercial exploitation. This study examined the use of a mixed sulphate reducing bacteria population to produce a highly magnetic sulphide to enable easy, low cost magnetic separation recovery. Sorption/desorption behaviour of the microbially produced sulphide on typical heavy metals found in commercial effluents was also investigated.

Culturing of the magnetic biosorbent using a mixed iron, ferrous rich modified Postgate growth medium and an alternating batch-continuous growth cycle produced a material with a magnetic susceptibility an order of magnitude greater than previously documented. Characterisation using chemical and x-ray diffraction tests indicated the presence of iron, sulphur (elemental and sulphide) and phosphate. Mackinawite (FeS_{1-x}) was inferred as the magnetic iron sulphide.

Sorption of metals to the sulphide followed the Langmuir isotherm model suggesting the occurrence of monolayer binding. The studied metal uptake affinity followed the order Cd>Zn>Cu>Ni, with the maximum calculated sorption capacity being an order of magnitude greater than other commercially tested biomasses, indicating its efficiency on a single application and suitability for commercial applications. Ethylenediamine-tetra-acetic acid (EDTA) was found to be the most effective desorbing agent eluting 30-90% of the bound metal. However the biomass oxidised during the process and subsequent sorption efficiency was poor.

In summary, this thesis describes a pathway to produce a highly magnetic iron sulphide and characterises its biosrobent properties. The work has demonstrated the potential of this material to be applied to heavy metal pollutant recovery.

TABLE OF CONTENTS

LIST OF FIGURES

LIST OF TABLES

ACKNOWLEDGEMENTS

I would like to express my sincere gratitude to Dr. Abubakr Bahaj, Dr. Patrick James and Dr. David Smallman for their guidance and encouragement throughout this project.

I would also like to recognise the following persons:

Dr Edward Young, Dr. Yifeng Yang (School of Engineering Sciences, University of Southampton) and Dr. Kevin O'Grady (Department of Physics, University of York) for assistance with saturation magnetisation measurements; Mr. Ross Williams (National Oceanographic Centre, Southampton) for technical support in X-ray diffraction, Dr. Barbara Cressey (School of Chemistry, University of Southampton) for assistance in field of electron microscopy; Julie Vaclavick, Earl Peters and Ken Yates (School of Civil Engineering and the Environment, University of Southampton) for their assistance during the experimental stages of this work; my family and friends, for their continuing support and encouragement.

ABBREVIATIONS

AMD	Acid Mine Drainage
AO	Acridine Orange
ATP	Adenosine Triphosphate
BS	British Standard
CC	Continuous Control
DO	Dissolved Oxygen
DSV	Desulfovibrio spp
EDTA	Ethylenediamine-tetra-acetic acid
EPA	Environmental Protection Agency
HGMS	High gradient magnetic separation
IUPAC	International Union of Pure and Applied Chemistry
LPS	Lipopolysaccharide
mgL^{-1}	Milligrams per litre
MSB-Auto	Magnetic Susceptibility Balance (automatic)
MTB	Magnetotactic Bacteria
OFN	Oxygen Free Nitrogen
ppm	parts per million
SBC	Switch-Batch-Continuous
SEM	Scanning Electron Microscope
SRB	Sulphate Reducing Bacteria
TSS	Total Suspended Solids
XRD	X-ray Diffraction

Chapter 1.

INTRODUCTION

'Heavy metal' is a ubiquitous term used with great generality to refer to metals and metalloids that have been associated with contamination and potential (eco)-toxicity (Duffus, 2002). It is often meant to refer to elements between copper and lead, on the periodic table inclusively (Figure 1.1). They are normally released into the environment in trace amounts and can be readily used by organisms for structural and catalytic functions (Ehrlich, 1997) or sequestered, thus removing them from the environment. This natural relationship generally serves to regulate dissolved metal concentrations within a range that poses no adverse effects to the environment or its inhabitants.

The structural properties of heavy metals make them very malleable with a high electrical conductance, which makes them highly favourable for large scale industrial applications such as electroplating and battery production. As a consequence of their increased usage with the onset of industrialisation, these metals are entering the environment at a faster rate and at increasing higher concentrations, most notably nowadays in countries with weak environmental legislation. At these elevated levels, the natural attenuation processes are incapable of sequestering the metals rapidly enough, resulting in the progressive accumulation and pollution of the receiving ecosystems.

Heavy metal pollution as a result of anthropogenic usage is classified in accordance to its origin: (i) non-point sources which refer to those inputs which occur over a wide area and are associated with land usage such as urbanization and agriculture; or (ii) point sources which are readily identifiable inputs where waste is discharged via a pipe or drain. Industrial wastes are generally classed as point source pollution, as discharge is often via a drainage network.

In response to widespread point source pollution and the resulting degradation of the receiving environments, integrated EU/UK legislation has been instituted to stem the damage to the receiving ecosystems by specifying the quantity and quality of waste effluent that can be discharged at a particular location. In an effort to be in accordance with discharge limits and licences, many industries have implemented in-house treatment plants modelled on conventional metal recovery strategies to achieve target limits and avoid penalty fees. The following section gives an overview of the more commonly utilised methods of heavy metal recovery.

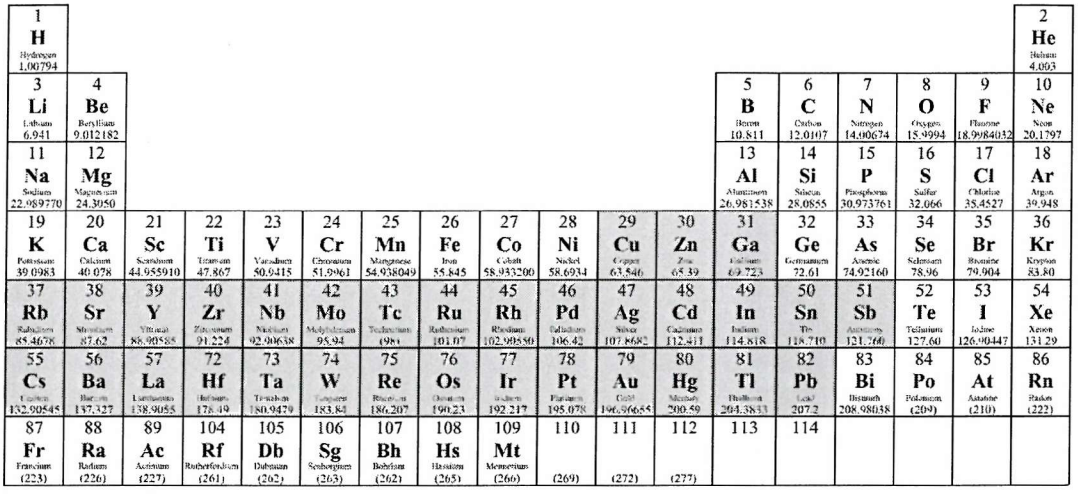

Figure 1.1 Periodic table showing location of heavy metals (shaded grey).

1.1. Overview of conventional recovery technologies

The recovery and removal of heavy metals from waste streams has been practiced for several decades and covers an extensive list of procedures (Table 1.1). These procedures when loosely grouped according to their basic recovery mechanisms employ either 1 of 2 principles (Van Deuren *et al.*, 2002):

1. Destruction or alteration of the contaminant.

This is achieved by altering the chemical structure of the contaminant using thermal, biological or chemical methods. Included in this group is chemical precipitation and neutralisation of the target metal.

2. Extraction or separation of contaminants

The treatments commonly associated with this technology involve a change in the physical state of the pollutant to enable recovery. Solvent extraction and ion exchange are two procedures that are included in this category.

Method	Description	Industrial Use
Chemical Precipitation	Precipitation of metal by the addition of coagulant and flocculation agent	Water Softening
Reverse osmosis	Metal ions separated using applied pressure via a semi-*permeable membrane*	Water Purification Desalinaton
Electrochemical Treatment	Metal ion solution used to complete an electrical circuit. When current is applied, metal ions migrate and are deposited on cathode.	Electroplating Industry
Ion Exchange	Aqueous metal ions exchanged with non toxic ions of equivalent charge attached to a solid matrix	Plating Industry
Phytoremediation	Use of plants in polluted soils or in specially designed ponds	Land Remediation

Table 1.1: *Conventional removal technologies of metals from waste water*

Chemical precipitation and ion exchange are two of the more commonly used procedures that exemplify the mechanisms described.

1.1.1. Chemical Precipitation

This process involves the conversion of soluble metal ions into insoluble salts that precipitate out of solution. This is readily achieved by pH adjustments or the addition of coagulants such as aluminium sulphate (alum), calcium hydroxide

(lime) or organic polymers. The resulting toxic precipitate can then be physically separated. For example, in the drinking water industry, water hardness is caused by high concentrations of dissolved calcium carbonate and bicarbonate. The addition of lime causes the dissolved metal species to form insoluble hydroxides that precipitate out of solution. Polymer coagulants are often added to accelerate settling through the formation of coarse flocculants (EPA, 2000).

This method of metal removal is very costly as the applied chemicals are not recoverable, and the precipitated metal sludge often requires de-watering and compaction prior to recovery and disposal. The efficiency of recovery is also limited as it is generally only effective at high concentrations.

1.1.2. Ion Exchange

This metal recovery process is a reversible chemical reaction wherein the ions in solution are exchanged for charged ions attached to a solid particle. Solid ion exchange particles occur naturally in the form of inorganic zeolites and are part of the natural trace metal sequestration process. For large scale industrial recovery purposes, ion exchange particles have been synthesized in the form of resins with characteristics tailored for specific recovery applications.

1.2. Innovative heavy metal recovery

Conventional methods for the recovery of metals, although practiced for several decades and which are effective within very specific parameters, are often expensive, provide incomplete metal removal and result in numerous adverse environmental effects (Ahalya *et al.*, 2003). In recent years however, increased emphasis has been placed on developing and implementing innovative, environmentally friendly and economical measures for reducing the concentration of heavy metals in discharge effluent (Kotrba *et al.*, 1999). At the forefront of this wave of innovative technologies is *biosorption*; the metal removal processes exhibited by naturally abundant biomass types through metabolically mediated or physico-chemical pathways of uptake.

Biosorption as a process is often described in terms of a *sorbent* (solid phase) and *solvent* (liquid phase) which contains the *sorbate* (metal ions). The affinity of the sorbent for the sorbate initiates the attraction and resultant removal of the sorbate species from solution via binding mechanisms. Upon attaining equilibrium between the bound sorbate and the aqueous sorbate the reaction ceases.

The complexity of microbial biomass structures suggests that there are many binding mechanisms which are used for metal uptake by a microbial cell (Figure 1.2). These mechanisms are often identical to those employed by conventional recovery treatments, with ion exchange, precipitation and physical adsorption being the most commonly identified mechanisms cited in the literature (Volesky, 2003). It is however the ready and sustainable abundance of the biomass materials and resourcefulness of the materials being used to carry out this recovery that makes the procedure innovative.

Conventional biosorption experiments cited in the literature have focused on the use of seaweeds, yeasts and bacteria for the immobilization of the target metal (Patzak *et al.*, 1997, Davis *et al.*, 2000). The range and specificity of the metal sorption varies greatly with the type of biomass used, the homogeneity of the solution mixture in terms of the components as well as the environmental conditions (eg. pH, temperature) (Volesky, 2001). More recent experiments have focused on employing traditional waste materials such as tea waste, bagasse (sugar cane pulp), wood sawdust, and bone char with varying degrees of success (Cheung *et al.*, 2001, Mahvi *et al.*, 2005, Sciban *et al.*, 2006).

Following this trend of using by-products as sorbents a number of studies have focussed on the use of bacterial metabolic by-products such as phosphates and sulphides to enable metal sequestration via precipitation of the metal ions (Lloyd and Macaskie, 1996, Thomas and Macaskie, 1996, White and Gadd, 1996, Patzak *et al.*, 1997).

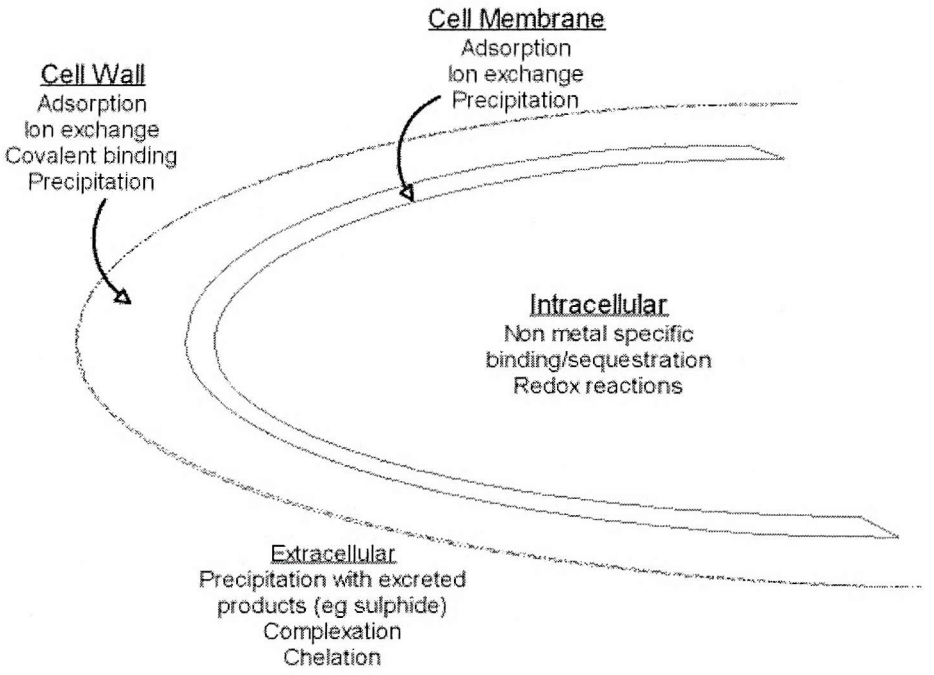

Figure 1.2: Diagram representing the processes contributing to the microbial uptake and detoxification of toxic metals (adapted from (White *et al.*, 1995))

The use of the sulphide by-product is most notable in iron rich environments, where the microbially liberated sulphide readily reacts with iron to form an iron sulphide which, on occasion, has been found to have magnetic characteristics (Thomas and Macaskie, 1996, White and Gadd, 1996, Patzak *et al.*, 1997, Lloyd, 2002). The sorption capacity of this microbially produced Fe_xS_y has been researched as an alternative biosorbent for heavy metal recovery and has been actively implemented and tested on common wastewater cations and industrial acid mine drainage wastes (Basu *et al.*, 1995, White *et al.*, 1995, Jalali and Baldwin, 2000, Smith and Gadd, 2000, White and Gadd, 2000, Garcia *et al.*, 2001). Additional work on its suitability for biomagnetic separation has indicated that the bacteria are an ideal candidate (Bahaj *et al.*, 1989) with the potential to produce a highly magnetic Fe_xS_y.

To date, the magnitude of 'magnetic responsiveness' of metal sulphides generated by sulphate reducing bacteria (SRB) has been of the order of 10^{-5} (Bahaj *et al.*, 1989). This low magnetic response restricts the industrial magnetic separation applicability of the material due to the need for large applied magnetic

fields (>1T) to enable efficient separation of the heavy metal load material resulting in high process costs (Watson *et al.*, 1996). In order to achieve efficient, low cost magnetic separation recovery, the magnetic properties of the iron sulphide would ideally be such that a magnet separator operated using only permanent magnets could be efficiently used.

1.3. Aims and Objectives

This research programme focuses on the development of a highly magnetic microbial iron sulphide. The combined properties of high heavy metal sorption capacity and high magnetic susceptibility would enable its use as a novel treatment method via biomagnetic separation.

To achieve the principal aim, several investigative experimental objectives were prioritised:

1. Investigate the effects of culture mode, (batch, continuous, semi-continuous) of the SRB on the magnetic susceptibility of the iron sulphide product.

2. Investigate the compositional growth medium effects on the SRB culture produced (magnetic susceptibility and cell growth).

3. Chemically characterise the highly magnetic iron sulphide produced as a result of the changes in culture mode and growth medium

4. Investigate the heavy metal affinity of the iron sulphide produced via the use of batch sorption studies.

5. Investigate the regeneration/potential reuse of the iron sulphide biomass using progressive sorption/desorption and heavy metal recovery experimental procedures.

1.4. Thesis Structure

This thesis is presented in 8 chapters. In this, the Introduction, Chapter 1, an overview of the heavy metal pollution problem is presented along with existing conventional (section 1.1) and new innovative methods of metal recovery (sections 1.2). In Chapter 2, a detailed review of the literature as it pertains to the use of sulphate reducing bacteria, their metabolic by-product, hydrogen sulphide, and precipitated iron sulphides as biosorbents is presented. The magnetic characteristic of the microbially produced iron sulphide is discussed and its use in high gradient magnetic recovery is presented.

Chapter 3 presents sorption/desorption fundamentals, including isotherm and kinetic models essential for the assessment of the effectiveness and appropriateness of a biosorbent. Experimental procedures and materials used to produce the magnetic microbial biosorbent, and to investigate and understand its characteristics and biosorption properties are presented in Chapter 4. The results of the experimental procedures along with discussion of the findings are summarised and presented in chapters 5-7. The major research conclusions are presented in chapter 8, along with recommendation for further works.

Chapter 2.

LITERATURE REVIEW: Sulphate Reducing Bacteria as a Biosorbent Medium

In this chapter, a review of the existing bodies of knowledge relevant to this thesis is presented. As a foundation, the sulphate reducing bacteria group which the research utilises is overviewed and their importance in the global sulphur cycle as a sulphur precipitator as a result of the formation of iron sulphide and the transient nature of the sulphide species is discussed. Data on the experimental uses of the bacteria as a biosorbent (through cell wall sorption, biosulphide production and microbial iron sulphide) are presented. Existing studies have shown that the iron sulphide precipitated by the bacteria possesses weak magnetic properties, which enable them to be magnetically recovered. The environmental and economic feasibility of the combined sorption ability and magnetic recovery potential are also analysed.

2.1. Sulphate Reducing Bacteria

Sulphate reducing bacteria (SRB) are a morphologically diverse group of anaerobic prokaryotes which play an integral role in the biological sulphur cycle (Castro *et al.*, 2000) (Figure 2.1). First discovered in the latter part of the 17th century by Beijerinck (1895) in the canals of Holland, this ubiquitous group have since been identified in a diverse range of anaerobic environments including sediments, marine habitats and the gastrointestinal tract of humans and other animals (Loubinoux *et al.*, 2002, Matias *et al.*, 2005).

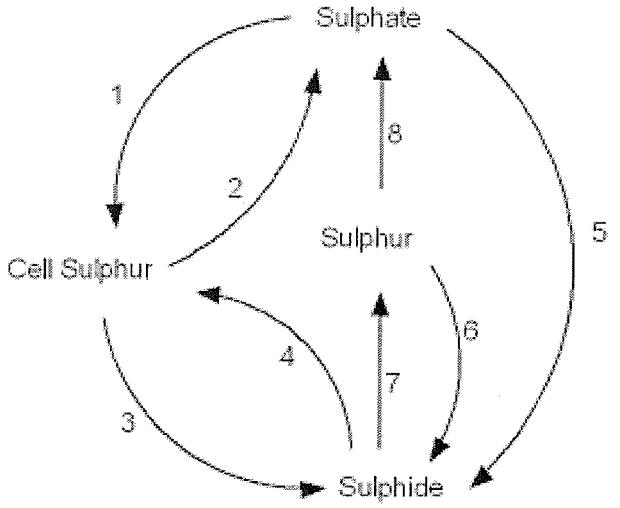

Figure 2.1 Schematic showing biological sulphur cycle where (1) represents the assimilatory reduction of sulphate by bacteria and plants, (2) sulphate excretion, (3) putrefication of dead animals, (4) sulphide assimilation, (5) dissimilatory sulphate reduction, (6) sulphate reduction, (7) sulphide oxidation and (8) sulphur oxidation (Fu, 2005).

SRB are predominantly found in sulphur rich environments and as the name suggests they are capable of performing the dissimilatory reduction of oxidised sulphur compounds such as sulphate, thiosulphate and sulphite in the presence of a carbon source (lactate, acetate ...etc). Of the sulphur reduced, a small amount is assimilated by the bacteria, but a significant proportion is released in the form of hydrogen sulphide (Postgate, 1979). This sulphide producing reaction can be represented by the following reactions:

$$2CH_2O+SO_4^{2-} \rightarrow S^{2-} + 2CO_2 + 2H_2O \qquad \text{(Equ. 2.1a)}$$

$$S^{2-}+2CO_2+2H_2O \rightarrow H_2S+ 2HCO_3^- \qquad \text{(Equ. 2.1b)}$$

The carbon source when oxidised by the bacteria liberates electrons which are used as an energy source for the growth and the production of adenosine triphosphate, (ATP) and other metabolic processes. The manufactured ATP is in turn used for the reduction of the sulphate to sulphide. The following schematic diagram (Figure 2.2) shows a representation of the carbon usage, ATP production and sulphate reduction.

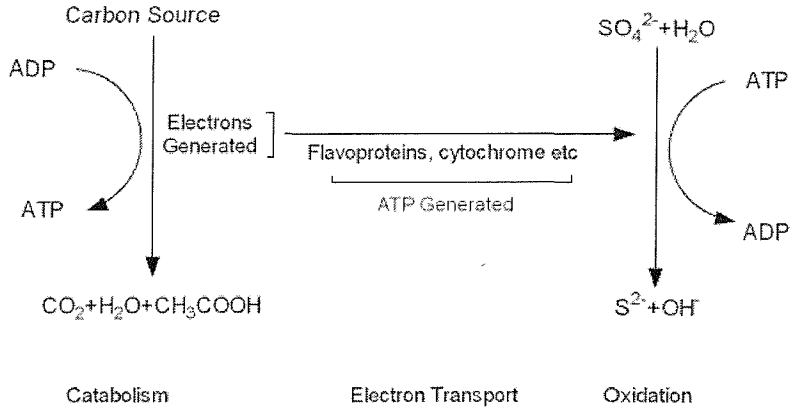

Figure 2.2 Schematic representation of dissimilatory sulphur reduction (Postgate, 1979).

Of the numerous species of SRB that exists, there is an equally extensive list of carbon sources that can be used (Table 2.1), some with a high degree of specificity depending on the SRB species. Lactate is however the most widely used carbon source (Postgate, 1979).

Genus	Carbon source	pH range	Temperature ^{O}C
Desulfobacter spp	Acetate	6.2-8.5	28-32
Desulfobulbus spp	lactate, ethanol, Propanol	6.0-8.6	28-39
Desulfocarcina spp	formate, acetate, butyrate, propionate	6.9-7	33-38
Desulfovibrio spp	Lactate	6.5-7.5	25-35
Desulfococus spp	formate lactate, acetate, pyruvate	-	30-36
Desulfotomacium spp	lactate acetate, ethanol	-	-

Table 2.1 Morphology, carbon source and optimum growth temperature and pH for a selection on SRB (Widdel, 1988).

In addition to carbon source, the environmental parameters of pH and temperature influence the growth of the bacteria. Sulphide concentrations in the immediate environment of the bacteria also affect growth.

2.1.1. Temperature

SRB are an extensive group of species with temperature adaptations which allows them to be active over a wide range of temperature (Postgate, 1979), which is alluded to by their pervasiveness. This adaptation facilitates grouping into three categories: (i) psychrophiles (growth temperature < 30^0C); (ii) mesophiles (grow best at temperature below 40^0C); and (iii) thermophiles (which are tolerant of conditions greater than 45^0C with optimum growth above 60^0C).

Desulfovibrio desulfuricans, a mesophile, is one of the most commonly used strains in laboratory experiments, and under laboratory conditions bacterial productivity has been shown to increase with increased culture temperature (Okabe *et al.*, 1995). However temperatures in excess of 35^0C have been shown to have a negative impact on the bacteria whereby the enzymes which enable the effective functioning of the bacteria are denatured. Reduced temperatures conversely have the same effect, in which at temperatures below 20^0C, bacterial productivity decreases. Thus under the environmental conditions of the temperate region (UK and Western Europe), bacterial productivity is highest during the summer months and lowest during winter.

2.1.2. Sulphide concentration and pH

In the aqueous environment, speciation of reduced sulphur occurs in three main forms; dissolved hydrogen sulphide (H_2S) and its dissociated products S^{2-}, HS^- (Equ. 2.2a and Equ 2.2b).

$$H_2S_{(l)} \leftrightarrow HS^- + H^+ \qquad \text{(Equ. 2.2a)}$$

$$HS^- \leftrightarrow S^{2-} + H^+ \qquad \text{(Equ 2.2b)}$$

The presence of these forms of sulphur is dependant on the solution pH as shown in Figure 2.3. At neutral pH, pH 7, sulphur readily exists in both its dissociated form; HS^- and as H_2S. In acidic environments, H_2S dominates and under alkaline conditions complete dissociation occurs. This pH dependence on the occurrence of environmental sulphide is also linked to its toxicity effects (Utgikar *et al.*, 2002).

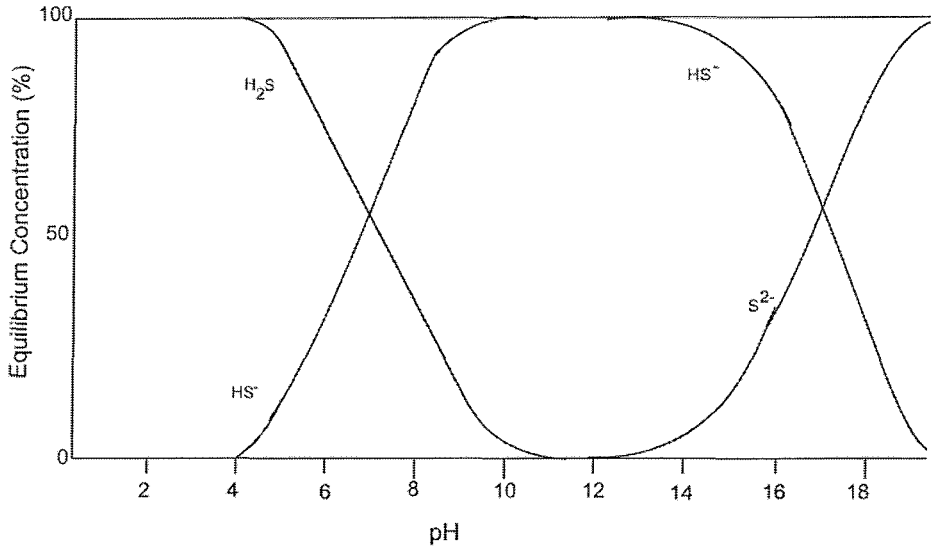

Figure 2.3 Schematic detailing prevalent forms at sulphur in relation to pH (Arfin *et al.*, 2006)

The presence of undissociated sulphide; H_2S, in the surrounding environment is known to have a negative effect of the growth and productivity of SRB andnaerobic bacteria in general (Utgikar *et al.*, 2002). Although SRB produce the sulphide in conjunction with their metabolic processes, it serves as a toxin in high concentrations. At H_2S concentrations in excess of $1000mgL^{-1}$, SRB activity can be reduced by 50% (Utgikar *et al.*, 2002). The alkalisation of the bacteria micro-environment through the production of carbonate ions during sulphate reduction (Equ. 2.1a and Equ. 2.1b) enables the conversion of the aqueous sulphide species into a form which is less toxic to the organism.

2.2. Iron Sulphide

An understanding of the complexity of the sulphur cycle as it relates to the process of formation of iron sulphide species is essential as it is has been linked

to SRB, which have been recognised as being responsible for major geologic sulphur deposits (Lennie *et al.*, 1997). Despite extensive research in this area, there is great disparity in the reported literature findings.

Iron sulphides are known to exist as six recognisable species (Rickard, 1969), of which pyrite is the most common and stable (Figure.2.4). It is well established in the literature that all the iron sulphide species are interlinked with some species being metastable precursors to pyrite (Rickard, 1969, Rickard, 1995, Lennie *et al.*, 1997, Hurtgen *et al.*, 1999, Benning *et al.*, 2000, Wolthers *et al.*, 2003, Rickard and Morse, 2005). Also suggested in the literature is the significant occurrence of an amorphous iron sulphide which forms rapidly, is highly reactive and serves as a precursor to all iron sulphide reactions at ambient temperature (Jeffrey and Melchers, 2003, Wolthers *et al.*, 2003).

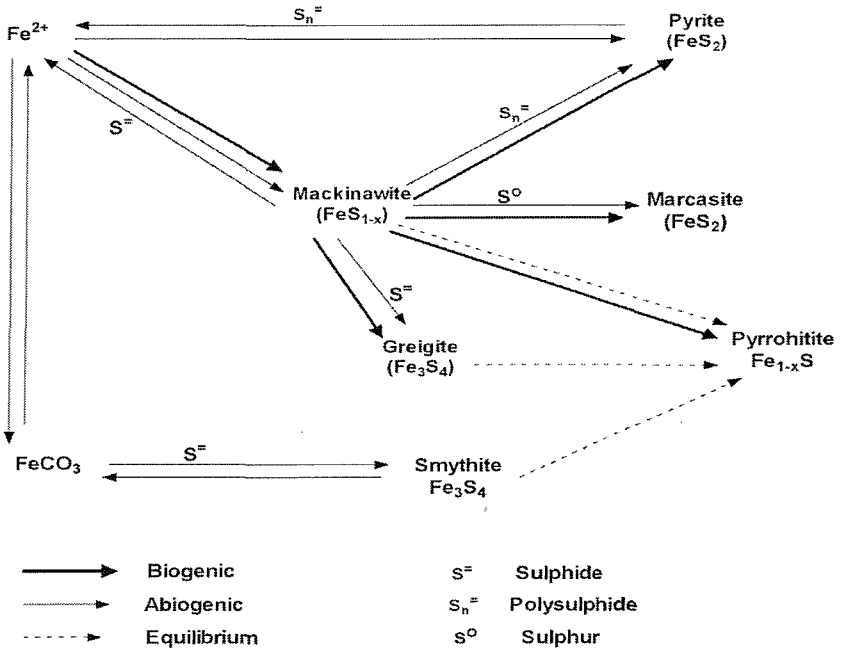

Figure.2.4 Schematic detailing the biogenic and abiogenic linkages between the 6 iron sulphide species (Rickard, 1969).

Wolthers *et al* (2003) however have put forward recent findings which go contrary to this theory and contend that there is no such compound, but that instead a disordered mackinawite form exists which undergoes progressive long range mackinawite ordering. For purposes of simplicity and convenience in this text, the

term mackinawite will be used to encompass both the disordered (amorphous) and ordered phases of the compound.

In one of his earlier works, Rickard (1969) proposed a series of interlinked biogenic and abiogenic processes (Figure.2.4) with mackinawite being an essential precursor for the formation of greigite, pyrrhotite and pyrite; however these minerals were not directly linked in the reaction pathway. More recent works (Lennie *et al.*, 1997, Benning *et al.*, 2000) investigating pyrite formations have included both mackinawite and greigite as sequential precursors to pyrite formation (Benning *et al.*, 2000), however the pathway specifics are numerous and equivocal in the literature

2.2.1. Iron sulphide formation

The recognised pathways which are as a result of the extensive pyrite formation studies include:-

(i) the *polysulphide pathway* (Equ. 2.2) endorsed by Rickard (1969) which assumes the sulphidation of a generic iron monosulphide (an all encapsulating term used to include mackinawite and greigite), using zero valent sulphur. This reaction between two solids however has been disputed as being highly improbable (Wilkin and Barnes, 1996),

$$FeS(s) + S^{o}(s) \rightarrow FeS_2(s) \qquad \text{(Equ. 2.2)}$$

but the aqueous chemistry of sulphur offers an alternative reaction state for the pathway to proceed (Equ. 2.3);

$$FeS(s) + S_n^{2-} \rightarrow FeS_2(s) + S_{n-1}^{2-} \qquad \text{(Equ. 2.3)}$$

(ii) the *iron loss pathway* which assumes iron disulphide nucleation via the loss of a ferrous iron (Equ. 2.4).

$$2FeS(s) + 2H^{+} \rightarrow FeS_2(s) + Fe^{2+} + H_2(g) \qquad \text{(Equ. 2.4)}$$

In this reaction hydrogen ions (protons) act as electron acceptors and are consequently reduced to hydrogen gas. The ferrous iron liberated is potentially reprecipitatied as FeS. X-ray powder diffraction studies conducted by Lennie (1997) confirmed this mechanism and indicates the ready transformation of mackinawite to greigite via the iron loss mechanism; and

(iii) most recently the *hydrogen sulphide pathway* (Equ. 2.5) which suggests that hydrogen sulphide acts as an oxidizing agent (Benning *et al.*, 2000).

$$FeS(s) + H_2S \rightarrow FeS_2(s) + H_2(g) \qquad \text{(Equ. 2.5)}$$

The rates and specifics of this proposed pathway is also ambiguous with little corroboration in the literature. Findings by Rickard and Luther (1997) detail rapid transformation from FeS to pyrite via the H_2S pathway at temperatures below 125^0C. This finding however is inconsistent with other published works by Benning *et al* (2000) and those cited therein which found that under strict anaerobic conditions, FeS is highly stable in the presence of H_2S, under a range of temperatures and pH, provided it is the only sulphide species present. Under controlled oxidation conditions, Bennings' results also concur with other literature (Schoonen and Barnes, 1991a,b, Wilkin and Barnes, 1996) and shows that transformation to pyrite is a slow process with either (1) incomplete oxidation of the FeS species with little pyrite being formed (over 240hr) or (2) complete oxidation of FeS via greigite for longer periods of exposure (>580 hrs)

The hydrogen sulphide pathway is most relevant to low temperature biogenic mechanisms with mackinawite formation by SRB being cited as one of the main routes for synthesis (Watson *et al.*, 2000). Of the other biogenically formed species referred to in Rickard's model (Figure.2.4), greigite and pyrrhotite, are of particular interest as they show innate magnetic characteristics when assessed using Mossbauer spectroscopy (Morice *et al.,* 1969). The magnetic property of these iron sulphides can be attributed to the crystallographic packing of the compounds which facilitates ionic interactions and the movement of free

electrons around the crystal structure. Synthetically produced pyrite formed under laboratory conditions through the controlled oxidation of iron monosulphide, has been observed to display magnetic characteristics which have been linked to the formation process via a greigite intermediary, which is remnant within the pyrite core (Benning *et al.*, 2000).

2.2.2. Microbial Iron sulphides

The magnetic characteristic of the microbially precipitated iron sulphide was first identified, accidentally, by Freke and Tate (1961) whilst exploring the iron precipitating capabilities of SRB. Attempts to reproduce the iron sulphide proved successful only when the SRB were cultured using an undefined "intermittent basis". An empirical analysis of the magnetic material revealed a Fe_4S_5 structure with a specific density of 2.9 (Freke and Tate, 1961). In later works with this material, characterisation using powdered x-ray diffraction identified a mixture of iron sulphides and oxides, namely greigite, goethite and hematite (Rickard, 1969).

In recent times, various researchers at the University of Southampton have devoted extensive efforts on developing a culture regime that would yield an iron sulphide bearing highly magnetic properties (Bahaj *et al.*, 1991, Watson *et al.*, 1995, Watson *et al.*, 1996, Marius *et al.*, 2005). One of the first documented attempts employed a continuous culture regime using the Freke and Tate medium. The experiment yielded a sulphide which, when analysed inconclusively showed a pyrrhotite ($Fe_{1-x}S$) structure (Watson and Ellwood, 1994). Magnetic quantification of cultured microbial iron sulphide precipitate samples using the single wire cell theory (Paul *et al.*, 1979) resulted in a calculated magnetic susceptibility within the range of $4x10^{-5}$ to $3.9x10^{-4}$ SI units dependant on the sample incubation period utilised (Bahaj *et al.*, 1991).

Subsequent experiments by Watson (Watson *et al.*, 2000, Watson *et al.*, 2001, Watson and Ellwood, 2003) to characterise and optimise the magnetic characteristics of the microbial iron sulphide using a feed back chemostat design (Watson *et al.*, 1996) proved limited as the magnetic susceptibility of the material remained too low for effective use in a magnetic separation process.

Identification of the sulphide also remained inconclusive with unidentified structures varying from; a mackinawite-greigite mix (pure Fe_xS_y structures) (Herbert *et al.*, 1998, Watson *et al.*, 2000, Watson *et al.*, 2001, Watson and Ellwood, 2003) to an impure Fe_xS_y mix; tochilinite-mackinawite mix (Watson and Ellwood, 2003).

2.3. SRB Sorption

Biosorption of heavy metals has been extensively researched, with various new biomass materials being tested to determine their metal binding capacities. As a group, bacteria are potentially excellent biosorbents due to their high surface area to volume ratio and have been extensively tested with encouraging results. However an evaluation of existing literature, as conducted by Volesky (1998, , 2000) has shown that a significant proportion of bacterial experiments measured the metabolically mediated process of bioaccumulation in addition to biosorption which relies on the principle of using dead biomass. However in these studies the high levels of the metal toxin often metabolically compromised the cells or caused death. No distinctions between the active bioaccumulation or passive sorption mechanism of metal uptake were therefore made herein.

Conventional bacterial biosorption processes often rely only on the cell wall chemistry to passively sequester metals. Experiments (Watson and Ellwood, 1994, Christensen *et al.*, 1996, Chen *et al.*, 2000, Jalali and Baldwin, 2000, Foucher *et al.*, 2001, Luptakova and Kusnierova, 2005) with SRB have explored 3 ways of using the bacteria and its metabolic by-products to sequester metals:

1) Cell wall sorption using the polymer structure of the cell wall;
2) Biosulphide production and resultant pH alterations to precipitate metals; and
3) Microbially produced iron sulphide to sorb metal ions from solution.

2.3.1. Cell wall sorption binding experiments

The bacterial cell wall is known to be highly effective in sequestering metals as it contains many chemically active compounds. In gram negative cell walls, such as that found in SRB, the outer most layer of the cell is made up of a highly anionic lipid, lipopolysaccharide (LPS) (Figure 2.5). The presence of this lipid makes the surface strongly electronegative and highly interactive with positively charged ions (SchultzeLam *et al.*, 1996).

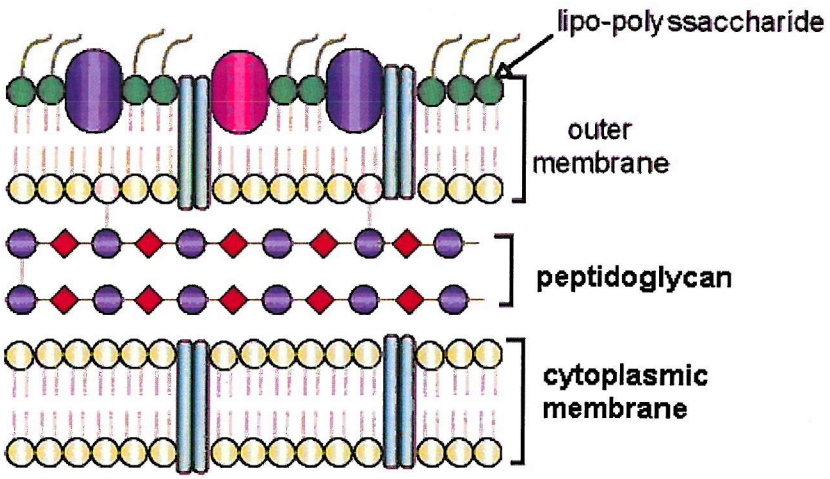

Figure 2.5 Diagram of the cell wall structure in a gram negative cell

Metals sorbed onto the surface of the bacteria are then able to act as nucleation sites, providing a surface for additional metal ions to adhere (Jalali and Baldwin, 2000). This double acting process is pivotal in the success of cell wall binding and of the sorption metals tested.

Chen *et al* (2000) examined the metal sorption capacity of *Desulfovibrio spp* (DSV) biomass using copper and zinc at various pH values. The effect of pH on metal uptake is significant as it affects the metal chemistry and the receptiveness of the functional binding groups. Maximum sorption of zinc was observed at a pH of higher than pH 6.6, whereas peak copper sorption occurred at pH 5. For experiments with a pH greater than pH 5, sorption capacity was reduced as the solubility of copper was decreased, thus altering the amount of aqueous copper available for uptake. The authors found that the DSV biomass had a higher

affinity for zinc than copper, with almost double the mass of zinc being sorbed per gram of biomass used. When viewed using a scanning electron microscope (SEM) at the end of sorption, the biomass showed an abundance of an extra-cellular polymer which is known to assist in the binding of the metal species (Schwartz *et al.*, 1998, Chen *et al.*, 2000).

Copper removal studies carried out by Jalali and Baldwin (2000) using various concentrations of aqueous metal ions also showed the presence of a polymer film encapsulating the bacterium and onto which copper was bound. The extent of the encapsulating film thickness around the bacterial cells was observed to increase as the concentration of the metal solution increased. This observation concurs with other literature which suggests that the extent of encapsulation of the bacterium with the polymer is a function of the aqueous metal surrounding the cell.

The ability of SRB to metabolise radioactive metals has also been researched with a view to developing and designing special treatment systems (Spear *et al.*, 2000, Watson and Ellwood, 2003). Spear *et al* (2000) showed better uptake in mixed culture systems, than in pure strain environments with on average, double the mass of metal being recovered per gram dry weight of cells. Work by White and Gadd (1996) endorses the use of mixed cultures over pure strains, as the effectiveness of the culture in bioremediation is optimised by the consortium growth. In addition, the stability of a mixed culture is generally not quickly compromised by minor environmental changes or the possibility of contamination (White and Gadd, 1996).

2.3.2. Biosulphide production

Dissimilatory sulphate reduction, the process used by SRB in respiration can be expressed chemically using the following equation (Equ. 2.6)

$$(C,H,O) + SO_4^{2-} \xrightarrow{SRB} H_2S + HCO_3^- \qquad \text{(Equ. 2.6)}$$

This method of sequestration optimises the metabolic by-products of the SRB respiration to sequester metals and is often used in conjunction with acidic metal solutions, in particular acid mine drainage (AMD). The effectiveness of this sequestration method is dependent on the ability of metal species present to form insoluble sulphides and at the same time minimise contact between the metal toxins and the cells so as not to compromise bacterial activity and structure.

Experimental configurations devised to ensure the longevity of the bacteria have included the use of nitrogen as a carrier gas to transport the liberated hydrogen sulphide from the culturing vessel to a separate vessel containing the metal solution (Figure 2.6) (Foucher *et al.*, 2001, Luptakova and Kusnierova, 2005). Alternatively an *insitu* sedimentation design has been investigated in which a vessel is used to simulate a mine pit with SRB living within the lower soil layers beneath the mine water. The hydrogen sulphide liberated gradually permeates the layers above, precipitating the metal ions from the bottom up (Christensen *et al.*, 1996).

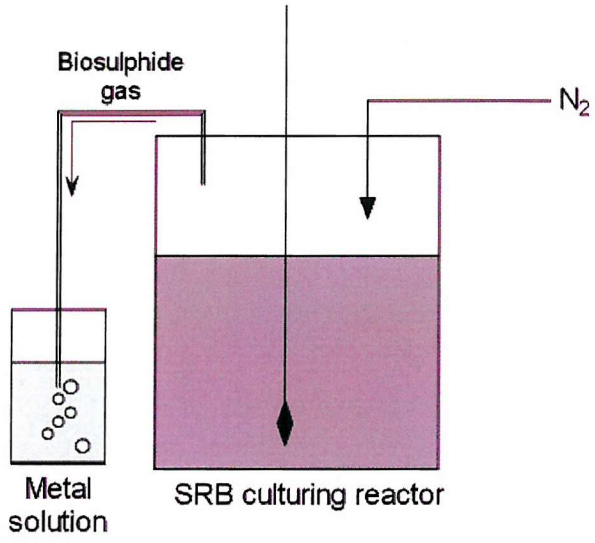

Figure 2.6 Schematic diagram showing biosulphide experimental configuration.(Utgikar *et al.*, 2002)

Foucher *et al* (2001), in their experiment using a separate sedimentation vessel were able to demonstrate the selective sulphide precipitation of copper and zinc by regulating the pH of the vessel. Similar results were documented by

Luptakova and Kusnierova (2005) using an initial concentration of 20 mgL^{-1} with almost 100% copper precipitation being achieved within 8 hours at pH 2.5. The economic viability of such a process assuming resale of the recovered metal; was investigated. However the procedure although successful was not sufficiently cost effective and/or efficient enough to cover basic operating costs (Foucher *et al.*, 2001).

In situ treatment as proposed by Christensen *et al* (1996) is a possible low cost treatment approach as the mine would serve as a sedimentation basin, thus alleviating the concerns of metal disposal. Generally a much slower sequestration process at start up is used as its success and subsequent efficiency relies on the successful establishment of an adequate bacterial population density. The experiment conclusively demonstrated that SRB, when provided with an adequate carbon source can produce a large ongoing source of hydrogen sulphide which readily reacts with metals forming precipitates and reducing metal concentration (copper and zinc) to levels not readily achievable by conventional precipitation technologies (< 0.05mg/L). With an increase in the pH of the effluent, alkalisation was also observed. Similar trends were documented in other studies (Garcia *et al.*, 2001) and thought to be as a result of the carbonate ion production (Equ. 2.6). Metal hydroxide precipitation as a consequence of pH manipulation is well documented and practiced in conventional treatments, and is thought to play a contributory role in the *in situ* metal sequestering process (EPA, 2000).

2.3.3. Microbial iron sulphide biosorption

This mode of metal recovery is the most recent, is two tiered and builds on the biosulphide precipitation method. The bacteria are first cultured in an iron rich environment, which results in the sequestering of metal iron species. This microbially precipitated iron sulphide is then used to further sequester other metal species. In conjunction with the metal sorbing properties of the iron sulphides, their observed magnetic properties also offer the potential for recovering the sulphide material after use.

Early work conducted by Watson and Ellwood (1994) utilised a laboratory grown microbially generated sulphide to conduct onsite treatment of mercury rich industrial effluent. In a single application the sulphide precipitate was able to reduce the mercury concentration by more than 90% of the original concentration. In the same paper Watson and Ellwood (1994) also conducted bench scale recovery of metals from a precious metal industry. The results obtained showed that a wide range of metals, including those that under normal circumstance would not form insoluble sulphides, could be recovered by this material. The authors postulated that the structure of the iron sulphide, was responsible for this recovery by allowing metal ion substitution in the lattice defects (Watson and Ellwood, 1994).

Subsequent experimental studies by Watson *et al* (Watson *et al.*, 1995, Watson *et al.*, 1996, Watson *et al.*, 1999, Watson *et al.*, 2000, Watson *et al.*, 2005) have focused on the recovery of heavy metals typically found in industrial waste water and mining effluent (Cu, Zn, Al, Pb, Cd). The predominant characteristic of the sorption processes exhibited was an 80%-97% removal of the test metal from solution. The initial uptake was rapid wherein most of the metal was sorbed to the available binding sites. Uptake slowed or plateaued after this period indicating saturation of the microbial Fe_xS_y material or the establishment of a pseudo-equilibrium (Jong and Parry, 2004).

The potential use of microbial iron sulphide for the recovery of radioactive metals was also investigated with tests on actinides, pertechnetate ions and uranium (Spear *et al.*, 1999, 2000, Watson and Ellwood, 2003). High levels of metal recovery were documented with uptake levels of approximately 1mg/g dry weight biomass (Watson *et al.*, 2001, Watson and Ellwood, 2003).

2.4. SRB Desorption Data

The process of desorption, as defined by the International Union of Pure and Applied Chemistry (IUPAC) is "*the converse of sorption*", implying reversibility of the reaction. This however is seldom true due to the nature of the binding mechanisms.

The pervasiveness of desorption data or regeneration of the sorbing agent/biomass in the literature in relation to the initial sequestering of the heavy metals is constrained with most data being related to cellulose rich biomasses (Amorim *et al.*, 2003, Saeed and Iqbal, 2003, Min *et al.*, 2004). Desorption data as it relates to SRB is extremely limited and of little interest as the regeneration of the sorbing agent is often impractical (ie biosulphide method) or highly destructive. In most studies, desorption is often determined using a batch method in which the sorbing biomass is transferred to an aqueous environment free of the target metal and the release of the metal measured. The nature of the aqueous desorbing environment is often such to optimise metal recovery without excessive damage to the sorbent (Vijayaraghavan *et al.*, 2004).

The effective use of pH manipulation using mineral acids on a wide range of biomass types is well documented in the literature with hydrochloric acid (HCl), sulphuric acid (H_2SO_4) and nitric acid (HNO_3) being the most commonly used (Chu *et al.*, 1997, Merroun and Selenska-Pobell, 2001, Vijayaraghavan *et al.*, 2005) at concentrations between 0.01-1M. In cases where the binding between the metal and the biomass cannot be readily overcome by pH adjustment or the biosorbent is incapable of enduring the pH extremes, as is the case with microbially produced iron sulphide, mineral salts and chelating agents including sodium citrate, and ethylenediamine-tetra-acetic acid (EDTA) provide a viable alternative (Saeed and Iqbal, 2003) for desorbing the metal from the sorbent biomass.

Work by Watson *et al* (2001) using an iron sulphide biomass investigated the recovery of the sorbed metal species using a pH 6 sodium citrate buffer. The chemical mediating effects of the desorbing agent were such that at least 20% of the sorbed metals were recovered within 3 hours. The affinity of cadmium for the sorbing biomass however was not overcome by the desorbing solution resulting in no metal being recovered. The poor recovery of cadmium using a mineral salt is in agreement with other literature which attributes the inefficient desorption of alkaline metal complexes with weakly alkaline agents (Saeed and Iqbal, 2003).

Mineral acids and EDTA are however well documented as efficient desorbing agents for cadmium (Holan *et al.*, 1993, Saeed and Iqbal, 2003).

2.5. High Gradient Magnetic Recovery of Biomagnetic Particles

High gradient magnetic separation, HGMS, is one of many devised processes used to separate a material with magnetic properties from a non-magnetic medium (Figure 2.7). The particles targeted tend to have either weakly magnetic traits or are very small in size. The principle of HGMS employs a filamentous ferromagnetic matrix connected to an electromagnet. When a magnetic field is applied, the connected wire matrix dehomogenizes the field producing large magnetic gradients around each wire. These induced fields are then able to attract and trap magnetic particles. The effectiveness of the matrix is often related to the particulate size so that maximum capture is achieved (Equ. 2.7) (Oberteuffer, 1974).

$$F_m = \mu_0 V_P M_P \bullet H \qquad \text{(Equ. 2.7)}$$

Where F_m is the force exerted on the particle, μ_0 is the permeability of free space, V_P is the volume of the particle, M_P is the magnetisation of the particle and H is the magnetic field at the location of the particle.
Successful recovery of the magnetic particles is also influenced by the fluid drag and particulate forces within the fluid.

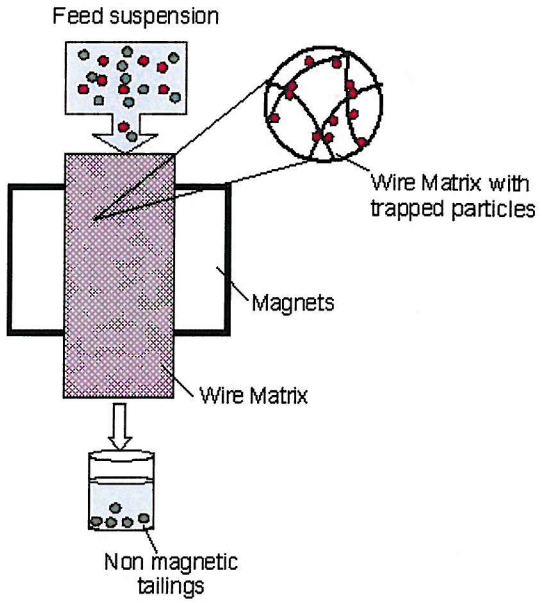

Figure 2.7 Generalised HGMS process

Naturally occurring bacterial magnetism was first identified by Blakemore (1975) during the microscopic analysis of bacteria found in brackish water sediments. His discovery was that of a unique strain of prokaryote, the magnetotactic bacteria (MTB), which displayed intrinsic magnetic abilities as a result of an internal chain structure of iron crystals. Subsequent investigations into the nature of the chain of crystals revealed the octo-rhombohedral iron-oxide structure of magnetite (Fe_3O_4) (Frankel *et al.*, 1979). Magnetic studies conducted on these bacteria showed that the magnetite crystals were magnetically aligned, thereby giving the bacterium cell a definite pole orientation.

Similar structures, although irregular in size have since been identified in a fresh water species of SRB RS-1, a close relative to the *Desulfovibrio spp.*, giving rise to displays of magnetoaxis (Sakaguchi *et al.*, 1993, Kawaguchi *et al.*, 1995).

The magnetic ability of bacteria and their metal adsorption characteristics were combined in the early 1990's with several studies focussing on the magnetotactic bacteria for pollution control (Bahaj and James, 1994, Bahaj *et al.*, 1998a, Bahaj *et al.*, 1998c). The pole specific orientation magnetic orientation of the magnetotactic bacteria initially made it a preferred species for investigation. In

magnetic recovery studies conducted by Bahaj *et al* (1991) using MTB and SRB, the SRB were captured rapidly in comparison to the MTB. This observation was a result of the magnetic iron sulphide not only having a highly magnetic susceptibility but also a net zero polarity thereby allowing instantaneous response, irrespective of the direction of the applied magnetic field, thus enabling rapid capture (Bahaj *et al.*, 1991, Bahaj *et al.*, 1996).

2.6. Applications and Viability as an Effective Biosorbent

The transition from a laboratory scaled test to industrial scaled applications can be very complicated with several limiting considerations of which economic feasibility in relation to existing technologies is most significant. Figure 2.8 shows some of the conditions to be considered when developing a biosorption process.

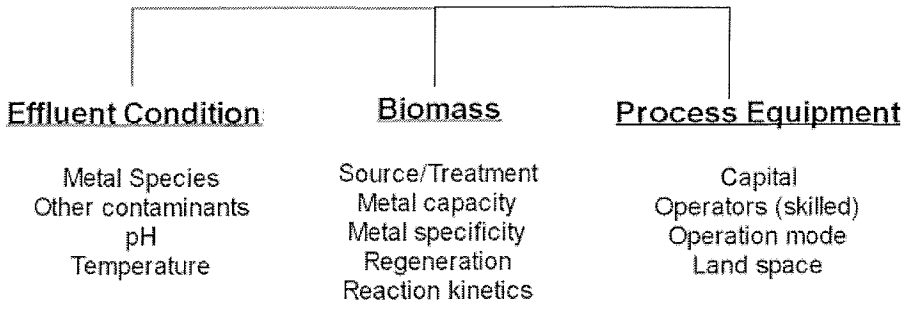

Figure 2.8 Areas of consideration when determining the feasibility of a biosorbent (adapted from Atkinson *et al.*, 1998).

The initial capital outlay required for the setup of a biosorbent system can be considered to be equivalent to that required for a conventional chemical precipitation system, as they utilise the same basic structural system requirements (Atkinson *et al.*, 1998). However, the more intricate the biosorbent system, the greater the incurred costs, both in relation to the structural design and to the required labour force. The ability of a biosorbent system to be incorporated into an existing treatment plant greatly reduces the initial capital outlay.

The cost and sorptive capacity of the biomass contributes significantly to the feasibility of use. The ready availability of biomass such as algae and bacteria greatly reduces costs as these can be readily be grown and harvested on a large scale at minimal costs. Their high sorption capacity in turn means that the amount of biomass required per treatment cycle is also low. Other industrial waste by-products such as sludges and fibres are often low cost and may also have a comparative sorption capacity; however, their bulk can make transportation costs prohibitive.

The recovery and reusability of the biomass is another important consideration. Most conventional treatments require a continual input of 'fresh' agents which are lost in the process, effectively adding to the process costs. Reusability of the biomass in conjunction with the recovery of the metal species increases the favourability of the procedure in addition to making the process highly lucrative.

Several independent groups have conducted extensive laboratory research on the potential for use of heavy metal biosorbents with consistently high metal removal (sorption) levels. These however have failed to be translated into widespread use in industrial wastewater treatment plants, as in most instances the treatment plants have long been established and to switch to this treatment method would incur substantially high costs. Companies are therefore content to pay the cheaper pollution control fine, if it arises (Watson and Ellwood, 1994).

Similarly, failure to exploit the magnetic properties of the microbial Fe_xS_y has been due to numerous mitigating factors including the magnetic inconsistency of the product and the cost of production and operation. Bioseparation work done by Bahaj, *et al* (1991) on their Fe_xS_y material has shown that it is an ideal candidate for this process, however due to its weak magnetic strength a large magnetic field had to be applied to enable efficient separation. The generation of a high magnetic field using either an electromagnet or superconducting magnets incurs prohibitively high expenses and hence its limited use.

Therefore with a view to implementing the use the microbial iron sulphide as an innovative and efficient biosorbent, the magnetic strength of the material would

have to be increased by at least an order of magnitude, without significant compromise to the sorption capacity. This increase in magnetic strength would enable easy manipulation and recovery with a low magnetic field such as that produced by a permanent magnet. Most imperative to this process is the constraint on production costs so as to ensure economic viability.

Chapter 3.

THEORY: Interpreting Sorption Data

This chapter details the theory behind sorption/desorption data analysis inclusive of isotherm and kinetics modelling. Sorption isotherms models enable an appreciation of the macroscopic processes and facilitate comparison between existing studies by quantification of sorption capacities. Kinetics models provide a basis for process design by providing insight into reaction rates.

Sorption is a naturally occurring process responsible in part for the attenuation of trace metals in the environment. Sorption sequesters the pollutant thereby reducing its mobility, toxicity and bioavailability (Veglio and Beolchini, 1997, EPA, 1999a, Volesky, 2001). The specific pathway by which the pollutant is sequestered is seldom obvious as it may be physically attached to the solid (adsorption) and/or incorporated into the internal structure of the solid (absorption) (Pagnanelli *et al.*, 2005). Sorption is therefore used as an all encompassing term which is independent of the binding mechanisms (EPA, 1999a).

The mechanism of sorption is motivated by either of 2 processes: (1) attraction forces between the sorbent and the solute or (2) dislike of the contaminant for the solvent (repulsive /hygroscopic forces). Biosorption investigations carried out using microbial biomasses and heavy metal pollutants (cations) have indicated that sorption is driven primarily by the affinity of the sorbent for the contaminant resulting in electrostatic binding and ion exchange (Volesky, 2003).

Sorption as a system process has been extensively studied under laboratory conditions with equilibrium being attained for various initial solvent concentrations

by altering the sorbent mass until an appropriate solvent to sorbent/liquid ratio is attained. At first glance the high percentage of metal binding can often be misleading, so to enable a true appreciation of the efficiency, capacity of uptake of the biomass and to allow comparison between experiments using different parameters sorption and kinetics models have been developed.

3.1. Sorption models

Sorption models are widely employed by researchers to demonstrate the performance of the sorbing biomass. The simplest model presents a calculated estimate of the contaminant retardation or partition as a ratio of the amount of solute (metal of interest) sorbed per unit weight of the tested biomass to the amount of sorbate remaining in solution (Equ. 3.1).

$$K_d = \frac{A_i}{C_i} \qquad \text{(Equ. 3.1)}$$

Where K_d is the partition coefficient, A_i represents the amount of sorbate on the biomass and C_i is the total dissolved sorbate remaining in solution.

This simplistic model is not prevalent within the literature pertaining to heavy metal recovery as the assumptions used to define K_d; (i) contaminants exist only in trace amounts, (ii) a linear relation between contaminant concentrations in the liquid and solid and (iii) an abundance of equally accessible sorption sites, are not upheld during laboratory determinations (EPA, 1999b).

Sorption isotherm models are robust and most commonly used within the literature for the analysis of sorption data (EPA, 1999a). The models vary in complexity ranging from single sorbate to multi-sorbent systems; as they explore the effects of different conditions on the partition coefficient and therefore have a wider practical application. Volesky (2003) in his review of biosorption models expressed a preference for the use of simple binary parameter models over more complex models provided a suitable fit is attainable. Langmuir and Freundlich isotherm models are considered the simplest models for sorption data analysis.

3.1.1. Langmuir Model

The Langmuir isotherm, derived from first principles, is one of the simplest models and was initially devised to describe gas sorption onto a linear or planar surface (Langmuir, 1918). Its usage has since been extended to characterize the partition of a solute from an aqueous phase (Equ. 3.2), however applicability of the model is limited to batch systems where sufficient time is provided to allow equilibrium to occur (Celik and Demirbas, 2005). Its primary use remains in single sorbate environments and assumes the occurrence of planar surfaces and monolayer binding.

$$q = \frac{QbC_f}{(1 + bC_f)} \qquad \text{(Equ. 3.2)}$$

Where: q is the metal uptake (mg/g biomass), C_f is the final concentration, Q is the maximum sorbate uptake and b is a coefficient related to the affinity between sorbent and sorbate.

When transposed (Equ. 3.3), the Langmuir equation can be expressed linearly by plotting $\left(C_f/q\right)$ vs C_f (Figure 3.1).

$$\frac{C_f}{q} = \frac{1}{Qb} + \frac{C_f}{Q} \qquad \text{(Equ. 3.3)}$$

The simplicity of the model and its associated assumptions imposes constraints on its validity as most biomass surfaces are highly heterogeneous in nature. The resulting graphical profile therefore should not be used to implicate specific binding mechanisms, but instead can be used for descriptive purposes of the processes and trends occurring (Sparks, 1995, Volesky, 2003).

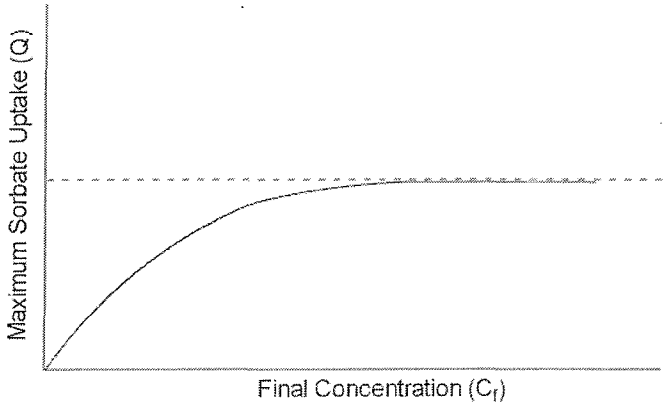

Figure 3.1 Diagram of a Langmuir Isotherm

Conformity to the Langmuir isotherm has been used by authors to indicate the occurrence of adsorption mechanisms (EPA, 1999a), however in keeping with the known short comings of the model, other works have documented the ability of the model to implicate both adsorption and precipitation mechanisms (Pagnanelli *et al.*, 2000, Schneider *et al.*, 2001).

3.1.2. Freundlich Model

The Freundlich isotherm is a nonlinear model based on an empirical equation in which uptake capacity (q) of the sorbate is infinite and the sorbent surface is heterogeneous (Equ. 3.4).

$$q = K_F \bullet C^{(1/n)} \qquad \text{(Equ. 3.4)}$$

Where: q is the sorbate uptake of the metal (mg/g), C is the final equilibrium concentration and K_F is the Freundlich sorption constant and n is a constant related to the degree of linearity (Figure 3.2).

The assumed heterogeneous surface morphology of the sorbing mass is more realistic than that of Langmuir's and as such allows this model to be used with a higher degree of confidence and wide applicability in both monolayer (chemisorption) and multilayer (van de Waals) adsorption (Yang, 1998)

The model equation is best used in its linear form by converting it to a logarithmitic expression (Equ. 3.5).

$$\log q = \log K_F + n \log C_f \qquad \text{(Equ. 3.5)}$$

In this form, the ratio of the solute sorbed (q) to the concentration left in solution (C) provided n=1 gives the Freundlich constant, K_F, which is equivalent to the partition coefficient (K_d).

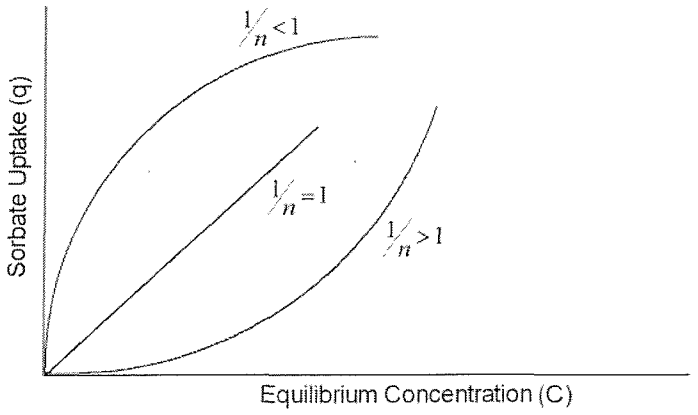

Figure 3.2 Schematic diagram of Freundlich isotherm, showing the effect of the linearity constant

Within the literature, both isotherm models are often applied to sorption data and the results presented in tandem. The suitability of each model in relation to the applied data is dependant on the sorbing biomass and its unique affinity for the metal pollutant. A statistical regression analysis is the primary means of evaluating the fit of the data to the model. Table 3.1 shows a compilation of some of the model parameters and correlation coefficients presented in the literature for a selection of test metal species.

		LANGMUIR PARAMETERS			FREUNDLICH PARAMETERS			
Metal	**Biomass**	**Q_{max}**	**B**	**R^2**	**K_F**	**N**	**R^2**	**Reference**
Cu	Green algae	74.63	0.008	0.957	4.268	2.351	0.983	(Vijayaraghavan *et al.*, 2005)
Cu	Peat	18.021	0.635	0.991	0.227	0.187	0.959	(McKay and Porter, 1997)
Cu	Sludge	294.00	0.018	0.996	9.19	1.5	0.986	(Gulnaz *et al.*, 2005)
Cu	Sago	12.42	0.069	0.991	4.21	0.185	0.915	(Quek *et al.*, 1998)
Cd	Peat	21.133	0.589	0.999	0.156	0.132	0.912	(McKay and Porter, 1997)
Cd	Juniper fibre	9.2	0.03	0.997	0.94	0.41	0.938	(Min *et al.*, 2004)
Cd	*Fucus spiralis*	64	0.053	0.996	10	2.85	0.912	(Cordero *et al.*, 2004)
Zn	Peat	11.708	0.445	0.999	0.139	0.181	0.949	(McKay and Porter, 1997)
Zn	Hazelnut shell	1.766	0.62	-	0.432	0.52	0.996	(Cimino *et al.*, 2000)
Ni	Sludge (granular)	7.899	0.034	0.956	1.669	0.572	0.989	(van Hullebusch *et al.*, 2004)
Ni	Grape stalks	10.67	-	0.99	-	-	-	(Villaescusa *et al.*, 2004)
Ni	Sludge (anaerobic)	12.02	0.98	0.99	-	-	-	(van Hullebusch *et al.*, 2005)

Table 3.1 Langmuir and Freundlich isotherm parameters for select metal ion sorption onto specific biomass types

3.2. Desorption

Sorption of heavy metals is well documented within the literature, however, its reverse process, desorption is not as extensively studied or as clearly understood (Gao *et al.*, 2003). Documented desorption studies show mixed results with sorption hysteresis (incomplete desorption) being observed (Namasivayam and Kadirvelu, 1997, Watson *et al.*, 2001, Panayotova and Velikov, 2002, Saeed and Iqbal, 2003). Panayotva and Velikov (2002) investigated the sorption/desorption of various metals including cadmium, copper, zinc and nickel on naturally occurring zeolites. Their results showed evident sorption hysteresis with desorbed metal concentrations ranging from less than 1% to 65%. Similar results were presented by Watson *et al* (2001) using a microbially produce iron sulphide, with partial to no recovery being recorded for zinc and cadmium respectively. Namasivayam and Kadirvelu (1997) presented their findings on the sorption of copper by carbonised coirpith and demonstrated partial (60%) to complete (100%) metal recovery using a weak acid. Similarly, Saeed and Iqbal (2003), documented the complete reversibility of cadmium sorption on black gram husk using EDTA as the desorbing agent for multiple elutions.

Elution of bound heavy metals from solids is performed in a similar manner to batch sorption experiments. The remobilization of the metal however is initiated by (1) lowering the solution pH (acidification), (2) introducing the metal loaded solid to a metal free solution and (3) sequestering bound metals with a complex-forming or chelating agent. As previously discussed (Section 2.4) the effectiveness of the desorbing agent is related to the nature of the binding between the sorbent and sorbate.

The nature of incomplete desorption has been identified as corresponding to either of 2 factors (Sander *et al.*, 2005); firstly, artificial hysteresis which is attributed to shortcomings in the experimental methods and can be corrected or eliminated by experimental modifications. The second factor, termed true hysteresis, is believed to be as a result of the formation of metastable states of the sorbate or permanent deformation of the sorbent by the sorbate. The

occurrence of sorption hysteresis indicates that the sorption/desorption pathways are not identical and therefore models and coefficients used to qualify sorption are made inadequate (Braida *et al.*, 2003). This is reflected in the literature as it pertains to heavy metal desorption, with amount of metal desorbed quoted in preference to isotherms parameters (Panayotova and Velikov, 2002, Saeed and Iqbal, 2003)

3.3. Kinetics Models

Sorption/desorption reactions between biomass and pollutant species proceed at rates which are governed by numerous factors including the reaction pathways and binding mechanisms. The speed of the reactions is dependant on metal specific affinities of the biomass relative to the solvent and therefore cannot be generically classified by solute. Ho *et al* (2000) in their review of biosorbent sorption kinetics provide a detailed list of sorption parameters which demonstrates the lack of correlation between sorption mechanisms and solute type. For the purposes of process design, the determination of these reaction rates are important as not only do they describe the pollutant uptake speed, but also the residence time at the solid-liquid interface. Pseudo- first and second order rate equations are most commonly used to describe sorption/desorption kinetics.

3.3.1. Pseudo-First Order

Pseudo-first order rate equations have been developed to express reactions found in sorption environments where one of the reacting species (biomass) remains unchanged in concentration at the end of the reaction. The reaction rate is therefore considered in relation to the removal of sorbent species from solution. This is generally described using the following equation (Equ. 3.6)

$$dQ_t/dt = K_1 \bullet (Q_{eq} - Q_t) \qquad \text{(Equ. 3.6)}$$

where, Q_{eq} is the amount of metal sorbed at equilibrium per unit weight of sorbent (mg/g); Q_t is the amount of metal sorbed at any time (mg/g); and K_1 is the rate constant (min^{-1}).

Integrating and applying boundary conditions, t = 0 and $Q_t = 0$ to t = t and $Q_t = Q_t$, equation 3.6 takes the form:

$$\log(Q_{eq} - Q_t) = \log Q_{eq} - {}^{K_1}\!/_{2.303} \bullet t \qquad \text{(Equ. 3.7)}$$

Or

$$\ln(Q_{eq} - Q_t) = \ln Q_{eq} - K_1 t \qquad \text{(Equ. 3.8)}$$

In order to obtain the rate constants, the straight-line plots of log (Q_e-Q_t) against *t* are made

Numerous studies have reported pseudo first order kinetics for the sorption of metals; (cadmium, nickel, copper, uranium), onto biomasses (peat, fly ash and SRB for example) (Spear *et al.*, 2000).

3.3.2. Pseudo-Second Order

In recent times, several authors including Ho and McKay (1999) have suggested that sorption kinetics are dependant not only on the metal species in solution, but also on that present at the surface of the biomass. A review of experimental data previously thought to be pseudo first order, when applied to a second order model showed a better correlation confirming that sorption mechanism is not strictly governed by the concentration of the aqueous metal (Ho and McKay, 1999).

The pseudo second order rate expression, is described by the following equation

$${}^{dQ_t}\!/_{dt} = K_2 \bullet (Q_{eq} - Q_t)^2 \qquad \text{(Equ. 3.9)}$$

Separating the variables, integrating and applying the boundary conditions t = 0 and $Q_t = 0$ to t = t and $Q_t = Q_t$, gives

$$t/Q_t = 1/kQ_{eq}^2 + 1/Q_{eq} \bullet t \qquad \text{(Equ. 3.10)}$$

Substituting h for the initial sorption rate $1/kQ_{eq}^2$, then Equ 3.10 becomes

$$t/Q_t = 1/h + 1/Q_{eq} \bullet t \qquad \text{(Equ. 3.11)}$$

where the plot of t/Q_t against t of equation 3.11 should give a linear relationship from which the constants can be determined.

Unlike sorption isotherm data, sorption kinetics data although applied to several models is predominantly presented using only the model to which the data best conforms. Alternatively, analysis is restricted to a predetermined model, usually the pseudo-second order. Table 3.2 show a summary of some the pseudo-second order kinetics data found within the literature.

Metal	Biomass	Pseudo Second order		Reference:
		K_2 (10^{-3}) (g/mgmin^{-1})	R^2	
Cu	Sludge	2.3	0.999	(Gulnaz *et al.*, 2005)
	Ulva Reticulata	0.011	1.000	(Vijayaraghavan *et al.*, 2004)
Cd	*Fucus Spiralis*	19.0	0.999	(Cordero *et al.*, 2004)
	Pumpkin skin	0.044	-	(Horsfall and Spiff, 2005)
Ni	Sludge	2.80	0.999	(van Hullebusch *et al.*, 2004)
	Peat	0.159	0.999	(Ho and McKay, 2000)
Zn	Pumpkin skin (acidified)	0.016	-	(Horsfall and Spiff, 2005)

Table 3.2. Pseudo second order rate parameters for metal sorption unto selected biomasses.

Chapter 4.

EXPERIMENTAL METHODS AND MATERIALS

4.1. Site Description

Salt marsh sediment containing a mixed bacteria culture was obtained from the Fawley-Calshot salt marshes on the Hampshire coastline on the south coast of the United Kingdom. Sedimentary material from this site, has been used in previous experiments (Bahaj *et al.*, 1998b, Macmillan, 2000) and is known to have a high population density of sulphate reducing bacteria (SRB), with *Desulfovibrio spp*, (DSV), being the most dominant genera (Macmillan, 2000). The Fawley-Calshot salt marshes, a designated site of special scientific interest, SSSI, is located on the leeward side of the Calshot spit (OS grid *448500,101550*) and covers an area of approximately 3 km^2 (Figure 4.1).

The stratigraphy of the area consists of three major geological units, dating from the Tertiary to Quaternary Period (Figure 4.2). The Tertiary deposit, from the upper Eocene epoch is Barton Clay. This grey brown clay has a sandy consistency and is highly fossiliferous (West, 2003). Overlaying the clays is Pleistocene river gravel, followed by Holocene deposits of peat, clays, and present day estuarine alluvium and gravel. Salt marsh samples were collected from the most recent estuarine silt.

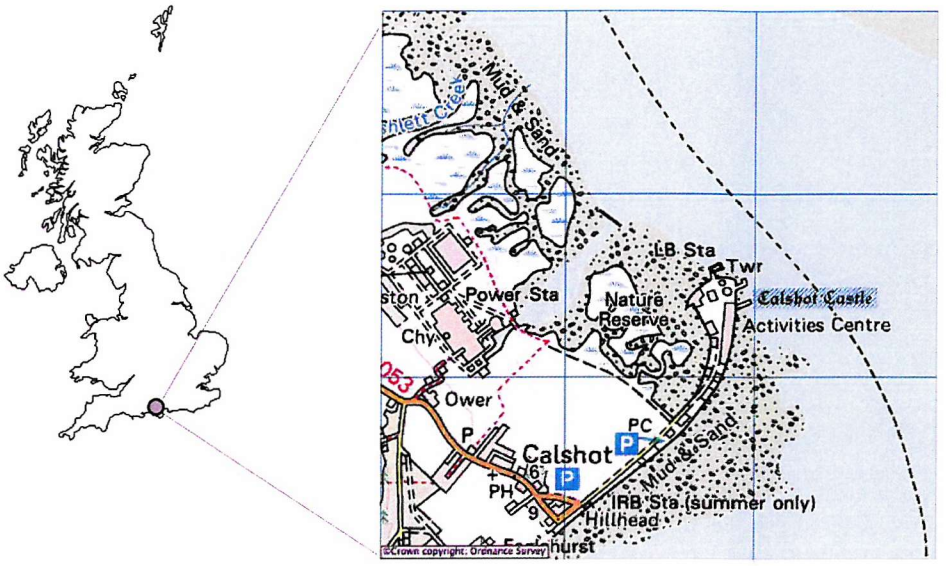

Figure 4.1 Map extract showing sample site location (OS grid 448500,101550)

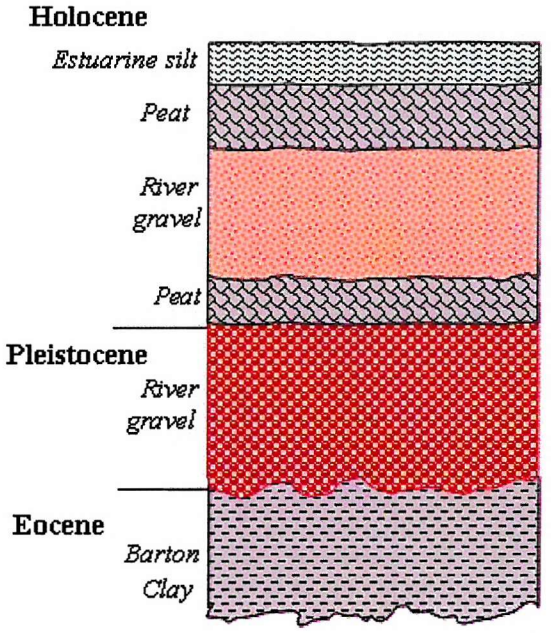

Figure 4.2 Cross section showing geological stratigraphy of sample site (not to scale) (adapted from West, 2003)

4.2. Bacteria Collection

Salt marsh sediment containing bacterial samples were collected approximately 3-5 hours after low tide thus allowing the sediment to drain of tidal waters. The sample sites were chosen using the following criteria which are known to indicate a high population of sulphate reducing bacteria (Luptakova and Kusnierova, 2005):

- black sediment;
- a hydrogen sulphide odour; and
- an oily film layer.

Soil samples were collected from the top 15cm of sediment and stored in sterile sealed glass bottles under marsh water to limit exposure to oxygen and maintain site conditions. Once in the laboratory, samples were stored at 4^0C until they were ready for use.

4.3. Bioreactor Set Up

The active culture of the SRB obtained from the salt marsh sediments was conducted in a growth vessel, here after referred to as a bioreactor, modelled on the Novick and Szilard (1950) chemostat. The operation of the bioreactor was such that the bacterial population growth was maintained for an indefinite period of time(Novick and Szilard, 1950).

The bioreactor consisted of a 2L vessel with an overflow set to maintain the active volume at 1.5L and an atmospheric headspace of 500ml (Figure 4.3). This is contrary to the accepted convention for the growth of anaerobic bacteria which prescribes that the growth apparatus be maintained under anaerobic conditions by the use of anaerobic cabinets or by the injection of oxygen free nitrogen (OFN) (Watson *et al.*, 1995). No attempt was made to maintain artificial anaerobic conditions as it was found that SRBs, in particular *Desulfovibrio spp* were able to facilitate their own anaerobic conditions required for their preferential growth, given a sufficient source of carbon in the growth medium. The growth medium for the bacteria (detailed in section 4.4 below), was introduced to the culture via tubing through the headspace at a dilution rate of $0.028hr^{-1}$.The bioreactor

contents were kept in constant suspension, maintaining a homogenous mix and optimising contact between the contents using a magnetic stirrer.

The optimum culturing temperature for SRBs is dependant on the strain of the bacteria present. In instances where mixed cultures are present the growth temperature is a means of preferentially culturing selected strains. Culturing conditions were regulated between 30-32^{0}C, by the use of a circulating water jacket to preferentially culture mesophiles and in particular Desulfovibrio *spp.,* which are known to have a high presence in the sample sediment utilised (Macmillan, 2000).

Where multiple bioreactors were being operated, the water jackets were connected in series to ensure uniformity of conditions between all vessels. The internal bioreactor parameters of pH and temperature were continually data-logged using probes inserted through the headspace. Redox and dissolved oxygen were recorded daily (see section 4.5 for a detailed description).

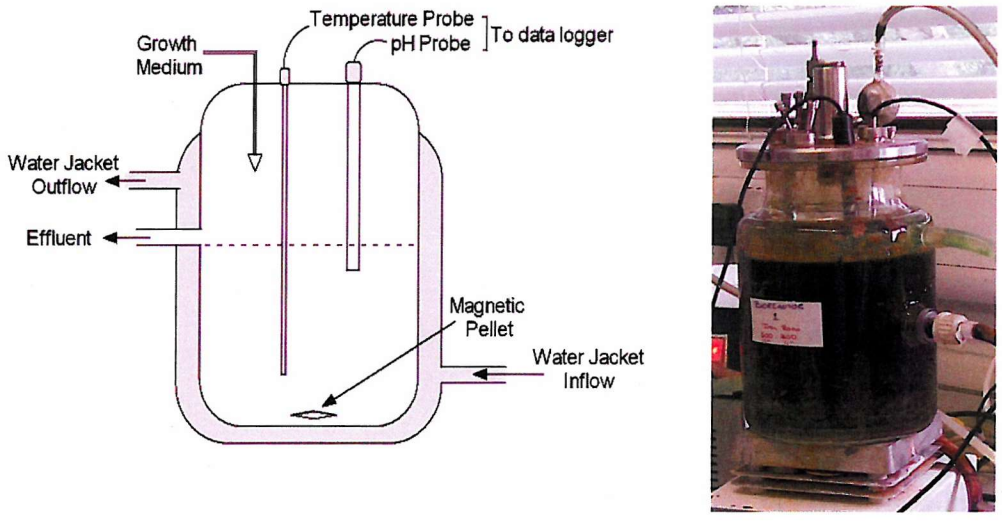

Figure 4.3: Schematic bioreactor design (left) along side photo of actual bioreactor (right).

4.4. Growth Medium

The growth medium used for the culturing of the SRB and to ensure a magnetic iron sulphide yield was an amalgamation of the Postgate C medium (Postgate,

1979) and the Freke and Tate mixed iron medium (Freke and Tate, 1961) with minor modifications. The resulting modified Postgate C medium, also later referred to as the "the mixed iron reference medium of ratio, (Fe^{2+}: Fe^{3+}), 650:150mgL^{-1}" is as follows: (in gL^{-1}), 3.22 $FeSO_4.7H_2O$, 0.58 $Fe_2(SO_4)_3.2H_2O$, 0.07 $(NH_4)_2SO_4$, 0.5 KH_2PO_4, 4.5 Na_2SO_4 (anhydrous), 0.06 $CaCl_2.2H_2O$, 0.06 $MgSO_4.7H_2O$, 5ml sodium lactate @70% w/v; and adjusted to approximately pH 6.7 using sodium hydroxide pellets.

Later modifications to the medium resulted in the alteration of the relative concentrations of the iron species (Fe^{2+}/Fe^{3+}) whilst maintaining the total iron concentration at 800mg/L (See appendix 1 for detailed medium permutation).

4.5. Physical Characteristics of Bioreactor

4.5.1. pH

pH conditions within the bioreactor was measured using a K-series ThermoRussell electrode (KDCE11) inserted directly into the bioreactor. The pH electrode was connected to a DataTaker DT505 logger (UK) which was programmed to sample the internal pH at 3 second intervals and log an averaged measurement every 60 seconds. To ensure the accuracy of readings, the electrode was calibrated weekly using pH 4, pH9 and pH7 buffer solutions.

4.5.2. Temperature

Temperature conditions within the bioreactors were monitored continually to ensure that optimum temperatures were maintained. Temperature was measured using a PT100 platinum resistance temperature sensor inserted directed into the culture.

4.5.3. Redox

Daily redox measurements were taken using a ThermoRussell K-series silver (Ag) electrode. The electrode was calibrated prior to each measurement using a

silver/silver chloride (Ag/AgCl) redox standard (250mV, ThermoRussell). The electrode was placed directly into the culture and allowed to stabilise prior to recording the measurement.

4.5.4. Dissolved Oxygen

The dissolved oxygen (DO) concentration within the bioreactor was measured daily using a YSI 5100 dissolved oxygen instrument system to determine whether anaerobic conditions were created and maintained within the bioreactor without artificial assistance. The DO probe was auto calibrated weekly, and manually calibrated monthly. The sensitivity of the probe was checked bi-weekly using a zero calibration standard (3mM sodium sulphite solution). The DO probe was inserted via the headspace directly into the culture. The reading was allowed to stabilise for 10 seconds and recorded.

4.6. Bacteria Growth Conditions

The growth of the bacteria was conducted in three distinct modes (i) batch, (ii) continuous, and (iii) mixed batch-continuous to determine their effect on the magnetic susceptibility of the microbial sulphide produced.

4.6.1. Batch Culture

Salt marsh sediment containing SRB was cultured under batch conditions to determine whether a highly magnetic iron sulphide could be readily produced (Figure 4.4). 100ml of the tidal marsh sediment sludge was used to inoculate 1900ml of the modified growth medium in a 2L flask. The flask was then sealed with a butyl stopper and laboratory sealing film, and placed in an incubator at 30^0C. The flask was gently shaken once a day to optimise bacterial contact with the medium. Samples for the monitoring of the magnetic susceptibility were collected on alternate days and immediately measured using a Sherwood Scientific magnetic susceptibility balance, MSB-Auto (section 4.10.3).

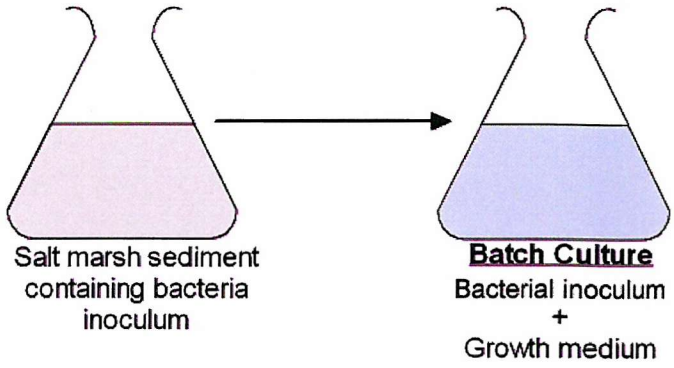

Figure 4.4 Schematic showing batch culture experiment set up

4.6.2. Continuous Culture

Bacterial growth under continuous culturing conditions was investigated to determine the magnetic strength of the material produced. The experiment was composed of two tiers of continuous culture (1) pure salt marsh sediment and (2) a magnetically refined culture similar to that used by Watson (1996) (Figure 4.5).

The modified Postgate C medium previously detailed in section 4.4 (1.4L) was inoculated with 100ml of unfiltered sediment sludge in a 2L bioreactor. The bioreactor was maintained at 30^0C with periodic gentle mixing in a batch growth mode until the bioreactor was made opaque (14 days) by the generation of iron sulphide. The bioreactor was then switched to a continuous culturing mode with a dilution rate of 0.028 hr^{-1}

Following an initial 4 weeks of continuous culture, the magnetic susceptibility of the culture was measured (section 4.10.3) and a simple test using boron-neodymium permanent magnets showed that only a small fraction of the iron sulphide produced by the continuous culture mode bioreactor was magnetic. The magnetic fraction of the microbial iron sulphide produced was recovered using an open gradient magnetic separator to be used for inoculating purposes (Figure 4.6).

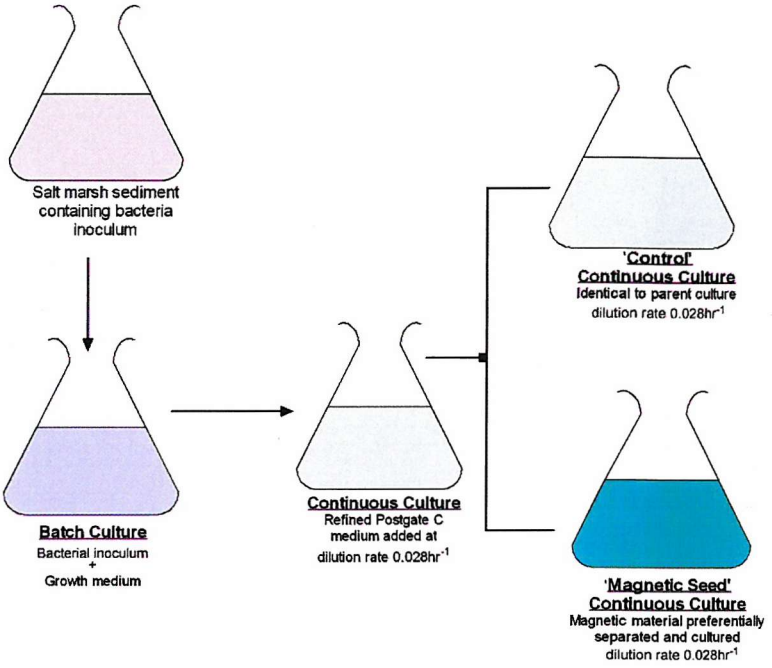

Figure 4.5 Schematic showing progression of bacterial culture from batch to the 2 tiered continuous culture experiments

Half of the bioreactor contents, 750 ml, were extracted and the concentrated iron sulphide precipitate was placed in a measuring cylinder adjacent to the magnetic pole of a 2T electromagnet, of which only one coil was energised. The magnetic fraction accumulated adjacent to the pole was recovered using a pipette. This recovered magnetic fraction was then used as a seed for a second, 'magnetic seed' bioreactor which was allowed to sit in batch for 14 days, prior to switching to continuous culture mode.

The original and magnetic seed bioreactors were then run in parallel under continuous culture conditions and the magnetic susceptibility of the produced material measured daily.

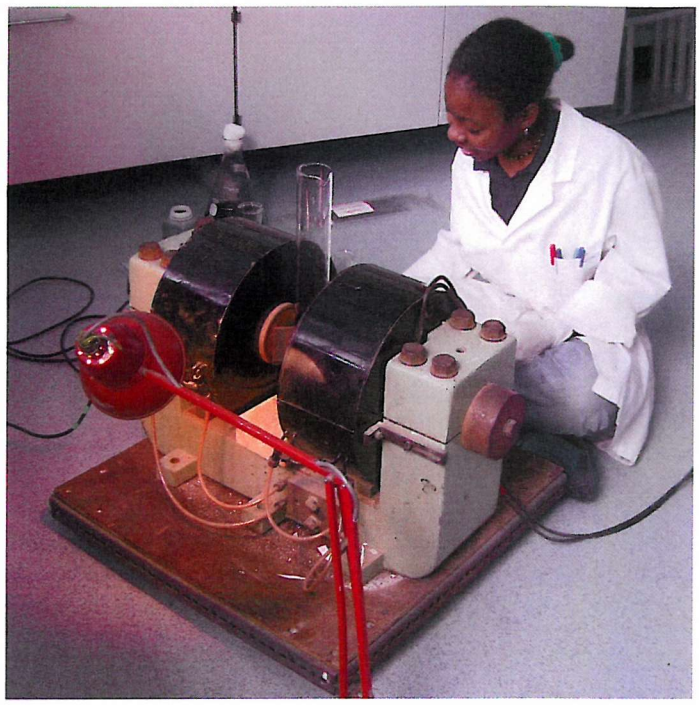

Figure 4.6: Magnetic separation of magnetic material produced during batch culture using a 2T electromagnet. Magnetic fraction collected and used as inoculum for continuous culture bioreactor.

4.6.3. Mixed Batch Continuous Culture

Successful laboratory culture of a magnetic iron sulphide was achieved by Freke and Tate in 1961 using an undefined semi-continuous culture regime (Freke and Tate, 1961). The effectiveness of a mixed culture mode was investigated using an alternating batch-continuous culture regime.

The contents of the magnetic seed bioreactor described above (section 4.62) was divided in half and used to create two identical bioreactors running in parallel. A comparison of the magnetic product produced by these two bioreactors running in parallel but under different growth conditions was undertaken (Figure 4.7)

The first bioreactor, termed 'continuous control' (CC), was initially operated in continuous culture mode at a dilution rate of $0.028hr^{-1}$ for 40 days. The dilution rate of the CC-bioreactor was then reduced to $0.015\ hr^{-1}$ to determine the effect and significance of the overall dilution rate on the magnetic susceptibility of the

iron sulphide yield The second bioreactor, termed 'switch batch-continuous' (SBC) was subjected to a 5 day batch: 6 day continuous growth sequence. During the 6 day continuous growth sequence, the dilution rate was identical to that of the CC-bioreactor, leading to an averaged dilution rate over an 11 day cycle of 0.015hr^{-1}.

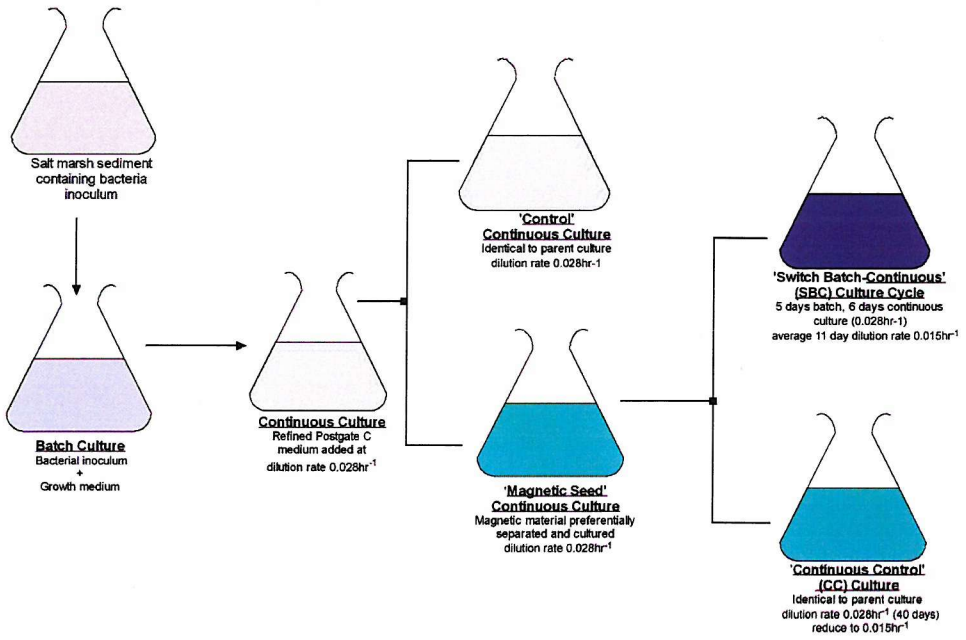

Figure 4.7 Culturing schematic showing the progression from batch culture to mixed batch continuous culturing

4.7. Valency Effect of Medium

At the end of the 'mixed culture conditions' experiment, (section 4.6.3 above), the SBC bioreactor was returned to a continuous culture mode with a 0.028 hr^{-1} dilution rate for 2 weeks. At the end of this period, the magnetic susceptibility of the biosorbent returned to a level identical to that established prior to the mixed culture test. The bioreactor contents (1500ml) were then divided into thirds and 1000ml of growth medium added to each. The three newly inoculated bioreactors were placed in batch growth mode for 5 days to allow the bacterial population to re-establish. They were then run continuously in parallel (dilution rate 0.028hr^{-1}) for approximately 3 days, until the variability in the magnetic product of the 3 bioreactors was 30%.

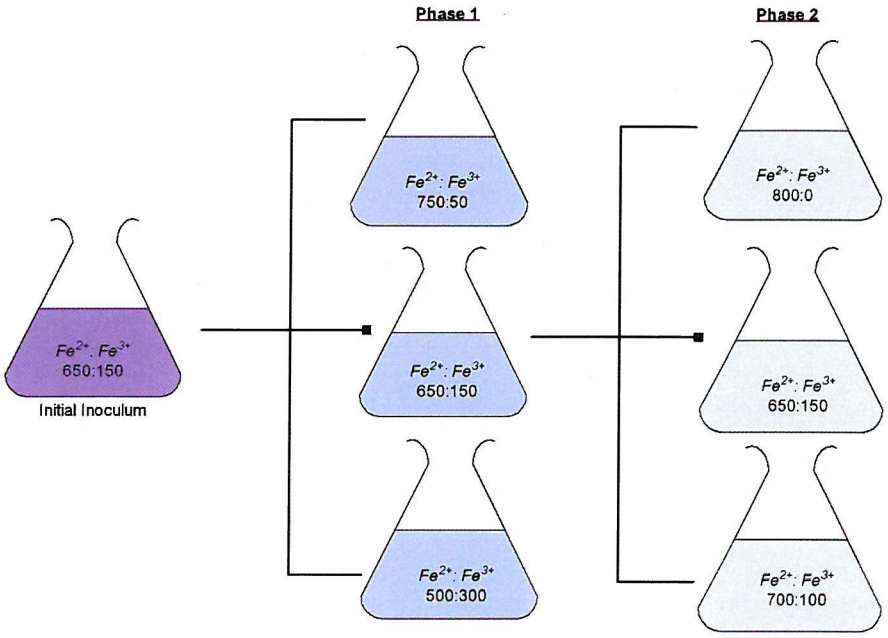

Figure 4.8: Schematic diagram detailing the relative concentrations of Fe (II): Fe (III) tested in the two phases of the experiment. The contents of the reference culture (650:150) served as the inoculum for each phase. Prior to the commencement of each phase the bioreactors were run continuously at a dilution rate of 0.028hr^{-1} until the measured magnetic susceptibilities were identical.

Where upon each bioreactor was run using the previously defined 11 day growth cycle (section 4.6.3), however the relative concentrations of Fe (II): Fe (III) in the growth medium was varied for each bioreactor (Figure 4.8). The total iron concentration, 800mgL^{-1} was kept constant and a 650:150mgL^{-1} mixed medium was maintained as the reference concentration throughout, as it represented the initial concentrations under which the magnetic characteristics of the associated products were first identified.

In this first phase of valency effect experiments the Fe (II): Fe (III) ratios in the medium were adjusted to 750:50 mgL^{-1} and 500:300 mgL^{-1} and run for the equivalent of three 11 day cycles. The second phase was then initiated by subculturing the reference bioreactor (650:150 mgL^{-1}) to form 2 further bioreactors. The newly inoculated bioreactors were allowed to establish as previous, then started on the 11 day mixed culture cycle using altered growth medium at concentrations of 700:100 mgL^{-1} and 800:0 mgL^{-1} Fe (II): Fe (III).

4.8. pH effect

As a result of metabolic processes, SRB create an alkaline microenvironment which facilitates the dissociation of hydrogen sulphide into its reactive constituents. The effect of externally regulating the pH environment of the bacterial culture on the magnetic susceptibility of the iron sulphide product was conducted using 2 pH regulating regimes as detailed below;

(1) Using a mixed batch continuous culture cycle, the bacterial culture pH was adjusted and maintained within the range of pH 6.5-7.5 for the duration of an 11 day culture cycle.

(2) The bacterial culture cycle was then altered to a continuous only cycle with a reduced dilution rate of $0.015hr^{-1}$ so that the total through-put of the bioreactor over 11 days was identical to that of the bioreactor operated under the 11 day mixed culture cycle. The pH of the bioreactor was then made to simulate that of bioreactor undergoing an 11 day mixed culture cycle, with pH restricted between pH 6.5-7.5 during continuous culture and pH 8.0- 8.5 during batch culture.

Adjustments to the pH were done using 1M sodium hydroxide and 1M H_2SO_4 solutions.

4.9. Bacteria Enumeration

4.9.1. Epi-fluorescence

Prior to the start of an experimental phase, bacterial numbers in conjunction with the measured susceptibility were used to confirm the similarity of the operation of the bioreactors. Bacterial enumeration was determined using fluorescence microscopy. In this 1ml sample aliquots were extracted from each bioreactor and placed into a scintillation vial. 1ml of a 2% formalin solution was added to the bacterial sample and agitated to fix the bacterial cells. The samples were stored

at 4^0C prior to bacterial enumeration. Storage time was limited to less than 4 weeks as bacterial numbers were observed to decrease with storage (Daley and Hobbie, 1975).

In addition to the natural tendency of some species of SRB to form biofilms, the deliberate generation of a charged extracellular iron sulphide coating further increased the natural tendency of the bacteria to form aggregates (Figure 4.9). As a result, samples extracted from the bioreactors consisted of free suspended bacterial particles as well as aggregates. In order to get a true appreciation of the bacterial population, bacterial enumeration was conducted in 2 phases – (i) unattached bacteria and (ii) total bacterial number.

Figure 4.9 Light microscope image of the formation of a bacterial aggregate by unattached SRB encased in Fe_xS_y coating. Magnification x100

4.9.1.1. Unattached Bacterial Numbers

Samples were diluted a hundred fold with Milli-Q water (Millipore) and 2ml aliquots centrifuged at 2000 *x g* for 12 minutes using an Eppendorf 5417C centrifuge. This operation pellets the solids leaving the unattached bacteria in suspension (Daley and Hobbie, 1975). 2ml of the supernatant was decanted into a test tube and 200µl of a 0.1% acridine orange (AO) solution added. This was allowed to stain for 1-5 minutes and then filtered onto a 0.45µm filter paper prestained with Dylon Ebony Black dye (Hobbie *et al.*, 1977). Filters were immediately prepared for analysis using a non-fluorescent, low viscosity

immersion oil as described by Daley and Hobbie (1975). Analyses were conducted under ultra violet light on a Diaplan standard microscope equipped with a 50W mercury lamp and interference filters set for blue excitation. Only green fluorescing particles with a definite boundary of bacterial shape and size were counted.

4.9.1.2. Total Bacterial numbers

In order to determine total bacterial numbers, bound cells were detached from particulates using a surfactant, Tween80. A 1ml aliquot of the ten fold sample dilution was taken and Tween80 solution (10mg/L) added (Yoon and Rosson, 1990). Samples were vigorously agitated and allowed to stand for 1-2 hours. This allowed the Tween80 to penetrate the particles and also allowed the larger particles to settle out of solution. Samples were homogenised for 1 minute and centrifuged at 150 *x g* for 10 minutes. 2ml aliquots of the supernatant were decanted and prepared for filtration and analysis as previously described (section 4.9.1.1).

4.10. Physical Characteristics of the Microbial Sulphide

4.10.1. Density

Particle density measurements were conducted using the BSI small pyknometer standard method (BSI, 1990). Bacterial samples were collected, centrifuged and initially dried anaerobically in a nitrogen/carbon dioxide environment at 30^0C to prevent oxidation of the metal sulphide and until constant weight was attained.

To a 10ml pre-weighed pyknometer 2mg of sample was added and weighed. Approximately 5ml of de-aerated water was added to the sample before the pyknometer was placed in a vacuum desiccator (~20mm Hg) for an hour. The sample was then sonicated to help displace any trapped air then replaced in the desiccator. When no further air was liberated from the sample, the density bottle was filled, stoppered and place in a temperature bath set at 30^0C until a constant temperature was attained. Water was added to the pyknometer until there were

no further signs of water loss. The pyknometer was then removed from the water bath and weighed. The procedure was then repeated with a sample of only water,

Particle density was then calculated using the following equation (Equ. 4.1):

$$\rho_s = \frac{\rho_L (m_2 - m_1)}{(m_4 - m_1) - (m_3 - m_2)} \qquad \text{(Equ. 4.1)}$$

Where

ρ_L = density of water at constant temperature (mg/m^3)

ρ_s = density of solid particles (mg/m^3)

m_1 = mass of empty density bottle

m_2 = mass of bottle and dry sample

m_3 = mass of bottle, sample and liquid

m_4 = mass of bottle when full with liquid only

For fine grained sediments with a high organic content, the accuracy of the calculated density can be easily displaced by the organic mass. The organic matter within sediments can be dissolved using the BSI standard method (1990).

4.10.2. Morphology

The shape and size distribution of the microbially generated iron sulphide was examined at the Southampton Electron Microscopy Centre using a JSM-5910 scanning electron microscope (SEM). Sulphide samples were extracted from the bioreactor, centrifuged and dried anaerobically to preserve the integrity and structure of the sulphide. Once dried, the samples were lightly ground with a mortar and pestle and secured to a mounted disc using a light adhesive. The sample was splutter coated with gold and prepared for SEM examination.

4.10.3. Magnetic Susceptibility

In the laboratory, the magnetic susceptibility of the microbially produced iron sulphide precipitate was measured as that of a wet sludge. Three samples measuring 20 ml each were extracted from each bioreactor on a daily basis and

centrifuged at 559 *x g* for 15 minutes using an MSE Centaur 2 centrifuge. The supernatant was decanted and the sludge extracted from the samples and used to measure the magnetic susceptibility (χ_v) by volume, of the biologically produced iron sulphide using a magnetic susceptibility balance, MSB-Auto (Sherwood Scientific Ltd). The three samples were then anaerobically dried to determine the moisture content to enable the calculation of the 'dry weight equivalent' magnetic susceptibility

The accuracy and precision of the balance was assessed using analytical grade chemical compounds of known mass magnetic susceptibility (χ_g) (Table 4.1)

Chemical Compound	Mass susceptibility $\chi_g (10^{-4})$		% Error
	Measured	Literature (Lide, 1996)	
Iron Sulphate $(FeSO_4 \cdot 7H_2O)$	0.462	0.403	15
Copper Sulphate $(CuSO_4 \cdot 5H_2O)$	0.057	0.0585	3
Manganese Chloride $(MnCl_2 \cdot 4H_2O)$	0.8	0.7377	8
Iron Chloride $(FeCl_2 \cdot 4H_2O)$	0.627	0.6489	3
Tris-ethylenediamine-nickel (II) thiosulphate $(Ni(en)_3S_2O_3)$	0.115	0.1105	4

Table 4.1 Accuracy of the magnetic susceptibility balance measured against published values.

4.10.4. Saturation Magnetisation

The saturation magnetisation of a material is a measure of the intrinsic magnetic properties of the material from which the nature and magnetic susceptibility can be deduced.

In preparation for the saturation magnetisation tests, large quantities (>100ml) of microbial iron sulphide samples were extracted from active bioreactors and centrifuged (MSE Centaur 2) at 559 *x g* for 15 minutes. The pelleted sludge was

dried anaerobically and ground to a fine powder (<0.024mm). The powdered sulphide was mixed with Emerson & Cuming Ecobond, a low magnetisation epoxy and moulded into bricks with dimensions of 0.4x0.2x0.05cm.

Saturation magnetisation was measured at room temperature using a Quantum Design physical particle measurement system, under an applied magnetic field varying between -0.5 and 0.5T.

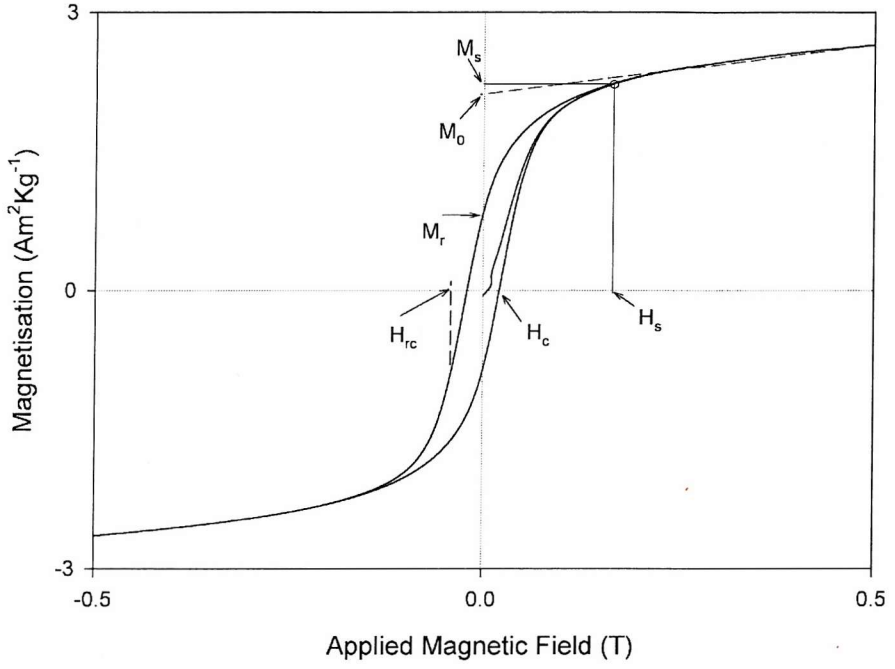

Figure 4.10 Hysteresis curve detailing important features used to describe and characterise the loop. M_s- magnetic saturation, M_0 - zero field magnetisation offset, M_r Magnetic remnance, H_c- bulk coercivity, H_s saturation field, H_{rc}- coercivity of remnance.

From the produced hysteresis loops (Figure 4.10) the magnetic susceptibility (χ) was calculated using the following derived equation

$$\chi = \left(M_{effective}\mu_o / B - (M_{effective}\mu_o) \right) \times \rho \qquad \text{(Equ. 4.2)}$$

Where, B is the applied external magnetic field (T), ρ is density of the material (gcm^{-3}), μ_0 is permeability of free space (NA^{-2}), $M_{effective} = M_{measured} - M_0$ ($Am^{-2}Kg^{-}$

^{1}) and M_0 ($Am^{-2}Kg^{-1}$) is the zero field magnetisation offset which is the predicted magnetisation at zero applied field extrapolated from the linear response region.

4.11. Chemical Composition of the Iron Sulphide

4.11.1. Chemical composition (X-ray diffraction)

The chemical composition of the biogenically produced sulphide was determined using X ray diffraction (XRD). The analysis was performed at the National Oceanography Centre (NOC), Southampton using a Philips X'Pert-Pro X ray diffractometer and related software.

Anaerobically dried samples were ground to a fine powder (~10μm) and loaded onto a silicon disk sample holder. The sample was compacted and made level using light pressure from a glass slide. The prepared sample was then irradiated with a cobalt source (CoKα 1.79Å) and the diffraction patterns produced were cross referenced with the Joint Committee for Powder Diffraction Studies (JCPDS) and International Centre for Diffraction Data (ICDD) databases to deduce the sample chemical composition.

4.11.2. Total Inorganic Sulphide

The total reduced inorganic sulphide (TRIS) content in the microbial sulphide samples were assessed using an adapted single step reduction method detailed by Ulrich *et al* (1997). Sulphide reduction was carried out in an anaerobic sealed 250ml flask containing 4ml of a 10% zinc acetate solution in a test tube, which functioned as a sulphide trap (Figure 4.11). So as to prevent premature oxidation of the samples and the liberated sulphide, all reagents were stored anaerobically and sample manipulation was performed in an anaerobic cabinet.

Centrifuge pelleted sulphide sludge samples (approximately 2ml) were added to the reaction flask, to which 8ml of a 1M Cr (II)-HCl solution followed by 4ml of a 12N HCl solution were added. The flask was immediately sealed and placed on a rotary shaker (150rpm) for the duration of extraction (approximately 30hrs).

At the end of the reaction time the precipitated ZnS in the sulphide trap was homogenised and serial dilutions performed using anoxic distilled water prior to quantification using the Cline methylene blue assay (Cline, 1969). The Cline reagent was prepared by mixing a prepared diamine solution ($16gL^{-1}$) and ferric chloride solution ($24gL^{-1}$) using a 50%v/v HCl solution as the aqueous phase. The Cline reagent (0.8ml) was added to the diluted sulphide solution, sealed and allowed to develop for 30 minutes. The resultant blue solution was measured spectroscopically using a UV spectrophotometer, Cecil Instrument, at 670nm.

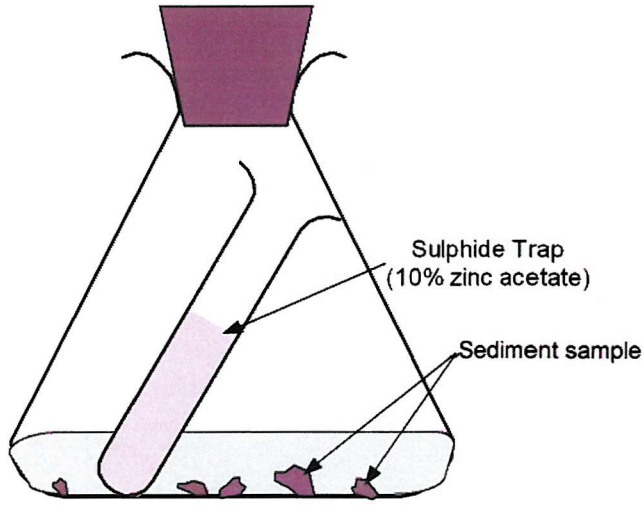

Figure 4.11 Schematic diagram showing experimental procedure used for the determination of inorganic sulphide in sediments.

TRIS sulphide is composed of chromium reducible sulphide (CRS) and acid volatile sulphur (AVS) as detailed in the following equation:

$$TRIS = AVS + CRS \qquad \text{(Equ. 4.3)}$$

Where CRS constitutes elemental sulphur and pyrite, and AVS is made up of free sulphide and all other iron sulphide species.

The AVS speciation was determined using the TRIS method; where the use of the chromium reagent was omitted. The composition of CRS was then deduced from TRIS and AVS values

Sulphide standards which were prepared from a 1000mgL^{-1} sulphide solution prepared from dissolving 0.75g $Na_2S.9H_2O$ / 100ml in anoxic distilled water.

4.11.3. Total Iron and Phosphorous Content

The total iron content of the microbial iron sulphide was determined by dissolving the microbial sample. A bacterial sludge sample (~1ml), was acidified with 12MHCl (4ml) and allowed to react. The resultant solution was serially diluted and analysed by atomic absorption flame spectrometry (Varian AAS 100/200).

The sample used to determine the total dissolved phosphorous content was prepared in a similar manner to that used for total iron analysis. A bacterial sludge sample (~1ml) was dissolved using 4ml of 12M HCl. The solution produced was serially diluted in Milli-Q water (Millipore) and prepared for analysis using a Machery-Nagel viscolour Phosphate photocolour test. The reacted solution was photometrically measured using a Machery-Nagel filter Photometer PF11.

4.12. Heavy Metal Sorption Experiments:

The metal sorptive capacity and associated reaction kinetics of the biogenic sulphide was studied with selected heavy metal ion species that typify industrial effluents; (cadmium, zinc, copper and nickel) using batch sorption experiments (Figure 4.12).

As discussed in section 2.6, excessive processing and pre-treatment of the sorptive biomass can result in inflated production costs which can reduce the marketability of a biosorption process. Previous works by Watson *et al* (2001) utilised freeze dried material to conduct sorption tests, however this method of preparation is time consuming and costly. In order to keep biomass costs low, no pre-treatment or processing was undertaken in these studies.

4.12.1. Batch Sorption Experimental Setup

In order to effectively use the cultured biomass for quantification of its sorption capacity, samples were extracted from the active bioreactor and centrifuged at 559 *x g* (MSE Centaur 2) for 15 minutes in a preweighed vial. Centrifuging separated the phases and concentrated the sample into residue sludge and an overlying supernatant. The supernatant was decanted and the vial reweighed to determine the wet mass of the biomass sample. The pelleted residue sludge was applied directly to the aqueous metal solutions. A duplicate residue sample was prepared in a similar manner, and then dried at 105^{O}C to determine the water content and the sample dry weight equivalent.

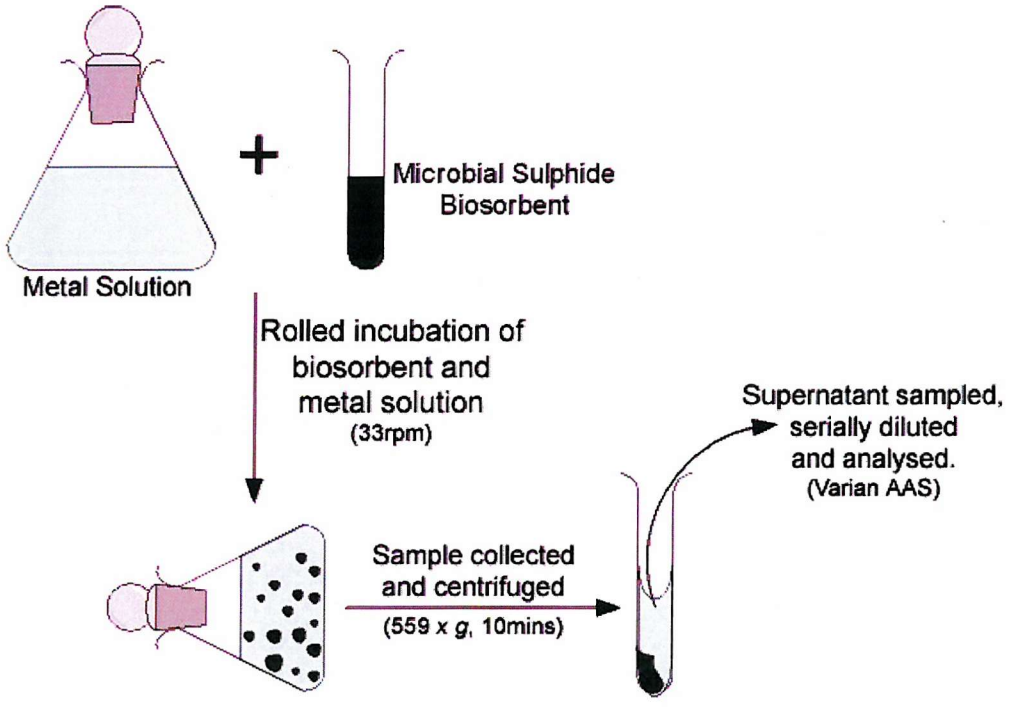

Figure 4.12 Schematic of batch sorption experiment

To optimise sorption by ensuring good contact between the biomass and the metal solution, the samples were maintained in a constant state of suspension by agitating the samples on roller beds (Stuart Scientific Roller/Mixer SRT2) at 33 rpm. Aliquot samples were taken at regular intervals during the sorption incubation period, centrifuged at 559 *x g* (MSE Centaur 2) for 10 minutes to separate the phases and the supernatant sampled and serially diluted as

necessary in preparation for metal analysis using a Varian AA200 atomic absorption flame spectrophotometer

Aqueous metal ion solutions were prepared using analytical grade salts dissolved in ultra pure Milli-Q water (Millipore Ltd). Concentrated stock solutions (1000mgL^{-1}) were prepared for each metal, from which subsequent test solutions were prepared. The stock solutions were stored at 4^{0}C between experiments and discarded after 14 days. pH measurements of the concentrated solutions showed that all the solutions were weakly acidic (pH 5-5.5). Given the low stability of the microbial sulphide under acidic conditions and the narrow pH range of the stock solutions, no further pH adjustments were made.

4.12.2. Data Analysis

The concentration of metal sorbed from solution was determined by mass balance of metal ions in solution (Equ. 4.4). The mass balance assumed that the difference in concentration of metal at the sampling (C_{aq}) and that at the start of the experiment (C_o) is equivalent to the concentration sorbed (q) per gram of applied sorbent. Any losses to the sorption vessel are determined from the control experiments (section 4.12.3) and corrected for accordingly. The percentage metal sorbed from solution was determined using Equ. 4.5

$$q = \frac{(C_o - C_{aq})V}{M} \qquad \text{(Equ. 4.4)}$$

Where q is the metal sorbed (mg/g biomass), C_o is the initial metal concentration, C_{aq}, is the residual concentration in solution, V is the volume of metal bearing solution and M is the amount of dry biomass added as the sorbing agent.

$$\%sorbed = \frac{(C_o - C_{aq})}{C_o} \qquad \text{(Equ. 4.5)}$$

Where %sorbed in the percentage of metal sorbed from solution and C_o and C_{aq} are defined as per Equ. 4.4

4.12.3. Effect of Magnetic Susceptibility

Batch equilibrium uptake studies investigating the effect of the magnetic susceptibility on the sorptive capacity of the microbial sulphide were performed in triplicate, using 150ml glass sorption vials (Sigma-Aldrich, UK) containing 100ml of aqueous cadmium solutions of varying concentrations; (50mgL^{-}1, 150 mgL^{-1} and 500mgL^{-1}). To each test concentration 0.018g (dry weight equivalent) of biomass was added. Two distinct biomass samples were used (1) at peak magnetic susceptibility and (2) at lowest susceptibility. The sorption vials were agitated on the roller beds (Stuart Scientific Roller/Mixer SRT2) for 2 hours, with sample aliquots (1ml) extracted, centrifuged (Eppendorf 5417C) and prepared for metal analysis as described in section 4.12.1 above.

For each test concentration, two controls containing no biomass were prepared. Both were sampled at the start of the experiment to provide an initial aqueous metal concentration and at regular intervals during the experiment to document any changes in metal concentration as a result of sorption to the glass or precipitation.

4.12.4. Sorption Coefficient Studies

For the determination of sorption coefficients, batch experiments were conducted on individual test metals (Cd, Zn, Cu. Ni) for a range of concentrations from 10mgL^{-1} to 500mgL^{-1}. The experiments were performed in 50ml sorption vials using 40ml of metal solution. To each test vial, approximately 0.014g (dry weight equivalent) of sorbent was added and allowed to interact for 2 hours on roller beds (Stuart Scientific Roller/Mixer SRT2). Each test was performed in duplicate with a sample measured at regular intervals. At the end of the designated time interval, the sorption equilibrium process was interrupted, a 10ml sample aliquot extracted and the sample remnants discarded. The extracted sample was centrifuged (MSE Centaur 2) and the supernatant sampled and serially diluted in preparation for equilibrium metal analysis as previously described (section 4.12).

For each sorption concentration two control (metal solution devoid of biomass) vials were prepared. Both controls were sampled at the start of the experiment to

provide an initial aqueous metal concentration and at the designated intervals during the experiment to provide any indication of changes in metal concentration which could be attributed to sorption to the glass or precipitation.

The determined sorption data was applied to the mass balance (Equ. 4.4) to determine the amount of metal sorbed from solution then applied to the Langmuir and Freundlich models detailed in section 3.1. The model providing the best fit (least squared regression analysis) was then used to derive the coefficients of sorption.

4.12.5. Sorption Kinetic Studies

Biosorption equilibrium reactions are rapidly initiated and are driven by the affinity and binding mechanisms between the sorbent and sorbate. Kinetic investigations were performed over a 60 minute period with sample aliquots extracted at 15 minute intervals. Kinetic data was fitted to pseudo-first and second order equations summarised in section 3.3 and the model which best described the data used to determine the reaction rate.

Sorption kinetics experiments were conducted using 40 ml of a 125mgL^{-1} solution for each test metal in a 50ml sorption vial. To each vial approximately 0.017g (dry weight equivalent) of biomass was added and incubated for 1 hour. Aliquot samples were extracted at 15 minute intervals and prepared for metal analysis as described in section 4.12.1.

4.13. Heavy Metal Desorption Studies

Desorption experiments were performed to determine the potential reusability and longevity of the microbial sulphide biomass. Desorbing agents used on SRBs are numerous, covering the chemical groups of acid, mineral salts and chelating agents (section 2.4). A desorbing agent from each chemical group (Table 4.2) including distilled water was tested.

Desorbing Agent	pH / Concentration
Distilled Water	pH 6.7
Acetic Acid	pH 5.5 (0.1M)
Citrate Buffer	pH 5
EDTA	pH 8 (0.5M)

Table 4.2 Desorbing agents used for elution of bound metals from microbial sulphide biomass.

The desorbing capacity of each test agent was determined using a batch method similar to that employed for the sorption coefficient experiments (section 4.12.4), however metal sorbate solution concentrations was adjusted to 100mgL^{-1} and the volume of desorbing agent was reduced by half (20ml) to minimise the output volume produced (Figure 4.13).

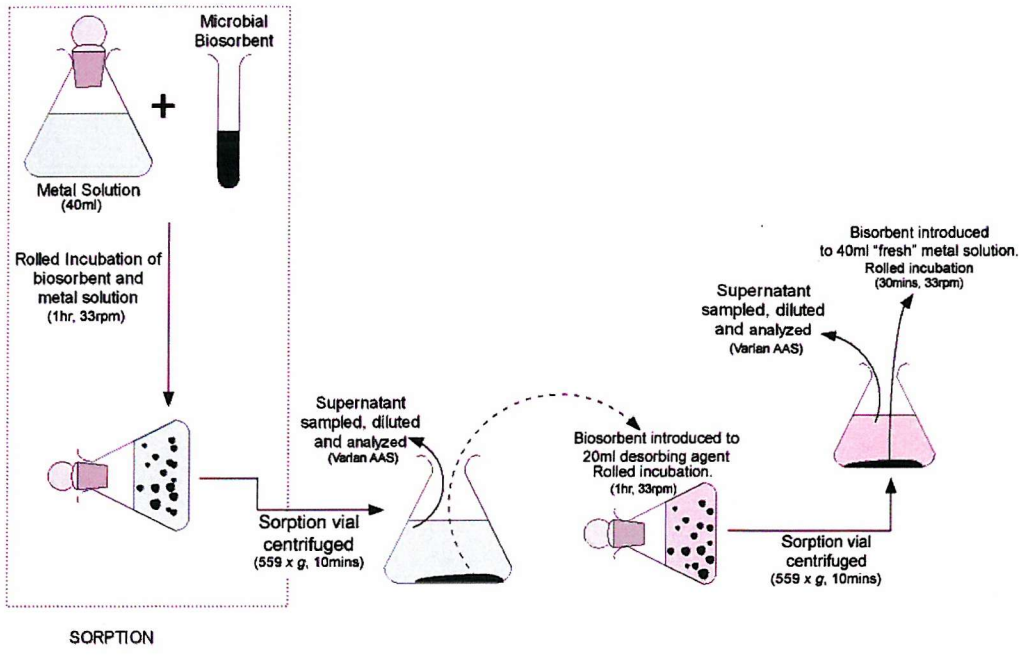

Figure 4.13 Schematic diagram detailing combined sorption and desorption experimental processes.

After 1 hour of undisturbed sorption and the attainment of an apparent sorption equilibrium (as determined from the susceptibility experiments section 4.10.3) the biomass was separated from suspension by centrifugation (MSE Centaur 2). The supernatant was sampled in duplicate for equilibrium concentration data. The separated biomass was introduced to the desorbing agent solution (20ml) and

allowed to interact for a period of 60 minutes. At the end of the allotted time, the solid and liquid phases were separated and the desorbing agent supernatant sampled in duplicate to determine the concentration of metal ion released into solution. A control desorbing agent sample (minus the biomass) was also prepared and sampled to measure any trace amounts of the test metal occurring naturally in the solution.

The desorbed biomass was then reapplied to 40 ml of a "fresh" 100mgl^{-1}metal solution. This second sorption stage was performed for 30 minutes, at the end of which the contents were centrifuged as previously done and the supernatant sampled for equilibrium metal concentrations.

A reference sorption/desorption experiment was conducted using identical test metal solutions to that described above and a synthetically produced iron monosulphide. The iron monosulphide was prepared as per Fossing and Jorgensen (1989). Ferrous iron (16.7g $FeSO_4.7H_2O$/100ml) and 14.4g $Na_2S.9H_2O$)/100ml) were mixed and the precipitated FeS washed with boiled anoxic distilled water to remove excess iron sulphide (Fossing and Jorgensen, 1989). This iron monosulphide is highly reactive and prone to rapid oxidation. Samples were therefore prepared fresh for each usage and used immediately once prepared

4.13.1. Data Analysis

As a reverse process of sorption, desorption data was quantified using a similar mass balance equation. The mass balance assumed that the increased presence of a metal ion in solution with time was as a result of the metal being released from its bound state on the biomass back into aqueous solution. All metal concentration increases were attributed solely to the eluting properties of the desorbing agent.

$Q_{des}= (C_b-C_{aq})/C_b \times (V/M)$

Where Q_{des} is the concentration of metal desorbed from the biomass, C_b is the concentration of bound metal, C_{aq} is the concentration of metal ions in solution, V is the volume of desorbing agent used, and M is the mass of biomass.

4.14. Effluent Sorption

Soprtion experiments conducted under laboratory conditions using pure water and only single metal samples give an idealistic approach to the sorption capacity of the tested biomass. Industrial and wastewater effluent often contain a mixture of metal species in addition to other suspended matter which may act synergistically or antagonistically with the biomass in the sequestration of the metal ion species.

In an attempt to determine the true sorptive capacity of the microbial biomass under commercial application conditions, untreated wastewater effluent was obtained from a municipal wastewater treatment plant in Devon, UK. Current UK legislation and guidelines prohibits the discharge of high concentrations of potentially toxic metals into municipal wastewater streams, thereby rendering the heavy metal concentrations void as the test metal species were in trace amounts and below the sensitivity of the analytical test machine (Varian AA200 flame spectrophotometer).

A synthetic commercial wastewater was prepared using the acquired wastewater sampled spiked with metal (Cd, Zn, Cu, Ni) stock solutions ($100mgL^{-1}$) to yield an effluent of uniform metal concentration of $12.5mgL^{-1}$. To 40ml of this spiked metal effluent approximately 0.02g (dry weight equivalent) of biomass was added and the mixture incubated on roller beds (Stuart Scientific Roller/Mixer SRT2) for 60 minutes. Aliquot samples were extracted at 15 minute intervals and prepared for metal concentration analysis as described previously (section 4.12.1).

Experimental controls containing no biomass were sampled in duplicate at 15 minute intervals to provide evidence of any metal losses from solution. Any such metal losses were primarily attributed to the presence of suspended solids in the effluent as other sorption control experiments using Milli-Q (Millipore) water showed no significant losses to the sorption vial or precipitation effects

Total suspended solids (TSS) within the wastewater sample (Equ. 4.6) were measured using the BSI standard methods (2005). 20mls of effluent was filtered through a pre-weighed 0.45um glass micro fibre filter paper. The filter was then dried at 60^0C overnight and cooled in a desiccator until a stable weight was attained.

$$SS = \frac{1000 \times (b - a)}{V} \qquad \text{(Equ. 4.6)}$$

Where SS is the content of suspended solids (mg/L), b is the final mass of the filter (mg), a is the mass of the filter before filtration (mg) and V is the volume of effluent sample used (ml)

A parallel experiment using a mixed metal solution of similar concentration ($12.5 mgL^{-1}$) was prepared using MilliQ (Millipore) water as the solvent. The experiment was operated under identical conditions to that of the spiked effluent sample to determine and quantify the effect of suspended solids on the sorptive capacity of the biomass.

Chapter 5.

RESULTS AND DISCUSSION: Development of a Highly Magnetic Iron Sulphide

This chapter details the sequence of experimental procedures used to achieve the development of a highly magnetic microbially produced iron sulphide. The reproducible culture of the highly magnetic sulphide product was achieved by studying the effect of varying the growth culture modes and growth medium composition on the magnetic yield. By experimenting with the growth culture modes, a time specific mixed culture cycle was developed whereby the desired highly magnetic results were produced. Concentration modifications to the reference growth medium were investigated and found to further improve the strength of the magnetic yield, as measured using the magnetic susceptibility balance, MSB-Auto, as previously described (Section 4.10.3). The effect of pH conditions within the bioreactor on the magnetic sulphide yield was also explored, as it was observed that when unregulated, peak magnetic sulphide production coincided with strongly alkaline (pH 8) conditions.

Section 5.1 discusses the progression of culture modes of the SRB, from batch, to continuous, to a mixed batch-continuous growth cycle. The resultant effects of the magnetic iron sulphide yield are outlined.

In section 5.2 the results of refining the relative concentrations of ferrous iron, Fe (II) to ferric iron, Fe (III) in the growth medium are presented. Finally section 5.3

explores the significance of pH conditions within the bioreactor and investigates whether the external regulation of pH conditions can be substituted for the devised mixed culture cycle.

5.1. Effect of culture conditions on the magnetic sulphide

5.1.1. Experimental Results for Culture Conditions

5.1.1.3. Batch culture

The results of the batch culturing experiments (described in section 4.6.1) are presented in Figure 5.1. The magnetic susceptibility of the marsh sediment when measured prior to inoculation averaged approximately $5.0x10^{-4}$ SI units.

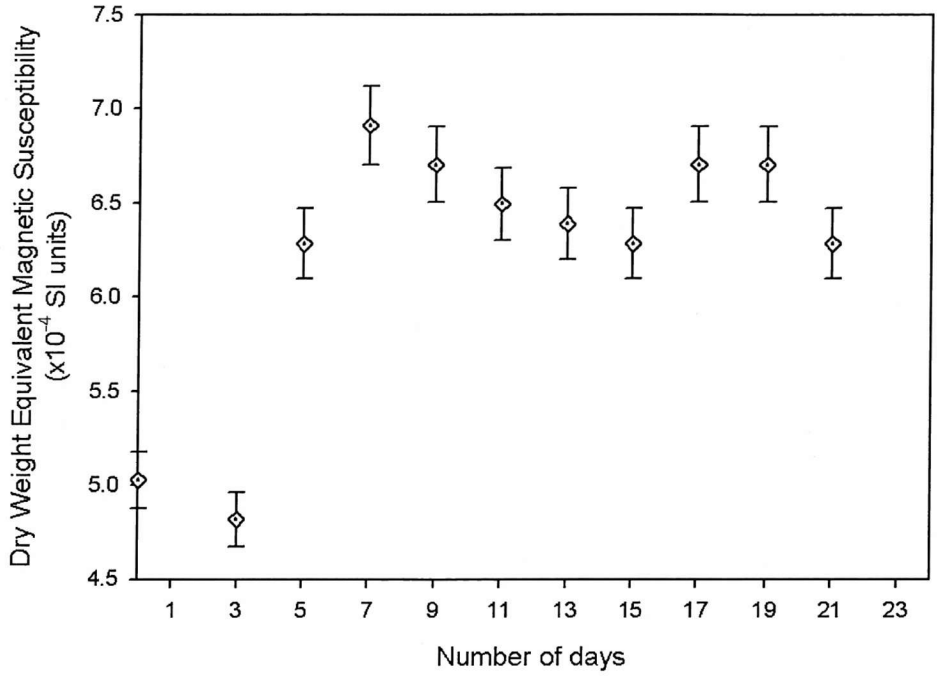

Figure 5.1 Measured magnetic susceptibility of the iron sulphide produced during batch culture.

Subsequent measurements of the sulphide, recorded on alternate days show an initial decrease in the susceptibility recorded. The magnetic susceptibility of the material then rapidly increases and fluctuates within the range of 6.2 -6.9 $x10^{-4}$ SI units. This increase was almost one and a half times that of the initial measured susceptibility; however when tested with a boron neodymium permanent magnet

the material showed little visible response to the applied 0.6T field on the face of the magnet.

5.1.1.4. Continuous culture

The continuous culture experiment undertaken comprised of 2 distinct stages (see section 4.6.2). In these, the effects of the inoculating sample on the resulting magnetic yield were investigated. The first stage of the experiments utilised a bacteria inoculum derived from unrefined salt marsh sediments and the second a magnetically refined inoculum from the salt marsh culture. The measured magnetic susceptibilities profiles are shown in Figure 5.2.

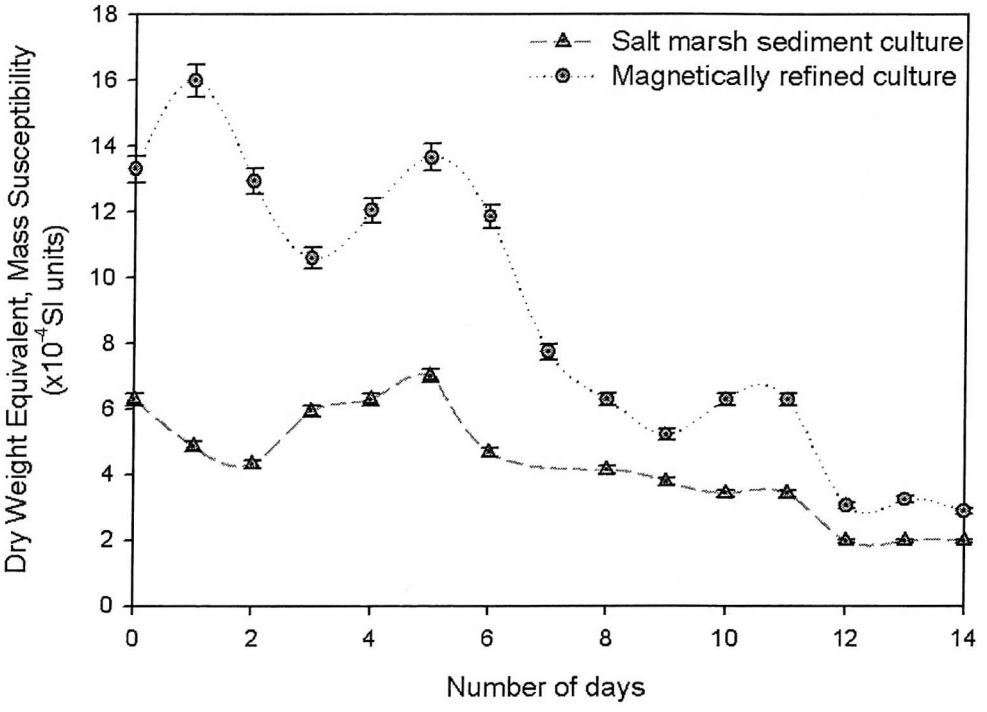

Figure 5.2 Magnetic susceptibility for iron sulphide produced using magnetically refined and unrefined inoculating cultures.

The unrefined culture was initially operated in batch to allow the bacterial population to establish and acclimatise, as immediate operation in continuous mode would result in the rapid dilution of a poorly established population. Within 5 days the bioreactor walls were opaque as a result of bacterial growth on the inner walls of the vessel and population enumeration indicated a ten fold

increase in bacterial density. Magnetic susceptibility measurements taken at end of the batch growth period averaged approximately $6.3x10^{-4}$ SI units.

Once switched into continuous culture at a dilution rate of $0.028hr^{-1}$, similar to that employed by Freke and Tate (1961) and that used by others (White and Gadd, 1996, Bahaj *et al.*, 1998b), the magnetic susceptibility was observed to initially decrease to $2.0x10^{-4}$SI units and then remain constant. A similar pattern in magnetic susceptibility was observed in the culture derived from the magnetically refined inoculum, however as a result of its selective culturing it maintained a consistently higher susceptibility, on average double that of the unrefined culture.

This observation was similar to that identified by Watson, and is what is believed to have instigated his feed-back chemostat design (Watson *et al.*, 1996), as the action of preferentially culturing the more magnetically producing species, should result in an increasingly highly magnetic yield. Later results however showed that the magnetic feed back process resulted in the production of large amounts of weakly paramagnetic material (Watson *et al.*, 1999).

5.1.1.5. Alternating batch-continuous culture

In this study a mixed batch-continuous culturing cycle using a magnetically refined inoculum as described in Section 4.6.3 was used to investigate the effects on an intermittent culturing cycle on the magnetic strength of the iron sulphide yield. A continuous culture bioreactor was also prepared using the same inoculum and served as a control against which all observed results were compared. Magnetic susceptibility measurements of the microbial iron sulphide from both bioreactors over a 60 day period are shown in Figure 5.3

During the period prior to the initiation of the mixed culture cycle, denoted as 'Day 0', both bioreactors were operated in continuous culture and were identical recording similar bacteria population numbers and a magnetic susceptibility value of $3.5x10^{-4}$ SI units.

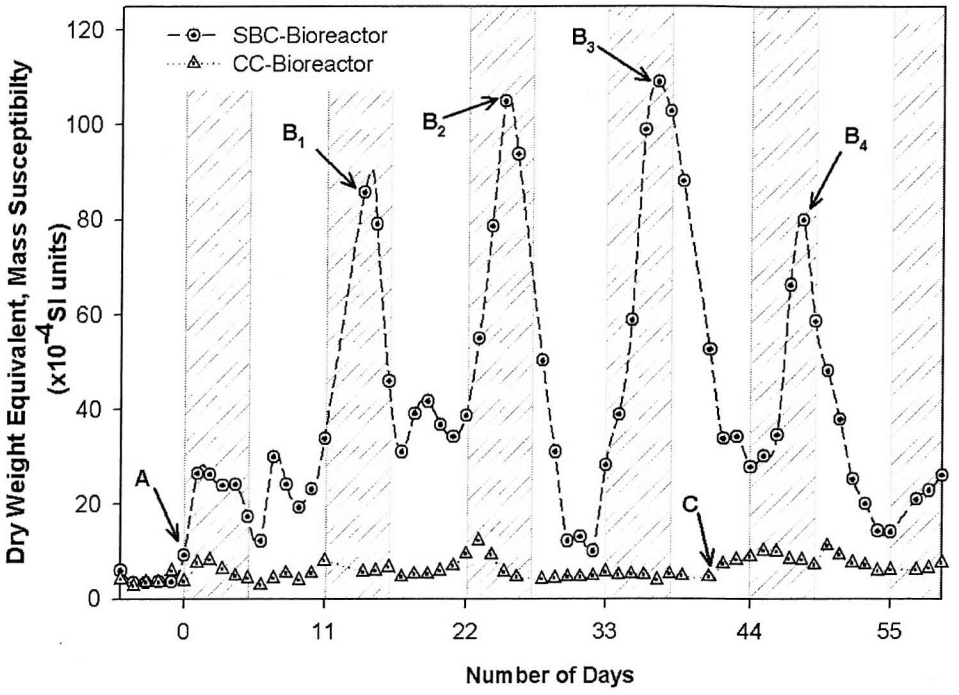

Figure 5.3: Magnetic Susceptibility of Fe_xS_y biosorbent produced by the Continuous Control (CC) and Switch Batch Continuous (SBC) Bioreactors: 'A' initial switch to batch of SBC bioreactor, B_1-B_4 peak susceptibility during batch culture phase, 'C' reduced dilution rate ($0.015hr^{-1}$) applied to CC bioreactor. Hatched areas batch mode cultivation.

The magnetic susceptibility of the iron sulphide from the control bioreactor in which a strict continuous culture (CC) was implemented remained consistently low, between $3x10^{-4}$ and $6x10^{-4}$ over the first 40 days of the test when the bioreactor was operated at a dilution rate of $0.028hr^{-1}$ (between 'A' and 'C' in Figure 5.3). These measurements are similar in magnitude to those recorded during the continuous culture experiments (section 5.1.1.4) and agree with published literature values for 'strongly magnetic iron sulphides' produced using the feedback chemostat method (Watson *et al.*, 2000).

The effect of lowering the dilution rate to $0.015hr^{-1}$ to coincide with the equivalent volume through-put of the bioreactor actively undergoing the mixed culture cycle, showed no significant increase (less than 5%) in the measured susceptibility. For the experimental duration (approximately 60 days) the bioreactor operating in switch-batch continuous (SBC) culture was observed to undergo 4 of the 11 day period culture cycles. The daily magnetic susceptibility measurements were

observed to rise when the culture was switched from continuous to batch mode. The peak magnetic susceptibility occurred between the third and fourth days of batch culture cycles (labelled B_1, B_2, B_3 and B_4) with the peak recorded magnetic susceptibilities averaging $95x10^{-4}$ SI units more than an order of magnitude higher than that quoted in previous studies (Watson and Ellwood, 1994). When returned to continuous culture mode an iron sulphide measuring a lower magnetic susceptibility was produced. Throughout the test period the magnetic susceptibility of the material produced by the SBC-bioreactor in continuous culture was consistently higher than that produced by the CC-bioreactor.

The internal pH of the CC and SBC-bioreactors was continually monitored with the aid of a K-series pH probe (ThermoRussel) attached to a DataTaker data logger (section 4.5.1). The pH measurement profile of the SBC-bioreactor for the duration of the experiment shows a definitive cyclic (11 day cycle) pattern that closely follows that of the magnetic susceptibility plot (Figure 5.4).

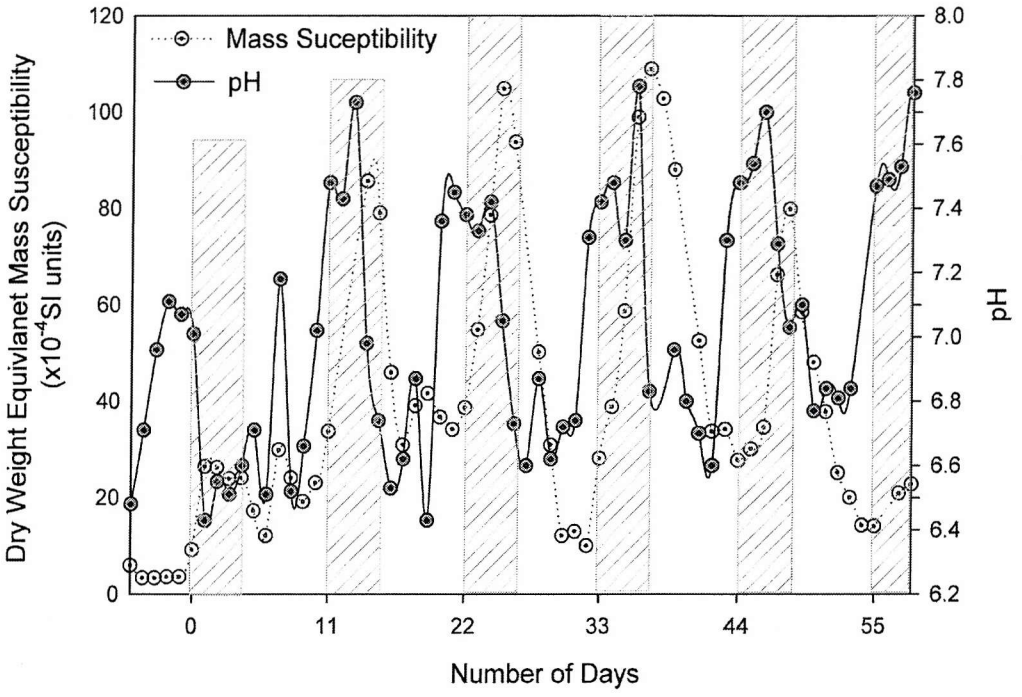

Figure 5.4 Comparison of magnetic susceptibility and pH response for switch-batch continuous (SBC) bioreactor. Hatched area signifies periods of batch culture.

The periods of highest pH (>7), for the SBC-bioreactor coincide with the batch phase of the culture period. This correlation is further addressed in section 5.3, but was presumed to be as a result of the bacteria altering the internal conditions of the reactor as a result of their metabolic processes and the production of carbonate ions (Equ. 2.1, section 2.1). During the days of continuous culture the regular influx of pH adjusted medium served to moderate the internal pH. In the case of the CC-bioreactor very little fluctuation is observed the pH due to the continual addition of medium.

Dissolved oxygen concentrations within the bioreactors as shown in Figure 5.5 was consistently maintained below 0.15mgL^{-1}. This result was obtained without the assistance of an artificially created external and internal environment and supports and confirms the theory that SRB are highly oxygen tolerant and are able to self regulate the conditions most suitable for their growth under the applied growth regimes.

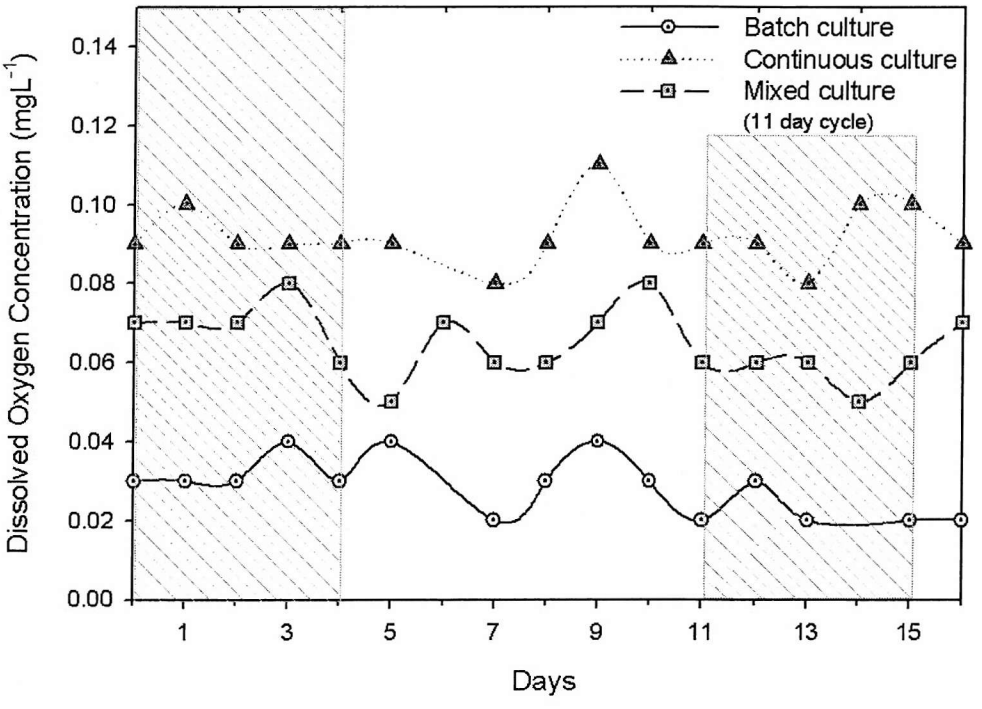

Figure 5.5 Dissolved oxygen concentrations within the bioreactors as a result of culturing conditions. Grey hatched area represents periods of batch culture during a mixed culture cycle.

Close examination of the graph also shows correlations between the pure batch, continuous cycles, and the mixed culture cycle. During pure batch and pure continuous culture cycles, the DO levels were measured at $0.03 \pm 0.01 mgL^{-1}$ and $0.10 \pm 0.01 mgL^{-1}$ respectively. During the mixed culture cycle, as was expected, the DO levels fluctuated within an intermediate range of $0.06\text{-}0.09 mgL^{-1}$, with lower DO concentrations generally being recorded during the period of batch culture.

The ability of SRB to create and maintain an anaerobic environment in the presence of the regular addition of an aerated growth medium is very significant and highly favourable for industrial development requirements as the need for a specially designed culturing environment and de-aerating medium pre-treatment is eliminated thereby reducing potential production costs.

5.1.2. Discussion and Summary of Findings for Effect of Culture Conditions on Magnetic Sulphide

The variation of culturing experiments revealed that under specific growth culture conditions a highly magnetic iron sulphide, Fe_xS_y, can be produced

5.1.2.6. Batch Culture

The batch culture experiments using fresh SRB rich salt marsh sediment diluted in a mixed iron growth medium Fe^{2+} [650ppm]: Fe^{3+} [150ppm] showed an initial decrease in the measured magnetic susceptibility of the material within the first 2 days of culture. This decrease is a reflection of the nature of the sample; as the initial measurement was that of the pure undiluted marsh sample. The pure marsh sediment has a high sand (silica) content which would contribute to the original magnetic reading. To alleviate the impact of the 'magnetic impurities' on the magnetic susceptibility of the produced sulphide, the culture was gently mixed prior to sampling to resuspend the sediments. The denser sand particles were observed to remain out of suspension and were therefore not included in the sample collected and magnetically tested. However, some fine grained sand particles were still included in the sample; but they are not considered to contribute as significantly to the measured magnetic susceptibility, thereby

making the readings subsequent to inoculation more representative of the produced iron sulphide.

The results obtained from the batch culture experiments showed an approximate doubling of its magnetic properties after 20 days of culture indicating that this mode of culture which is limited by the lifespan of the bacterial population and the finite amount of nutrients present in solution is capable of producing a magnetic iron sulphide. However the magnetic magnitude of the material was not sufficiently high enough to show an attractive response to an applied field of 0.5T; as produced by a permanent magnetic.

Bacterial enumeration during batch culturing (using epi-fluorescence, section 4.9.1) indicated a rapid growth response within the first 4 days of culture which was concurrent with conventional bacterial growth profiles. Population numbers however showed no apparent decline during the subsequent 10 days of culture. This result is in agreement with expectations outlined by White and Gadd (1996), as in the presence of a mixed culture the "life span" of the culture was prolonged due to the specific growth patterns of the constituent species in the growth culture. A decline in population numbers was observed after 2 weeks of culture. This observed decline is believed to be primarily as a result of reduced nutrient levels as opposed to the natural life span of the various bacterial species present.

5.1.2.7. Continuous Culture

Continuous culture is the growth mode most commonly cited in the literature as the means of maintaining a bacterial culture and producing a magnetic iron sulphide (Watson *et al.*, 1995). The continuous culture experiment undertaken comprised of 2 distinct stages (see section 4.6.2) conducted over 4 weeks using the same mixed iron growth medium (650mgL^{-1} [Fe^{2+}]: 150mgL^{-1} [Fe^{3+}]) at a dilution rate of 0.028hr^{-1}. In these, the effect of the inoculating sample on the resulting magnetic yield was investigated.

The bacterial culture was initially operated in batch to allow the bacterial population to establish and acclimatise. Results from the previous batch experiments (section 5.1.1.3) showed that incubation in batch conditions gave

rise to an increase in the magnetic susceptibility of culture. Once switch to continuous culture (denoted as 'day 0') an initial decrease was observed and presumed to be as a result of the diluting effect of the switch to continuous culture and the adjustment of the culture to the new growth conditions within the bioreactor. This decrease in magnetic susceptibility of the bioreactor contents was observed for approximately 12 days before stabilising. This measured decrease however was not linear as would be expected if the decrease was purely as a result of diluting effects which suggests that new magnetic material was consistently being produced, however equilibrium between the dilution effects and production of new material was not visibly achieved until 12 days into continuous culture.

Although the recorded susceptibility after 12 days of continuous culture was lower than that of the pure marsh sludge, and a third in magnitude to that produced during batch culture it is believed to be a more accurate measure of the iron sulphide properties, as the constant stirring and dilution would facilitate the removal of fine grained silicates and other magnetically oriented materials present in estuarine alluvium. Additionally, greater care was exercised when sampling to ensure that samples were not collected from the base of the bioreactor which would still contain the denser marsh sediments.

Whilst the magnetic separation and preferential culturing of bacteria was responsible for producing the magnetic material that is on average twice more magnetic than that produced by an unrefined inoculum, the magnitude of the magnetic susceptibility was still such that high magnetic fields (>1T) such as that used by Watson and others (Coe *et al.*, 1998, Watson *et al.*, 1999) would still be required for efficient recovery of the material.

5.1.2.8. Alternating Batch Continuous culture

Attempts by several researchers to reproduce the magnetic iron sulphide produced by Freke and Tate (1961) is well documented in the literature as cited in Section 2.3.3. The documented culture conditions were intended to be continuous in nature and appear to incorporate the weekends when the Freke and Tate bioreactors were turned off, in the operating dilution rate ($0.028hr^{-1}$)

(Watson *et al.*, 1995). The use of an intermittent culturing system (semi-continuous) as operated by Freke and Tate was attributed to being responsible for producing the highly magnetic material however this appears never to have been subsequently tested or documented.

The proposed culturing regime was comprised of 5 days of batch culture followed by 6 days of continuous culture at a dilution rate of $0.028hr^{-1}$ resulting in an overall dilution rate to $0.015hr^{-1}$. The results showed that the active switching of the bioreactor growth conditions from continuous to batch mode provided the appropriate conditions for the production of a highly magnetic microbial iron sulphide, which included the maintenance of an active bacterial population and nutrient supply. The most magnetic material was consistently produced during the batch growth phase and was on average 8 times more magnetic than that produced under continuous culture conditions and approximately an order of magnitude more magnetic than that of any other microbial iron sulphide documented within the literature (Watson and Ellwood, 1994). This magnetic sulphide was observed to be easily manipulated using a permanent magnet and could therefore be used in a low field biomagnetic separator powered by permanent magnets.

5.2. Varied Fe (II): Fe (III) ratio in Growth Medium

5.2.1. Experimental Results for effect of Iron Valency in Growth Medium on Magnetic Susceptibility

A dual phased programme was devised to determine the effect of the relative concentrations of ferrous to ferric iron in the growth medium on the magnetic susceptibility of the iron sulphide product. Figure 5.6 shows a schematic of the experimental design in which the relative concentration of the iron species was varied whiles maintaining the total iron concentration (Fe (II) + Fe (III)) at $800mgL^{-1}$, as used by Freke and Tate (1961).

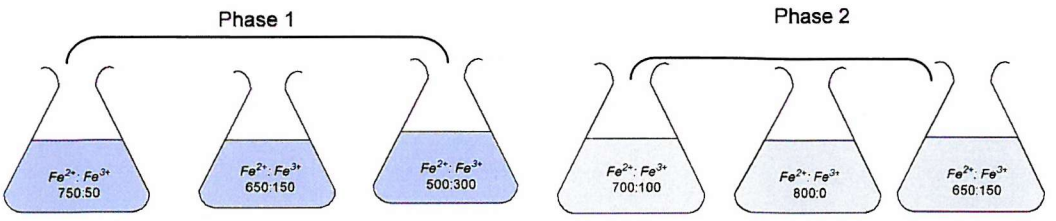

Figure 5.6 Schematic diagrams showing the 2 culture phases investigated (a) shows the relative concentrations (mg/L) initially employed relative to the reference concentration and (b) shows the refined concentrations attempted at the far extreme levels.

As previous, the contents of an established control bioreactor operating using the modified Postgate medium was divided and used as the inoculum. The newly inoculated bioreactors were allowed time to establish, and then operated in continuous culture using the standard reference medium at a dilution rate of $0.028hr^{-1}$ until the magnetic yields were similar ($3.8x10^{-4}$ SI) and bacteria population were within 20%.

At the start of the experimental period, day '0' (denoted as 'A' in Figure 5.7), the bioreactors were started in batch mode of the 11 day mixed culture cycle. After an initial 5 days of batch culture, the continuous cycle was started with each bioreactor using a different refined growth medium as detailed in Table 5.1Figure 5.6. The result of the medium effect on the magnetic susceptibility was therefore determined in the days subsequent to the first 11 day cycle. Magnetic susceptibility peaks are therefore quoted as averages of the second and third cycles.

Bioreactor	**Iron concentration (mg/L)** Fe^{2+}:Fe^{3+}
1	750:50
2 (ref)	650:150
3	500:300

Table 5.1 Relative iron species concentration used in medium for phase 1 experiment.

As observed in previous experiments using the semi-continuous culture cycle the daily log of magnetic susceptibility showed a cyclic pattern with an increase in magnetic yield strength during batch culture with peak susceptibilities; B_1-B_3, C_1-C_3 and D_1-D_3; being recorded at or near to day 5, the end of batch. Once returned to continuous culture, the magnetic susceptibility gradually decreased.

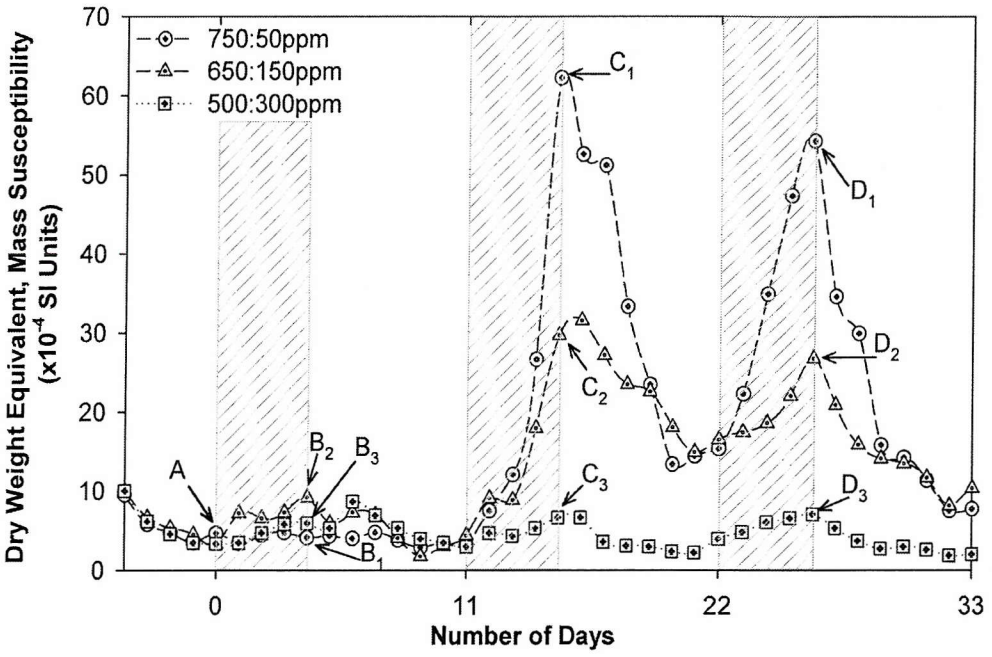

Figure 5.7 : Magnetic susceptibility of Fe_xS_y biosorbent produced during phase 1 of the varied Fe (II): Fe (III) ratio in the growth medium. 'A' denotes the beginning of the varied feed experiment. Prior to 'A' all three reactors were run using the reference medium 650:150ppm [Fe^{2+}:Fe^{3+}]. 'B_1-B_3', 'C_1-C_3' and 'D_1-D_3'are peak susceptibilities recorded during the batch culture phase for each applied growth medium.

Bioreactor 3, being cultured on a higher ferric iron concentration than the other active cultures, 500 (Fe^{2+}) : 300 (Fe^{3+}) mgL^{-1} recorded the least change between the batch and continuous culture stages with the peak recorded susceptibilities averaging $7x10^{-4}$ SI, less than double the initial recorded susceptibility.

The magnetic iron sulphide produced using the ferrous rich growth medium 750 (Fe^{2+}) : 50 (Fe^{3+}) mgL^{-1} recorded an average peak susceptibility of $58x10^{-4}$ SI, approximately 8 times more magnetic than that produced in bioreactor 1 and double that of the reference 650:150 culture in bioreactor 2.

The second phase of experiments focussed on refining the ferrous rich medium concentrations (Table 5.2) as it was shown that increased ferric concentrations had a negative effect of the magnetic properties of the iron sulphide yield.

Bioreactor	Iron concentration (mg/L) Fe^{2+}:Fe^{3+}
1 (ref)	650:150
2	700:100
3	800:0

Table 5.2 Iron concentrations used in phase 2 experiments

As previous, the bacterial inoculum to be used was obtained from the existing reference concentration culture, sub cultured and distributed equally between the new bioreactors. Further subculturing of the population was expected to have some deleterious effects to the magnetic susceptibility of the iron sulphide produced

Similar to other results in which the modified medium was introduced six days into the first 11 day mixed culture cycle, the effect on the magnetic susceptibility was not evident until the start of the second 11 day cycle. Magnetic susceptibility peaks were quoted as averages of the second and third cycles (labelled E_1-E_3 and F_1-F_3 in Figure 5.8)

Bioreactors 2 and 3 exhibited similar averaged peak susceptibilities of 2.64×10^{-4} and 2.60×10^{-4} SI units respectively during the 11 day cycles (Figure 5.8). These measured susceptibilities were less than half that of reference concentration, 650:150 mgL^{-1}, at an average peak value of 6×10^{-4} SI units, indicating that the total absence of ferric iron, and the experimental ratio of 7:1 Fe(II): Fe(III) both reduced the magnetic susceptibility of the iron sulphide produced.

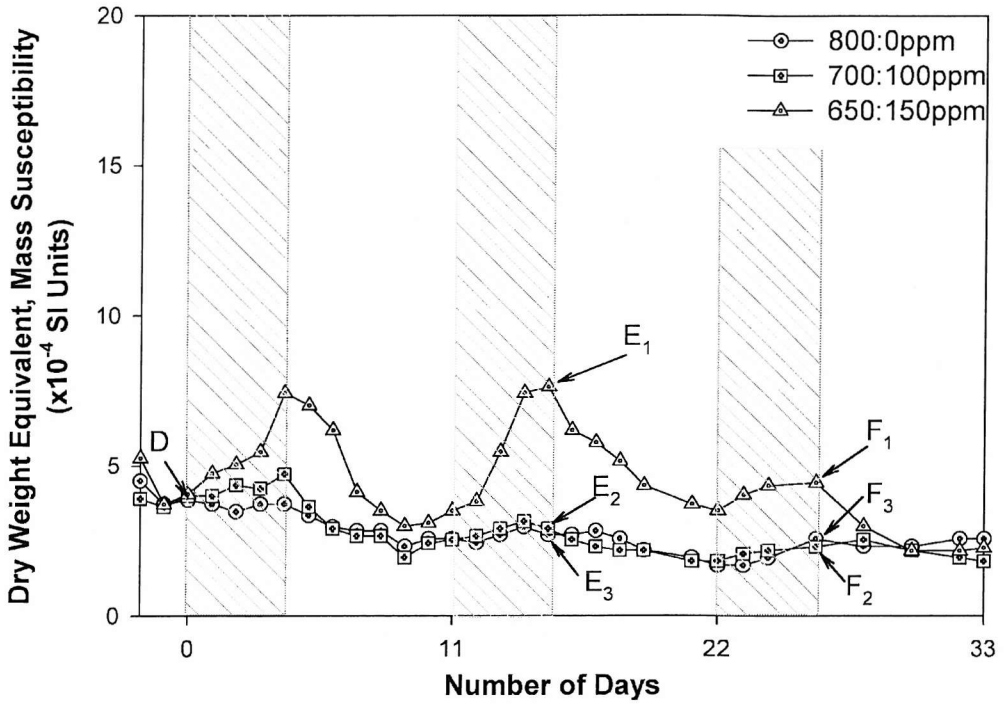

Figure 5.8 Magnetic susceptibility of Fe_xS_y biosorbent produced during phase 2 of the varied Fe (II): Fe (III) ratio in the growth medium. 'D' denotes the beginning of the varied feed experiment. Prior to 'D' all three reactors were run using the reference medium 650:150ppm [Fe^{2+}:Fe^{3+}]. 'E_1-E_3'and 'F_1-F_3'are peaks used to calculate the averaged peak susceptibility recorded during batch culture phase for each applied growth medium.

5.2.2. Discussion and Summary of Findings for Iron Valency in Growth Medium on Magnetic Iron sulphide

The standard growth medium (detailed in section 4.4) which was used for culturing purposes was a modification of Postgate's medium C (Postgate, 1979) by incorporating iron concentration used by Freke and Tate (1961) during the experiment in which the magnetic iron sulphide was first observed. Similar media modifications although not clearly specified have been previously used in attempts to produce the magnetic bacterial iron sulphide (Watson *et al.*, 1995, Bahaj *et al.*, 1998b, Watson *et al.*, 2000). The use and reduction of ferric iron to the ferrous species by SRB's is well documented (Coleman *et al.*, 1993), however the significance of the relative concentrations of the iron species present in the growth medium on the magnetic yield was unknown.

The experiments which investigated the refining of the growth medium by altering the relative concentrations of Fe (II): Fe (III) showed that the initial test medium (Fe^{2+} [650 mgL^{-1}]: Fe^{3+} [150 mgL^{-1}]) could be further refined to produce a more magnetic material.

The average peak magnetic susceptibility measurements for the reference culture in both phases of the experiment showed a significant decrease in relation to previously recorded measurements. This variation was expected and was attributed to natural variation as a result of using a mixed bacterial culture and the sub culturing process. Given that the operating bioreactors were subcultured from the same stock, and were identical prior to the application of the medium variation, comparisons of magnitude could be normalised relative to the specific reference control bioreactor. Comparisons across experiments were therefore restricted to trends.

Of the medium concentrations tested relative to their respective reference control, it was shown that ferric iron (Fe^{3+}) was essential in the production of a highly magnetic sulphide. When Fe^{3+} was absent from the medium (800:0), a decrease in magnetic susceptibility was measured. In high concentrations as shown by the 500:300 medium, ferric iron also decreased the magnetic strength of the sulphide yield.

An optimum concentration for producing a highly magnetic iron sulphide was achieved using the 750:50 (15:1 empirical ratio) medium. At this low concentration, ferric iron appears to act primarily as a promoter as under reducing conditions ferric iron is converted to the ferrous species.

5.3. Effect of pH on Magnetic Iron Sulphide

Previous observations of pH during a "regular" 11 day culture showed a cyclic pattern with high pH values (~pH 8) coinciding with batch culture and a reduction in pH (~pH 6.7) as a result of the introduction of pH adjusted growth medium during continuous culture (Figure 5.4).

The effects of external pH moderation on the magnetic susceptibility of the microbially generated iron sulphide throughout the 11 day culture cycle (section 4.8) was conducted by (i) restricting the internal pH within the range of pH 6.5-7.5 throughout an 11 day mixed culture cycle and (ii) implementing strict continuous culture whilst simulating pH conditions identical to that observed during batch culture (Table 5.3).

Culture mode	pH conditions
11 day mixed culture cycle (5 days batch, 6 days continuous)	Restricted within range pH 6.5-7.5
Continuous culture (dilution rate 0.015hr^{-1})	Simulated 11 day cycle (6 days pH 6.5- 7.5, 5 days pH 8)

Table 5.3 Culturing mode and induced pH environment

The experimental results for the effect of external pH regulation are shown in Figure 5.9 and Figure 5.10.

Maintaining pH conditions within the range pH 6.5-7.5 throughout an 11- day cycle (starting from point A - day 0 as shown in Figure 5.9), resulted in the magnetic susceptibility of the material produced remaining consistently low and showing no variation between batch and continuous culture modes. The control bioreactor which was pH regulated (~pH 6.7) during continuous culture and then allowed to self-regulate under bacterially produced conditions showed an increase in pH conditions during batch culture which also coincided with an higher magnetic susceptibility yield of the material produced. Once returned to continuous culture and a lower pH, the magnetic susceptibility of the produced sulphide was also observed to decrease.

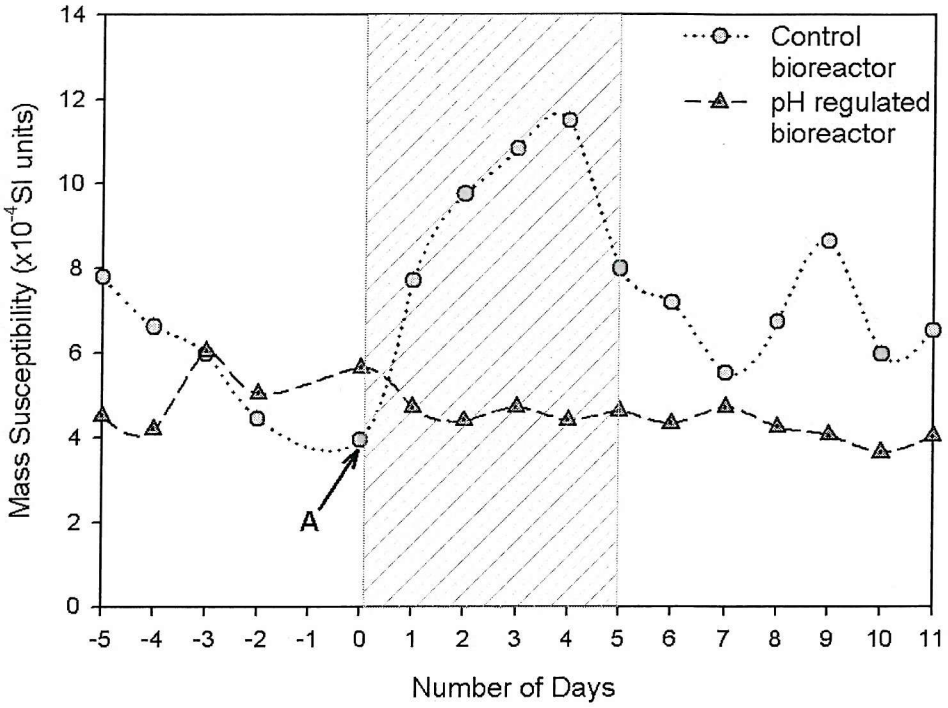

Figure 5.9 pH regulating effect on the mass susceptibility of microbially produced iron sulphide. The regulated bioreactor maintain between pH 6.5-7.5 for an 11 day mixed culture cycle starting from point A. The grey hatched area represents the 5 batch culture period for the control bioreactor under going unregulated 11 day mixed culture cycle.

When the bioreactor was operated in strict continuous culture and a dilution rate of 0.015hr^{-1} with internal pH conditions simulating the cyclic pattern observed during a 11 day continuous culture (see Table 5.3 for details) the measured magnetic susceptibility also showed a cyclic pattern. During simulated continuous culture the magnetic susceptibility of the produced material was low and during simulated batch (Figure 5.10) a higher magnetic susceptibility was measured. The average peak susceptibility of the material produced during simulated batch was 6.2 x10^{-4} SI, approximately double that produced during simulated continuous culture.

Relative to the control vessel undergoing unregulated 11 day culture, the simulated culture peak magnetic yield was approximately 75% in magnitude.

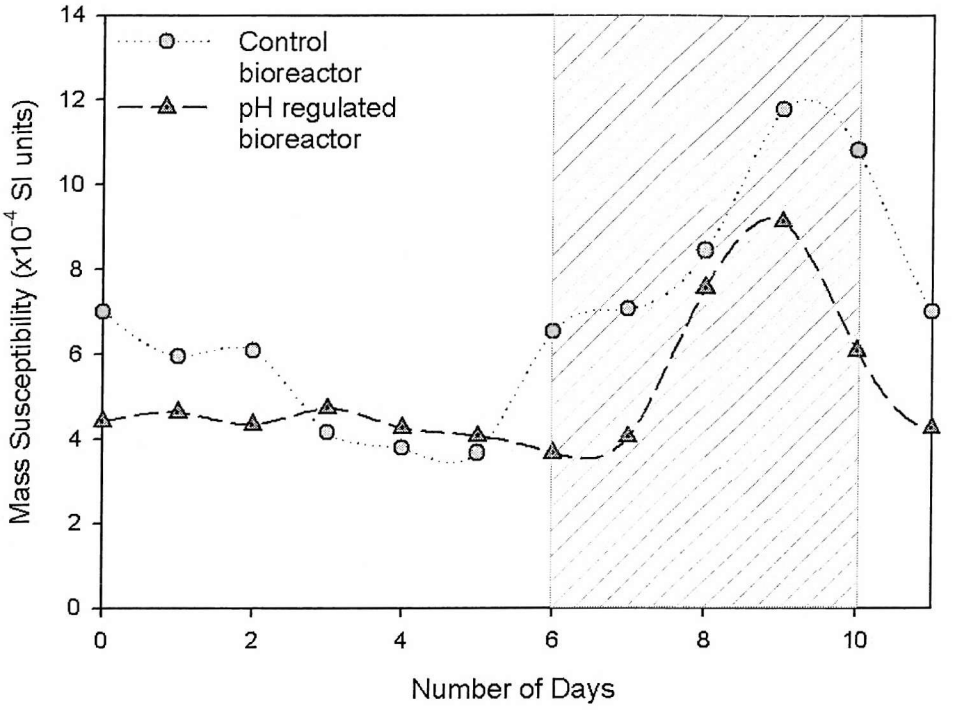

Figure 5.10 pH regulating effect on mass susceptibility of mircobially produced iron sulphide. Regulated bioreactor operated at a reduced dilution rate of 0.015hr^{-1} and pH manipulated between pH6.5-7.5 during continuous culture and pH8-8.5 during batch culture (grey hatched area).

5.3.1. Discussion and Summary of Findings for Effects of Culturing pH on Magnetic Iron Sulphide

The experimental results for the effect of culturing pH on the magnetic susceptibility of the iron sulphide reveal a partial dependence of the magnitude of the magnetic yield on the pH conditions. Restricting the bioreactor conditions to almost neutral pH (pH 7), the formation of a highly magnetic iron sulphide was not observed. Instead only a weakly magnetic sulphide of similar magnitude to that produced during the continuous culture phase of the control bioreactor was observed. This observation is possibly as a result of a low concentration sulphide ions (HS^-) in solution as under these pH conditions the most prevalent form is the protonated state (H_2S) and as previously discussed (section 2.1) is the form in which sulphide has been shown to have negative effects on the bacterial activity (Utgikar *et al.*, 2002).

Strongly alkaline conditions (>pH8), which are produced by the bacteria during metabolism appears to be integral to the production of a highly magnetic iron sulphide. Under these conditions, the hydrogen sulphide produced dissociates into its reactive ions, which in addition to not compromising bacterial activity can readily interact and bind with other ionic species present in solution

Artificially regulation of the bioreactor pH conditions to simulate that produced by the control bioreactor resulted in a similar magnetic susceptibility trend with peak yields being obtained during batch culture conditions. However, the magnitude of the yield was less than that obtained by the control bioreactor. Most noticeable in the results (Figure 5.10) was the magnetic response profile. The response of the chemically regulated bioreactor was almost instantaneous which can be attributed primarily to a chemical reaction in which the rapid introduction of the pH adjusting agents facilitated the formation of magnetic iron sulphide and the biological reaction occurred to a latter extent. This reaction would therefore be expected to be highly reproducible due to its chemically driven reactions.

The control bioreactor however showed a slower response to the change in batch culture conditions as the internal bioreactor conditions were controlled by the bacterial processes, which would therefore not have an instantaneous response. As was observed in previous experiments (section 5.2) the magnitude of magnetic response of sulphide produced varied with the culturing conditions and bacterial population. In comparison to other magnetic yields the measurements recorded herein was comparatively low, despite being greater than that attained during chemically regulated conditions. It is therefore fair to surmise that this observed difference in magnetic yield does not give a true appreciation of the effect of artificial regulation on the magnetic yield. However, these results are sufficient to conclude that although magnetic sulphide can be produced by regulating the pH conditions of the cultured bacteria, the magnitude of the magnetic susceptibility is lower than that produced when the culturing system is not externally regulated through the entire culture cycle. Additionally, with regard to applications beyond the laboratory context, the added costs which would be incurred from the need to constantly regulate the culturing pH could make the process less favourable.

..

Chapter 6.

RESULTS AND DISCUSSION: Characterization of the Highly Magnetic Iron Sulphide

Samples of the microbially produced iron sulphide were collected from the bioreactor over a period of 3 peak cycles and were prepared for characterisation using the methods described in chapter 3. The surface morphology of the material is discussed in section 6.1, and the particle density in section 6.2. The saturation magnetisation (section6.3) and elemental content as it relates to the relative composition of iron to sulphide is characterised in section 6.4

6.1. Surface Morphology

SEM measurements (section 4.10.2) were used to establish the shape, size and morphology of the biogenically produced iron sulphide. The shape and size of the iron sulphide particles were observed to be highly irregular and varied with particles ranging from 0.4μm coccooidal shapes to 5μm flakes (Figure 6.1a).

The particles possess a random dipole moment (Bahaj *et al.*, 1998b) and as such exert van der Waals forces which give rise to clustering and the agglomeration of the particles (see Figure 4.9).

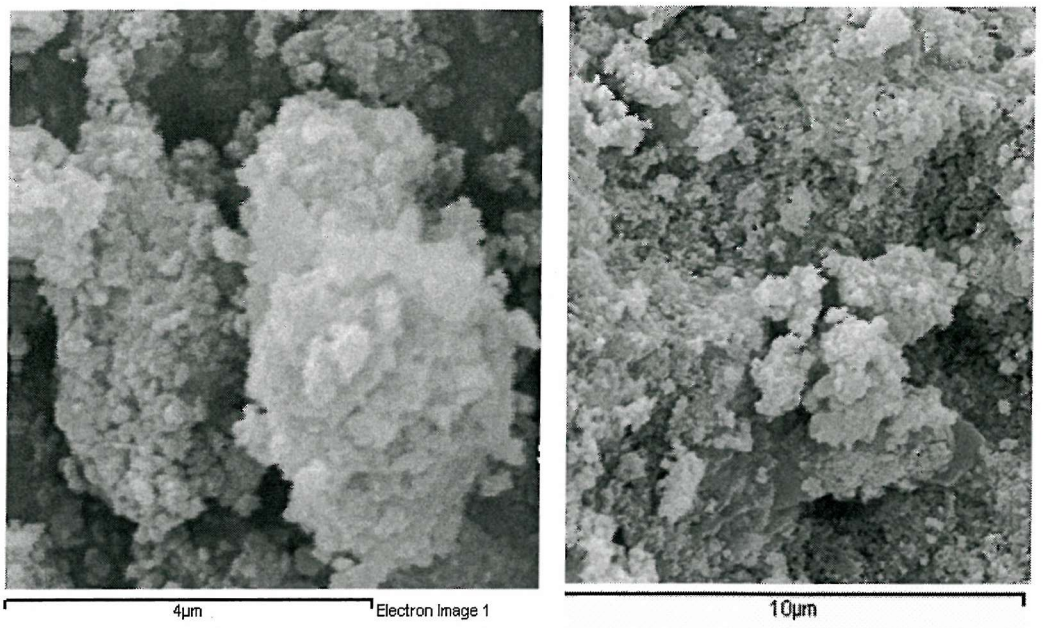

(a) (b)

Figure 6.1- SEM plates of microbially produced iron sulphide. (a) Sulphide particles deposited on bacteria surface and (b) vesicular nature of sulphide

6.2. Density

Particle density measurements were conducted on microbial iron sulphide samples using the BSI method (1990) outline in section 4.10.1. As shown in Table 6.1the averaged calculated density of the iron sulphide material in the bioreactors was within the range of 2.5 - 3.12mgm^{-3}. These results however do not correspond to known densities of magnetic iron sulphides (Table 6.1).

Iron Sulphide density (gcm^{-3})		**Reference**	**Measured sample density**	
Pyrrhotite	~ 4.6	(Rietmeijer, 2002)	*raw*	*corrected*
Mackinawite	~ 4.2	(Wolthers *et al.*, 2003)	3.039	5.810
Greigite	~ 4.1	(Tauxe, 2002)	3.144	3.647
Marcasite	~ 4.9	(Huggins, 1922)	2.526	4.668
Pyrite	~5.0	(Vallentyne, 1963)	2.540	4.691

Table 6.1 Measured density of microbially produced iron sulphide and known iron sulphide species.

The microbial sulphide samples, when treated with hydrogen peroxide to digest any organic matter present showed an average reduction of 23% in the sample mass.

6.3. Saturation Magnetisation

The magnetic saturation properties of 6 bacterially produced iron sulphide samples were measured, producing hysteresis loops (section 4.10.4). These loops are a measure of the magnetic response of a material to an applied field and are commonly used in rock and paleomagnetic studies to assist in the identification of minerals. The response of a material is strongly dependant on its mineralogy and physical properties with the presence of impurities adding distortion to the loop (Tauxe, 2002).

The hysteresis loops measured at room temperature for the 6 bacterial samples taken at different times during the 11 day culture cycles show a distinct trend in magnetic response. At an applied field of approximately 0.18T, the batch samples, day 2 to day 4, reached magnetic saturation, resulting in a linear response at higher magnetic fields (Figure 6.2). The gradient of the linear response for the batch samples progressively increased indicating an increase in the bulk magnetic susceptibility of the material. The averaged calculated magnetic susceptibility of the batch samples as shown in Table 6.2 is approximately 41×10^{-4} SI units, ten times more magnetic than that of material previously produced (Watson *et al.*, 2000).

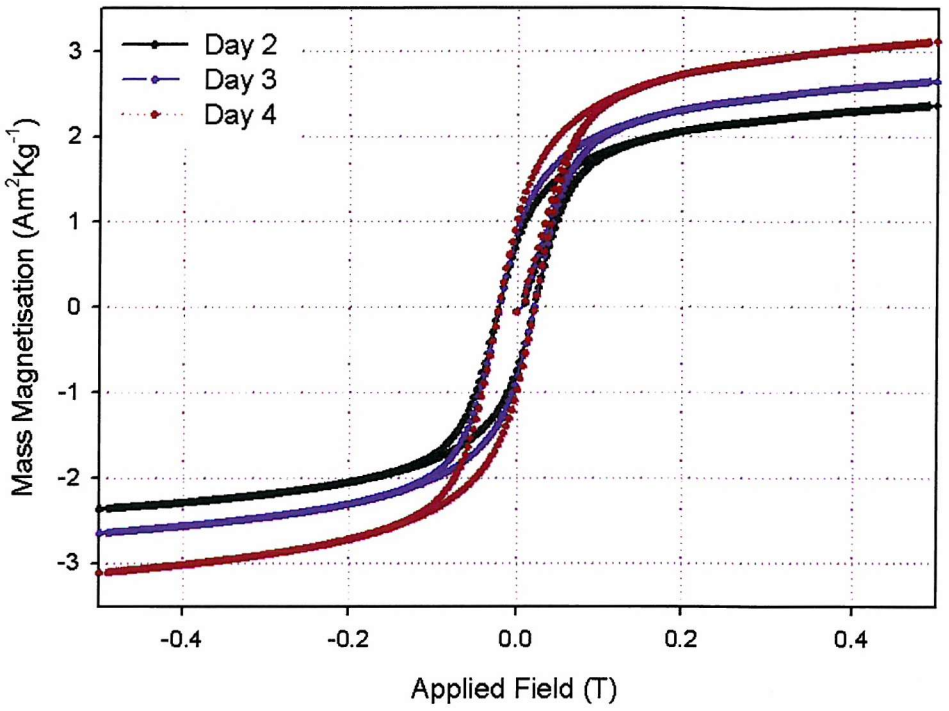

Figure 6.2 Saturation magnetisation response of batch samples isolated at day 2, 3 and 4 over an applied field of -0.5-0.5 T

At zero applied field a remnant magnetisation of $0.8Am^2Kg^{-1}$ was recorded for each of the 3 batch samples indicating that the tested material consisted in part, of permanently magnetized (ferromagnetic) material Figure 6.2).

	Samples					
	Batch Culture			*Continuous Culture*		
	D2	*D3*	*D4*	*D7*	*D9*	*D11*
M_0 (Am^2Kg^{-1})	1.95	2.15	2.55	0.35	0.25	0.15
Magnetic Susceptibility (χ) ($x10^{-4}$)	35.5	41.4	47.3	11.8	11.8	5.9

Table 6.2 Calculated magnetic susceptibility for microbial iron sulphides

The hysteresis loops for the continuous culture samples, days 7, 9 and 11, show saturation being attained at 0.1T (Figure 6.3). Almost no magnetization was

demonstrated at zero applied field indicating the absence of ferromagnetic properties.

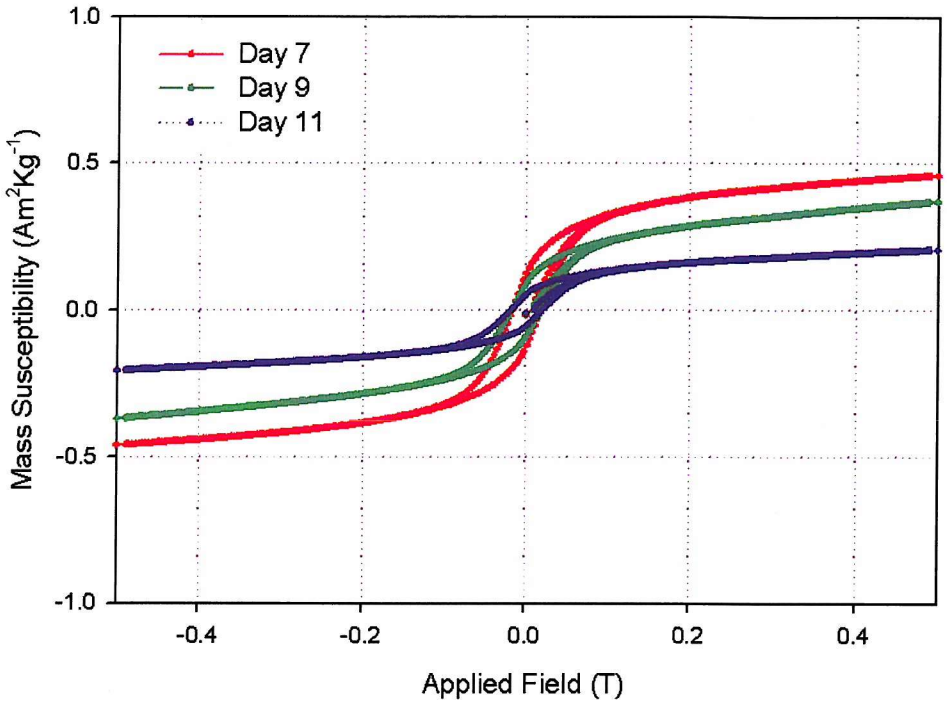

Figure 6.3 Hysteresis curves produced for a selection of continuous culture samples at an applied field of -0.5-0.5 T

6.4. Mineral Composition

Powder x-ray diffraction (section 4.11.1) was used as a qualitative procedure to determine the mineral composition of the highly magnetic microbial sulphide. The selected samples were irradiated using a cobalt source and produced diffraction spectra with 3 definitive mineral peak positions (Figure 6.4). Of the produced peak positions, 2 displayed narrow peaks with high intensities indicative of a crystalline structure and were readily identified as vivianite ($Fe_3(PO_4)_2$ $8H_2O$) and elemental sulphur (S^o). The third peak was not characteristed by the software being used in this study. This result was unexpected as all other published works on microbially produced sulphides (Rickard, 1969, Watson *et al.*, 1995, Watson *et al.*, 2000, Watson *et al.*, 2005) included mackinawite, greigite and other iron oxides in their mineral composition, but not vivianite. The difference in mineral content could however be attributed to the culturing regime and environment, as

other authors have used pure culture cycles and sterile, artificially created, anaerobic environments.

Table 6.3 shows the relative composition of the elemental species identified during XRD, which were determined by dissolving the microbial sulphide and analysing the liberated sulphide and the resulting solution. As can be seen from the results, the molar composition of phosphate is two orders of magnitude less than sulphide which confirms the dominance of the sulphide structure and the absence of a blue colour which would indicate a high vivianite content.

Total Fe (mM)	**TRIS** (mM)	**AVS** (mM)	**Phosphate** (mM)
14	20	12	0.1
15	19	7	0.5
39	35	16	0.7
25	44	27	0.6

Table 6.3 Elemental content of microbial sulphide samples

The empirical structure of the iron sulphide determined from the AVS and total iron concentrations (Table 6.3) suggest a Fe:S ratio within the range 1: 0.4 to 1:1.08, which includes possible mackinawite and pyrrhotite structures. The accuracy of this ratio however is questionable as work by Rickard and Morse (2005) suggested that during the AVS dissolution process some CRS species can become soluble thereby giving an false value.

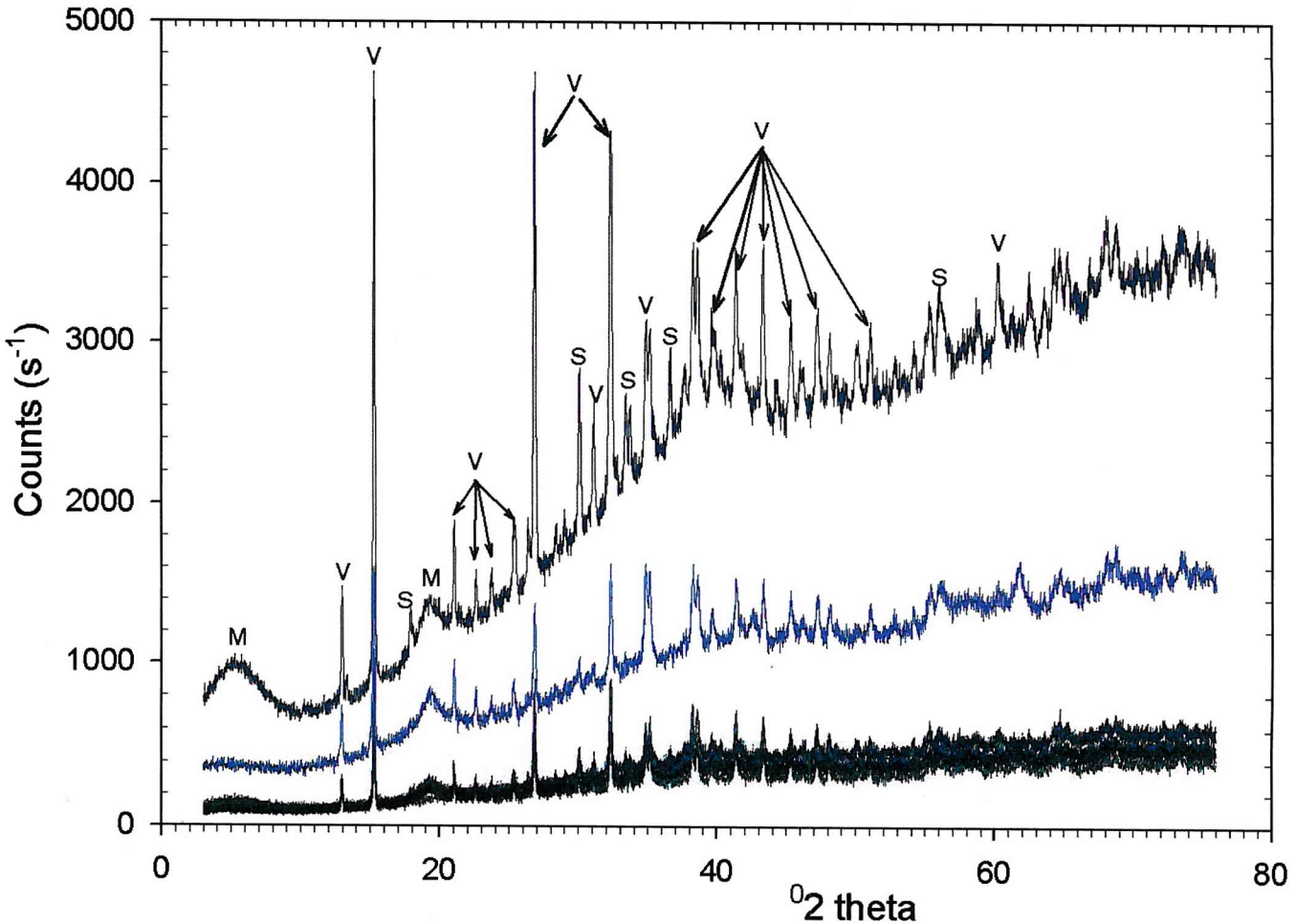

Figure 6.4 XRD diffraction spectra for microbially produced iron sulphide samples. Peaks are labelled with the identified minerals where (V) is vivianite, (S) is elemental sulphur and (M) is disordered mackinawite as identified by Wolthers et al (2003)

6.4.1. Discussion and Summary of Characterisation of FeS

The structure of the biologically produced iron sulphide was composed of fine grained particles which are deposited freely or as an extracellular coating on the bacteria. Bacterial metabolism is not hindered by this coating as its morphology is highly vesicular allowing the flow of nutrients (Figure 6.1b). This observed structure is similar to that reported by Watson and Ellwood (1994) and gives the material a high surface area to volume ratio, similar to that of activated charcoal (Watson *et al.*, 2000). Coe and Gerber (1998) later alluded to this vesicular structure being beneficial in metal adsorption as it provides physical vacuoles in which metal ions can be trapped.

The initial measured density of the microbially produced sulphide low and did not correlate with literature values for known magnetic iron sulphides. These low results were thought be attributable to structural and chemical alterations during the drying process which may have resulted in the partial oxidation of the material. Also the presence of chemical impurities in the sulphide which could be as a result of the environment of formation and the presence of bacterial material could help to influence the measurements. In a similar experiment Freke and Tate (1961) cited cellular inclusions and possible alterations of sulphide structure as plausible sources for the reduced values (Freke and Tate, 1961). Treatment with hydrogen peroxide to dissolve all organic matter within the sulphide product resulted in a change in mass which was translated into an increase (ranging from 1.5-1.8%) in the calculated particles densities. These corrected values although not identical were more closely correlated to published iron sulphide densities (Table 6.1).

Saturation magnetisation (hysteresis) loops are a measure of the magnetic response of a material to an applied field and are commonly used in rock and paleomagnetic studies to assist in the identification of minerals. The hysteresis loops for the continuous culture samples unlike the batch culture samples showed the no residual magnetisation (remnance) when the applied field was removed. This indicates that relative to the material produced during batch culture, the continuous samples consisted almost exclusively of paramagnetic particles and the batch samples are composed of some ferromagnetic material.

The calculated mass magnetic susceptibility for the continuous culture samples also showed a progressive decrease in magnitude as the duration of continuous culture was extended. This trend supports the theory that the dilution of the bioreactor contents removes dissolved H_2S from the system constantly and introduces more iron species into solution thereby maintaining a low relative concentration of iron to sulphide. This process acts to inhibit the formation of complex sulphides. Under batch culture conditions, no dilution occurs and H_2S in maintained in high concentrations thus facilitating the formation of complex sulphides with a high magnetic property.

The use of XRD to help determine the chemical composition of the sulpide reproduced similar results to that achieved by Davis (2000) while demonstrating competitive effects between sulphide and phosphate ions in an iron rich environment. It was found that under high sulphide conditions, the exclusive formation of iron sulphide occurred. In low sulphide environments iron sulphide was still preferentially formed, however iron phosphate was also present. The precipitated solid, similar to that produced microbially was completely black in colour which is indicative of a predominantly sulphidic composition as opposed to blue, which would be expected for a high vivianite composition. The produced XRD pattern did not reveal the presence of any form of iron sulphide, but showed 3 peaks positions, 2 of which matched vivianite and elemental sulphur with the third peak remaining undetermined (Davis, 2000).

Further examination of the diffraction spectra produced by the microbial sulphide sample showed a progressive elevation in the background profile (which was more evident in some samples than others). This feature is often indicative of a high amorphous content which could also explain the inability of the software to identify the third peak positions.

X-ray powder diffraction of synthetically produced disordered mackinawite as performed by Wolthers *et al* (2003) using a copper alpha source produced diffraction spectra patterns with intense peaks at around $4^0 2\theta$, $15^0 2\theta$, and $50^0 2\theta$. These peaks appear to coincide with the third unidentified peak position on the spectra produced by the microbial biomass. The apparent amorphous nature of the samples makes further identification very difficult and inconclusive.

From the cumulative results of the XRD and mineralogical composition it can therefore be inferred that the magnetic characteristics displayed by the microbially produced material can be attributed to a possible amorphous mackinawite structure.

Chapter 7.

RESULTS AND DISCUSSION: Sorption/Desorption Batch Results

This chapter details the results of the sorption/desorption experiments carried out using the highly magnetic microbially produced iron sulphide. The sulphide was applied to various test metal solutions to assess the feasibility of using the sulphide as a biosorbing agent.

Section 7.1**Error! Reference source not found.** explores the practicability of using the biomass as an effective biosorbent. The effect of the magnetic susceptibility of the biomass sample on its sorption capacity is presented (section 7.1.1). By experimenting with the metal ion concentrations, for a fixed mass of biosorbent, equilibrium sorption profiles (isotherms) were derived and applied to known models to help indicate the sorption process occurring and for determination of the coefficients of sorption (section 7.1.3). The microbial biosorbent was applied to single and binary metal solutions to determine rates of sorption and to investigate the occurrence of competition effects between metal ion species for binding sites on the biomass (section 7.1.5 & section 7.1.7).

Section 7.2 investigates the reusability of the biomass and explores the use of various desorbing agents. The resulting effect on the biomass structure and subsequent alterations in the sorption capacity is also determined.

In section 7.3, the efficiency of sorption of the microbial biomass is compared with a synthetic iron sulphide to evaluate the significance of the sorption potential of the microbial sulphide. Finally in section 7.4 the microbial biomass is applied to a wastewater sample and the effectiveness of the biomass to sorb metal ions from a commercial source is investigated.

7.1. Laboratory based Metal Sorption

7.1.1. Experimental Results for the Magnetic Susceptibility Effect on Sorption

Batch equilibrium sorption experiments were performed at controlled pH (5.5) and temperature (20±2°C) to determine the effect of the magnetic susceptibility on the sorption capacity of the microbial sorbate. This was evaluated using 2 distinct samples extracted at (i) peak and (ii) weakest susceptibility applied to cadmium metal solutions. The experimental conditions used are detailed in Table 7.1 below.

Experimental Parameters	**Conditions**
Initial concentration of Cd	$50mgL^{-1}$, $150mgL^{-1}$, $500mgL^{-1}$
Solution pH	5.5
Temperature	20±2°C
Mass of Biomass	18mg
Solution Volume	100ml
Biomass magnetic susceptibility	~$7x10^{-4}$ SI units (low), ~$98x10^{-4}$SI units (high)

Table 7.1 Experimental parameters used for magnetic susceptibility effects on sorption.

The concentration of aqueous cadmium metal ion was measured at regular intervals to determine the time required for sorption equilibrium to be attained within the closed system. Over the 2 hour test period, as shown in Figure 7.1 the measured cadmium concentration in the control vials ($50mgL^{-1}$, $150mgL^{-1}$ and $500mgL^{-1}$) containing no biosorbent was observed to fluctuate within 4%. This concentration variation was attributed to the precision of the spectrophotometer and indicated the absence of any significant losses to the reaction vessel. All

larger decreases in concentration in the vials containing biomass were therefore considered to be equivalent to the amount of metal ion sorbed from solution by the biosorbent.

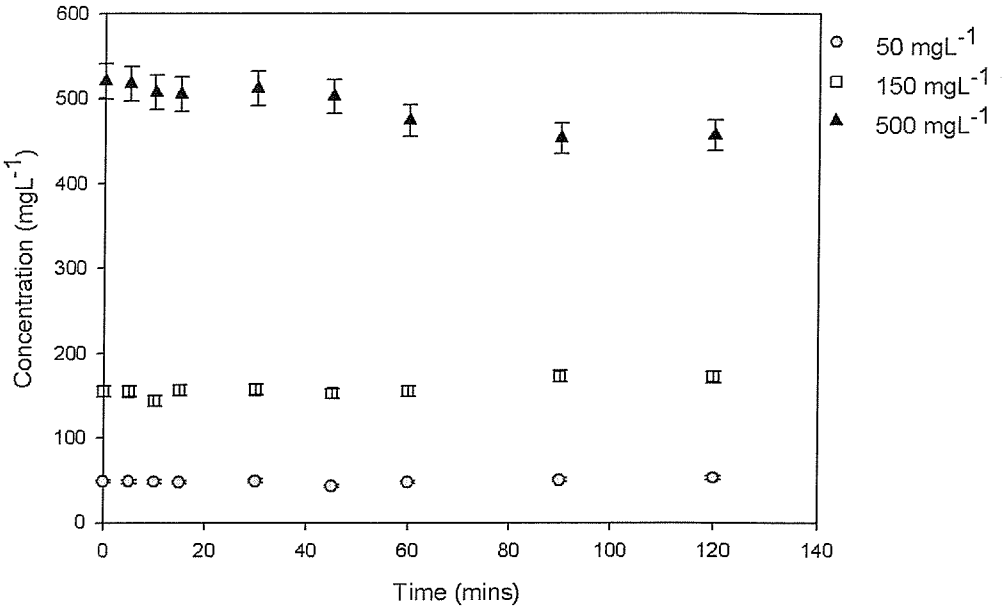

Figure 7.1 Cadmium concentration in control sorption vials (no biomass) for a 2 hours incubation period.

The percentage metal sorbed with respect to time for the sorption vials containing biomass is shown in Figure 7.2. For the tested concentrations and magnetic susceptibility of the biosorbent the sorption profiles showed a similar trend of rapid initial uptake followed by a gradual slowing to an equilibrium level irrespective of the initial metal concentration and the magnetic susceptibility of the biosorbent. The sorption process appears to have slowed significantly, tending towards equilibrium within the first 60 minutes of contact with the majority of the sorbed metal being acquired within the initial 10 to 20 minutes. One hour was therefore determined to be a sufficient time frame to be used to approximate equilibrium. Within the 2 hour test time, the amount of cadmium metal sorbed from solution by the weakly magnetic biomass decreased from 86% to 32% as the cadmium metal concentration increased (Figure 7.2). This correlates to an increase in sorption capacity from 0.23g to 0.91gCd per gram dry weight equivalent biomass. The highly magnetic biomass had an identical sorption

capacity of 0.23gCd/g biomass at the low initial metal concentration (50mgL^{-1}), which corresponds to an 82% reduction in Cd ion concentration.

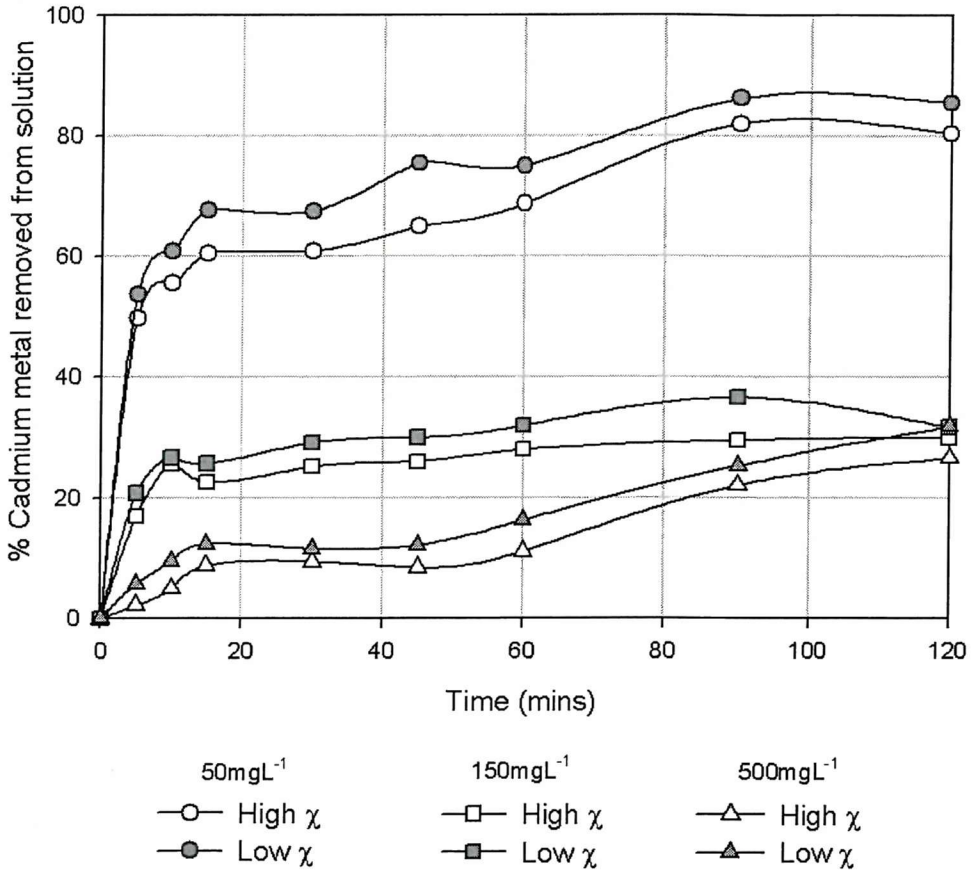

Figure 7.2 Percentage sorption of cadmium metal from 50, 150 and 500mgL^{-1} solutions using a microbial iron sulphide of high and low magnetic susceptibility.

At high metal concentrations; the percentage reduction of Cd in solution was only 26% which corresponds to a lower sorption capacity of 0.75gCd/g dry weight equivalent biomass, 7% less than that of the weakly magnetic biomass sample.

7.1.2. Discussion and Summary of Magnetic Susceptibility Effects on Sorption

The difference in the sorption capacity of the tested biomasses at the metal ion concentrations tested is indicative of a difference in the biomass structure. At low metal concentrations, identical sorption capacities, 0.23gCd/g and similar

removal percentages are achieved. This result is due to the ready availability of binding sites on which to sequester the metal ion species. At higher concentrations, the availability of binding sites on the weakly magnetic biomass appears to be more abundant and/or accessible, facilitating higher metal recovery than that achieved by the more magnetic biomass.

The outcome of the magnetic strength of the biomass on its efficiency as a sorbing agent appears to have an effect only at high metal concentrations. The significance of this effect however is generally low as the difference in sorption capacity between the tested low and high magnetic susceptibilities is less than 20%, whereas the measured difference in magnetic susceptibility of the samples used was approximately 93%. From the joint perspective of biosorption and magnetic recovery, the highly magnetic biomass, although having a lower sorption capacity at high metal concentrations offers a greater potential of low cost biomagnetic separation processing.

7.1.3. Experimental Results for Sorption Isotherms

The relationship between sorption capacity and equilibrium concentration was measured for a range of initial metal concentrations using the experimental parameters detailed in Table 7.2. The equilibrium concentration of aqueous metal ion was measured (in duplicate) after 2 hours of contact between the biomass and the metal ion solution. Langmuir and Freundlich sorption models were fitted to the data and least squared regression analysis performed (using SigmaPlot software) to evaluate the data fit to the models (Figure 7.3 and Figure 7.4).

Experimental Parameters	**Conditions**
Metal Species	Cd, Cu, Zn, Ni
Initial metal concentration	$10mgL^{-1}$, $50mgL^{-1}$, $100mgL^{-1}$, $200mgL^{-1}$, $500mgL^{-1}$
Solution pH	5.0 - 5.5
Temperature	20±2°C
Solution Volume	40ml
Mass of Biomass	14mg

Table 7.2 Experimental parameters used for determination of sorption isotherms

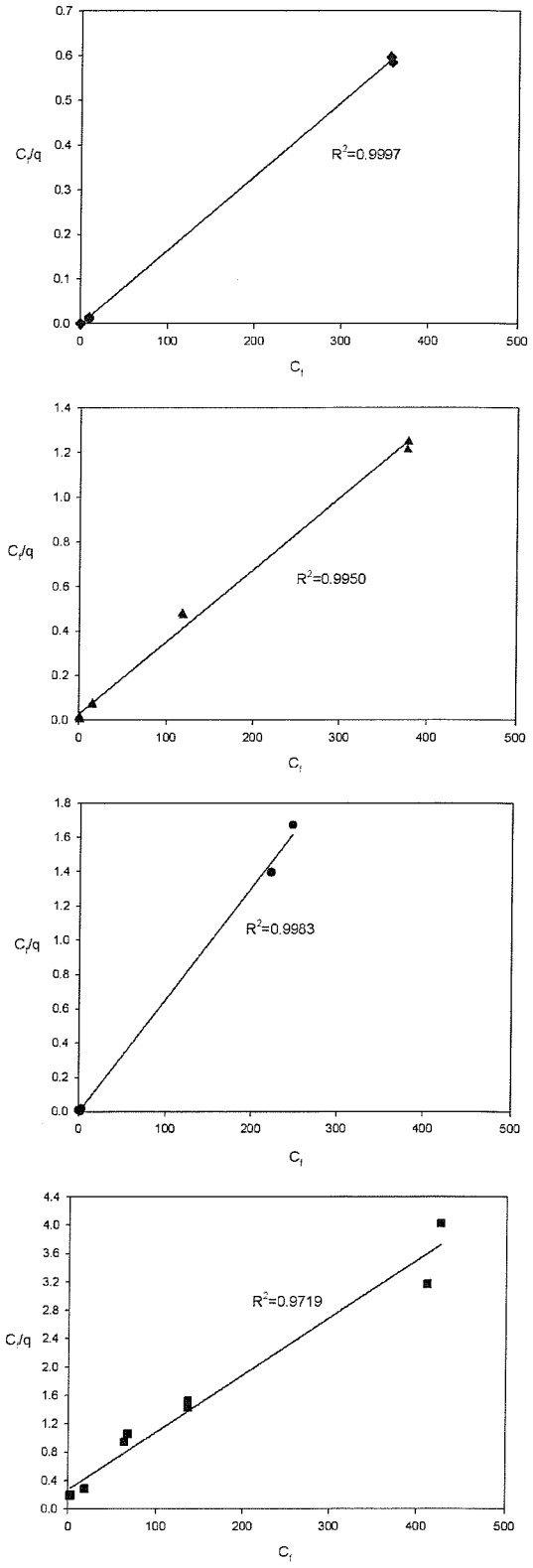

Figure 7.3 Linearised Langmuir sorption isotherms for (A) cadmium, (B) zinc (C) copper and (D) nickel by microbial iron sulphide

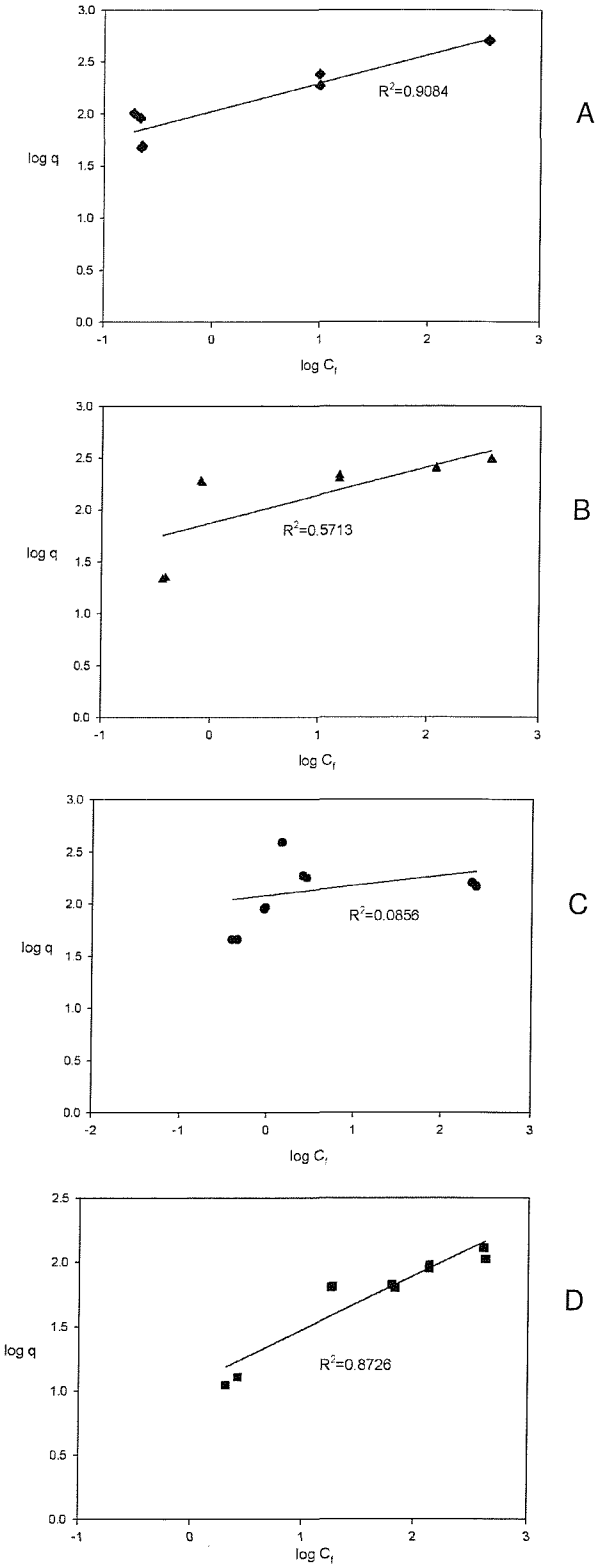

Figure 7.4 Linearised Freundlich isotherms for (A) cadmium, (B) zinc, (C) copper and (D) nickel by microbial iron sulphide.

Metal	*Q* (mg/g)	*b* (L/mg)	R^2
Cd	603	2.23	0.9997
Zn	308	0.11	0.9950
Cu	153	24.80	0.9983
Ni	11	0.04	0.9719

Table 7.3 Langmuir model parameters calculated from the fitting of experimental points for sorption of each metal species to linearised isotherm equation (Equ. 3.3).

Metal	Biomass	Uptake ($mmolg^{-1}$)	Reference
Cu	Microbial sulphide	2.41	This study
	Sargassum	0.93	(Davis *et al.*, 2000)
	DSV	0.26	(Chen *et al.*, 2000)
Cd	Microbial sulphide	5.36	This study
	Hazelnut shell	0.05	(Cimino *et al.*, 2000)
	Sargassum	0.79	(Davis *et al.*, 2000)
Zn	Microbial sulphide	4.7	This study
	Hazelnut shell	0.03	(Cimino *et al.*, 2000)
	Sargassum	1.18	(Davis *et al.*, 2000)
	DSV	0.09	(Chen *et al.*, 2000)
Ni	Microbial sulphide	0.19	This study
	Sargassum	0.09	(Davis *et al.*, 2000)

Table 7.4 Comparison of maximum sorption capacities of cadmium, copper, nickel and zinc for various biosorbents.

The Langmuir model (Equ. 3.3) and (Equ. 3.2) showed a better overall fit for the tested metal ion species with high calculated correlation coefficients (>0.9) The correlation coefficients (R^2) determined for the Langmuir isotherms and the related constants are presented in Table 7.3**Error! Reference source not found.**. A comparison of the uptake constant *Q*, for each metal shows that the capacity uptake of the microbial sulphide follows the order Cd>Zn>Cu>Ni, with cadmium uptake being 60 times greater than that of nickel

The sorption capacities of other biomasses on the tested metals, as performed by other researchers are presented in Table 7.4 alongside the results determined herein. The sorption capacity of the microbial sulphide for all the tested metal ions was considerably higher than that exhibited by other biosorbents used in metal recovery applications.

7.1.4. Discussion and Summary of Sorption Isotherm Results

The sorption isotherm data results show that the experimental data conforms best to the Langmuir isotherm model which indicates the possibility of adsorption (as well as precipitation) occurring to sequester the metal ion species (Pagnanelli *et al.*, 2000, Schneider *et al.*, 2001). This result was unexpected as the microbial material possesses a highly irregular (inhomogeneous) surface (Figure 6.1) as a result of the high porosity of the sulphide structure which is characteristic of a typical Freundlich model system and is contrary to the ideal Langmuir model assumptions. The finding however supports assumptions made previously (section 7.1.2) which relate to the occurrence of monolayer binding and the presence of a limited number of binding sites that become saturated at specific concentrations.

The uptake capacity of the microbial biomass for the metal ion species tested varies greatly with a calculated affinity trend of $Cd^{2+}>Zn^{2+}>Cu^{2+}>Ni^{2+}$ which relates to the affinity of binding between the metal ion and the sorbent mass.

Ion	Coordination	Ionic Radius (Å)	Pauling Electronegativity
Cd^{2+}	6	0.95	1.69
Zn^{2+}	6	0.74	1.65
Cu^{2+}	6	0.73	1.9
Ni^{2+}	6	0.69	1.91

Table 7.5 Selected properties of metal ions used for sorption

This trend can be explained in part using the metal ionic radii (Table 7.5) as metal ions with larger ionic radii have a greater sorption capacity than metal ions with smaller ionic radii. This relation is such because the larger the size of the ion the more frequent the interaction with the binding mass and hence a greater opportunity for binding to occur (Ali *et al.*, 1987).

The ion electronegativity however would suggest a reverse order; $Ni^{2+}>Cu^{2+}>Cd^{2+}>Zn^{2+}$, with previous studies intimating its direct effect on the observed sorption capacities (McKay and Porter, 1997, Han *et al.*, 2000). However it can be argued that although the binding potential of the smaller ions may be greater, a larger ionic radius guarantees more ready contact (under mixing conditions) between the interacting particles and therefore increases the likelihood of binding to occur.

The calculated uptake values for the SRB generated biomass also indicate a greater affinity for the test metals than other commonly used biosorbents This result is highly favourable as it indicates that the tested biomass is equally suited for recovery of the tested metals and can yield a treated effluent with significantly lower metal concentrations than that obtain when using other biosorbents.

7.1.5. Experimental Results for Single Metal Sorption Kinetics

SRB literature investigating sorption of heavy metals as reviewed by the author contain predominantly time course details of sorption (Chen *et al.*, 2000, Jalali and Baldwin, 2000), however the application of specific kinetics models is generally omitted. Literature focussed on the kinetic quantification of the other biomass however use a variation of pseudo first and pseudo-second order kinetic

models to evaluate the effectiveness of the tested biosorbent (Namasivayam and Kadirvelu, 1997, Cheung *et al.*, 2001, Ho, 2003, Gulnaz *et al.*, 2005). For purposes of clarification and analysis, both kinetics models were applied to the sorption data and assessed to determine which provided a more suitable fit for the experimental results. Table 7.6 summaries the parameters used to acquire sorption kinetics data

Experimental Parameters	**Conditions**
Metal Species	Cd, Cu, Zn, Ni
Initial concentration	$125mgL^{-1}$
Solution pH	5.0 - 5.5
Temperature	20±2°C
Mass of Biomass	~17mg
Solution Volume	40ml

Table 7.6 Experimental parameters used for kinetic sorption experiments.

Figure 7.5 shows a time dependant plot of sorption for cadmium along side the fitted model data. Rapid sorption of the metal is evident from the time course sorption graph (Figure 7.5A) with almost all the metal in solution being removed within 30 minutes of contact with the biomass.

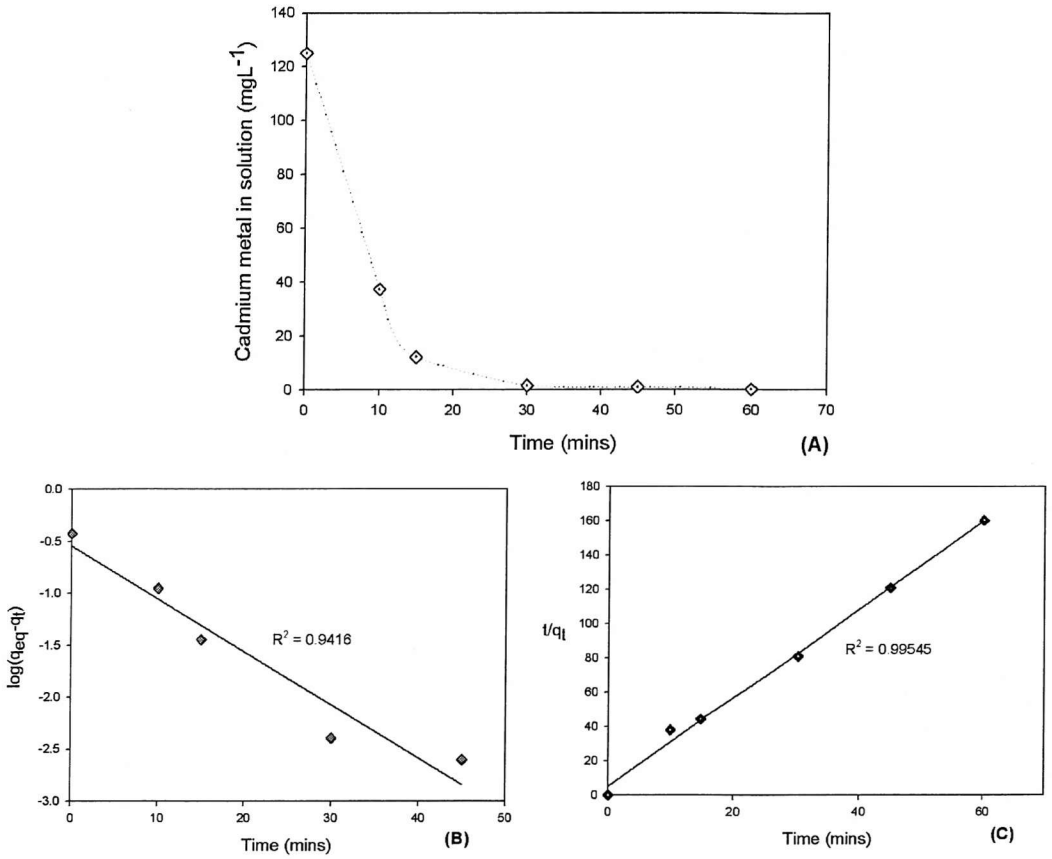

Figure 7.5 Kinetics of cadmium sorption. (A) Time dependant plot of sorption. (B) Pseudo first order kinetics model for uptake of Cd metal, (C) pseudo second order sorption kinetics model.

The correlation coefficients for both cadmium kinetic model plots are statistically high (>0.9) indicating a good fit to both models however the pseudo second order plot has a greater coefficient indicative of a better fit (Figure 7.5 C).

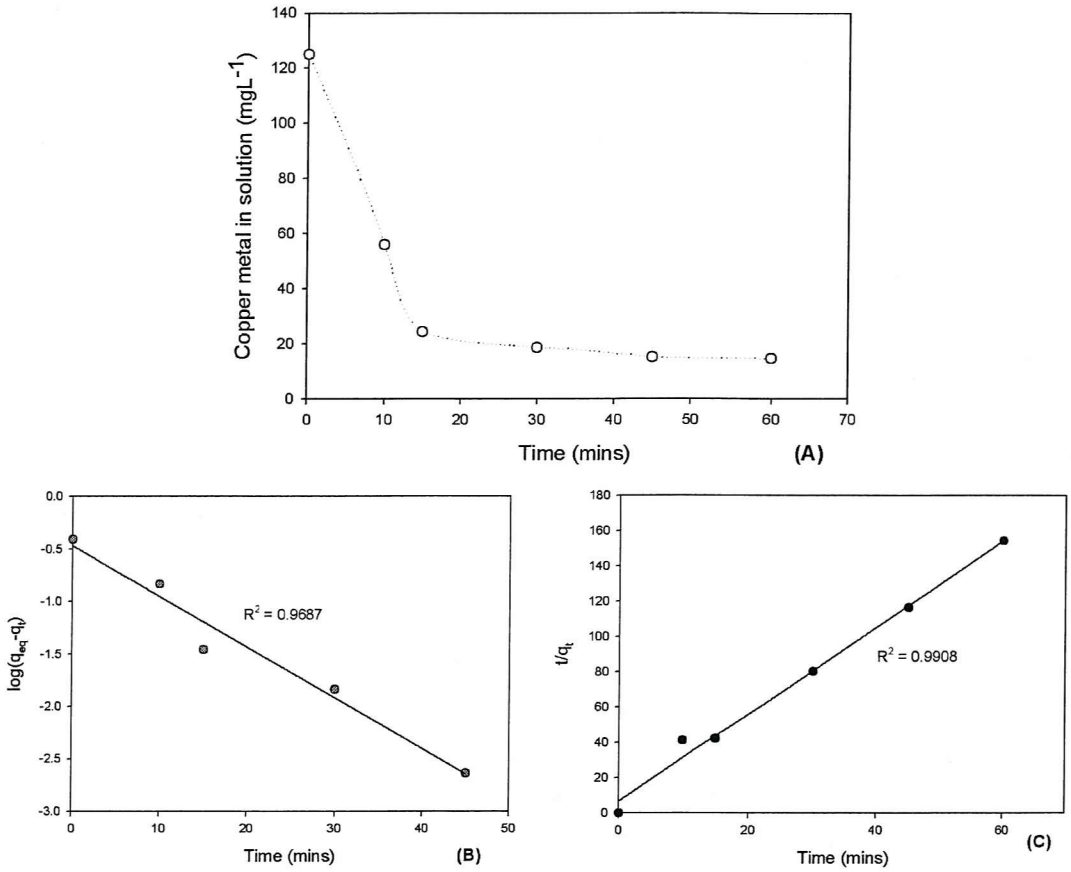

Figure 7.6 Kinetics of copper sorption. (A) Time dependant plot of sorption. (B) Pseudo first order kinetics model for uptake of Cu metal, (C) pseudo second order sorption kinetics model.

Similar results were attained for copper (Figure 7.6) with both kinetics models attaining high correlation coefficients but the better correlation occurring for the second order model (Figure 7.6C).

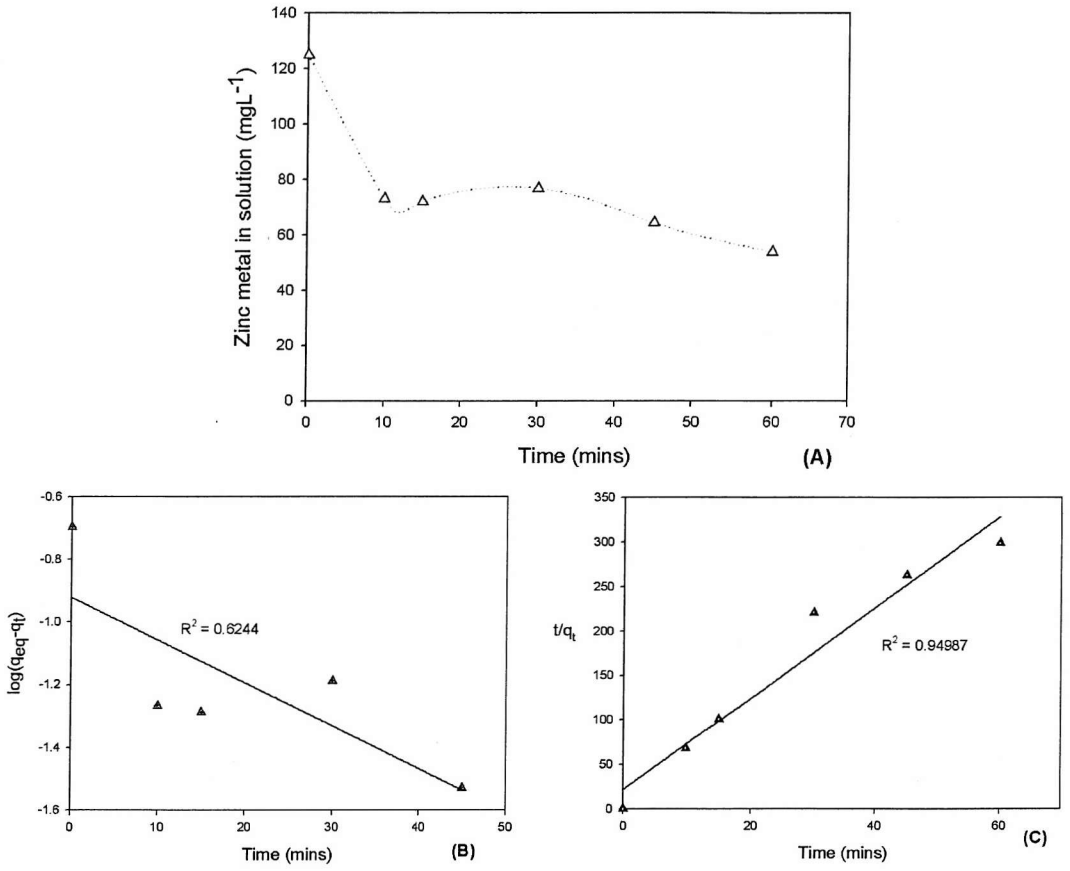

Figure 7.7 Kinetics of zinc sorption. (A) Time dependant plot of sorption. (B) Pseudo first order sorption kinetics model for uptake of Zn metal, (C) pseudo second order sorption kinetics model.

Figure 7.7A and Figure 7.8A show the time course sorption for zinc and nickel respectively. As shown with the other metal ion species, maximum metal uptake occurred within 30 minutes of the start, after which sorption slows until equilibrium is attained.

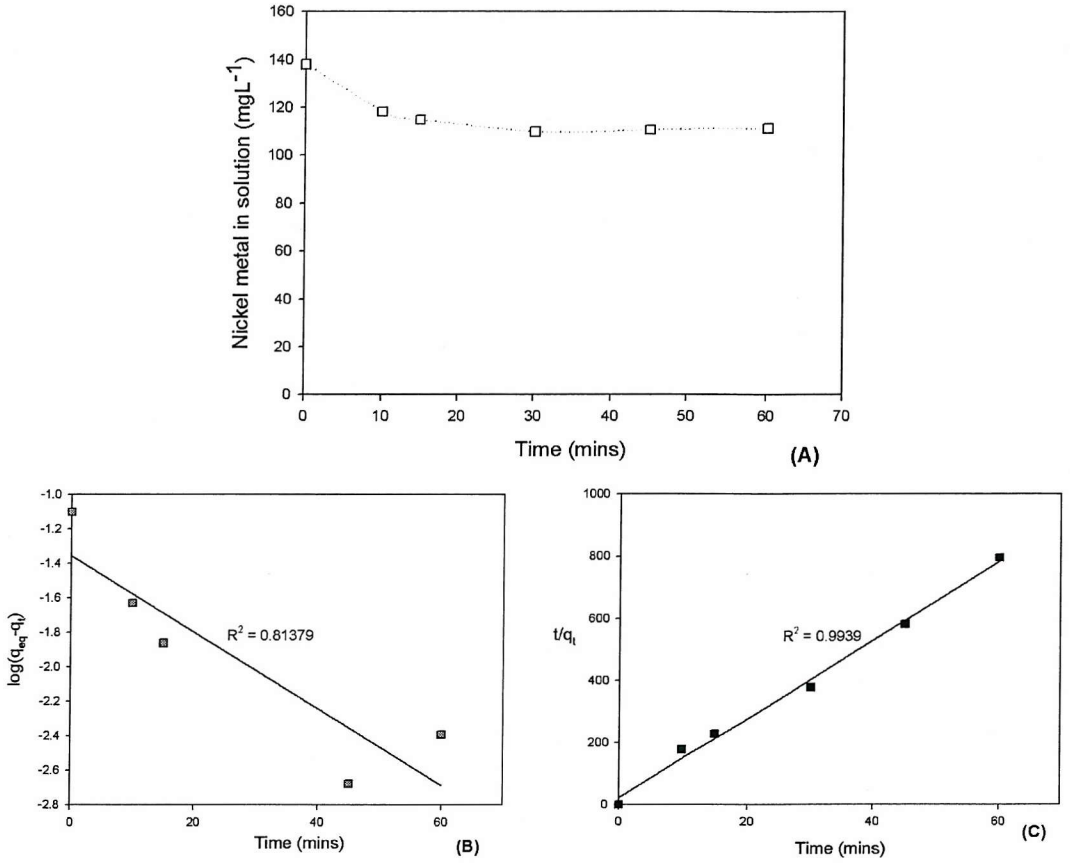

Figure 7.8 Kinetics of nickel sorption. (A) Time dependant plot of sorption. (B) Pseudo first order sorption kinetics model for uptake of Ni metal, (C) pseudo second order sorption kinetics model.

Unlike the other metal ion species (Cd^{2+} and Cu^{2+}) the calculated pseudo-first order correlation coefficients for both nickel and zinc (Figure 7.8B and Figure 7.8B respectively) are significantly lower than the second order coefficients (Figure 7.8C and Figure 7.8C). This therefore suggests that pseudo-second order kinetic mechanisms are dominant.

7.1.6. Discussion and Summary of Single Metal Kinetics Results

The rate at which sorption occurs is a significant consideration in the design and feasibility of a sorption system. As previously discussed, metal sequestering by biosorption occurs more rapidly than conventional methods; however the need to quantify the reaction rate by the use of models is still essential.

All the metal ions tested showed a 2 phased sorption process. The first phase was a fast reaction that occurs within 30 minutes wherein most of the metal ion sorption transpires. A slower, second reaction was also observed which ran until sorption equilibrium was attain/approximated. As with all rate determining processes, the kinetics of these sorption processes were therefore dependant on the slower observed reaction.

Sorption kinetics as modelled using the pseudo first and pseudo second order equations showed a close similarity between the model correlation coefficients attained for cadmium and copper. This result suggests that the rate determining mechanism of sorption is not exclusively dependant on the concentration of metal ions in solution as can be inferred from the pseudo-first order equation, but also chemical binding processes as proposed by the pseudo-second order kinetics model (Ho and McKay, 2000, Gulnaz *et al.*, 2005).

Modelled results for zinc and nickel however showed a clear distinction between the calculated correlation coefficients. Unlike the Cd^{2+} and Cu^{2+} results, the sorption systems for nickel and zinc are predominantly controlled by the chemical valency forces exerted between the biomass and metal ion species (Ho and McKay, 1999) which is indicative of pseudo-second order modelling.

Recent literature by Ho and McKay (1999), has suggested that pseudo-second order models generally provide a better fit to kinetic data as equilibrium is dependant not only on the concentration of metal ion species in solution as inferred by pseudo-first order models, but also on chemical interaction occurring at the solid–liquid interface.

7.1.7. Experimental Results for Binary Metal Sorption

Binary metal sorption was performed using two mixed metal ion combinations using equal concentrations of the target metal ions; Cd(II)-Zn(II) and Cu(II)-Ni(II). Table 7.7 shows the experimental parameters used.

Experimental Parameters	Conditions
Metal mixture	Cd(II)-Zn(II), Cu(II)- Ni(II)
Initial metal concentration	125mgL^{-1}
Solution pH	5.0 - 5.5
Temperature	20±2°C
Mass of Biomass	~18mg
Solution Volume	40ml
Contact time	60 minutes

Table 7.7 Experimental parameters used for binary metal sorption experiments

The uptake of metal ions from single and binary metal environments is shown in Figure 7.9 to Figure 7.12. The results show that uptake efficiency for cadmium is similar in both single and binary metal environments with approximately 99% recovery recorded. The uptake of zinc, Figure 7.10, in the binary environment with cadmium is reduced by almost a third of that measured in the single metal environment.

In the Cu(II)-Ni(II) binary system , less than 5% of nickel ion present in solution was sequestered (Figure 7.12). This represents a 75% decrease in the amount of metal removed from solution in the single metal environment. The uptake capacity of copper in the Cu(II)-Ni(II) binary environment is also reduced in comparison to a pure copper environment; however the reduction in copper sorption is less than 20% (Figure 7.11)

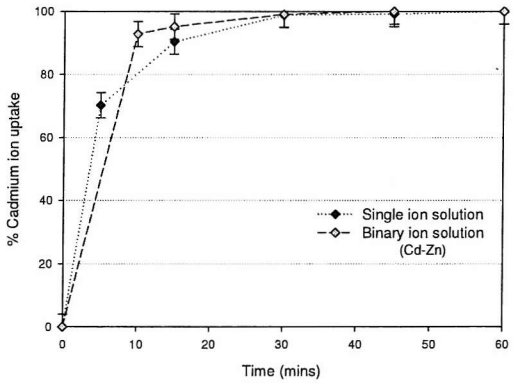

Figure 7.9 Uptake of cadmium ion from single and binary metal ion (Cd(II)-Zn(II)) solutions using microbially produced iron sulphide.

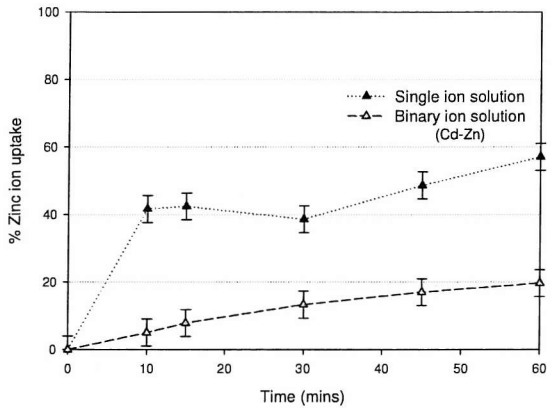

Figure 7.10 Uptake of zinc ion from single and binary metal ion (Cd(II)-Zn(II)) solutions using microbially produced iron sulphide

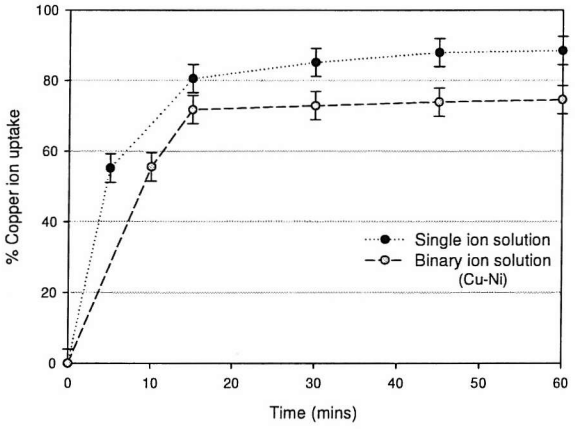

Figure 7.11 Uptake of copper ion from single and binary ion (Cu(II)-Ni(II)) solutions using microbially produced iron sulphide.

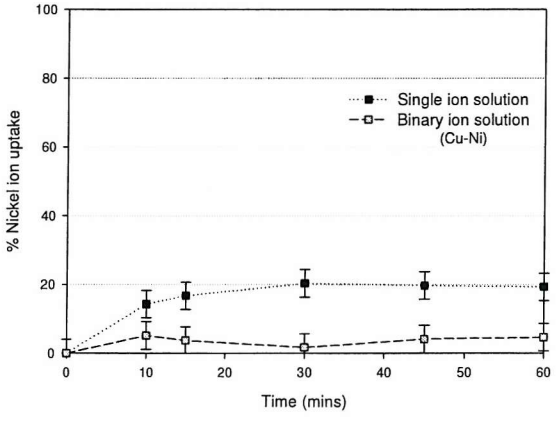

Figure 7.12 Uptake of nickel ion from single and binary ion (Cu(II)-Ni(II)) solutions using microbially produced iron sulphide.

The sorption rate constants as derived from the application of the pseudo-second order model to the sorption data is presented in Table 7.8 below.

Both cadmium and copper, the metals species preferentially sorbed in their individual binary environments showed an increase in the sorption rate when in the binary environment. Zinc and nickel, the accompanying metal in the respective binary environments, however showed a decrease in the rate of sorption in the binary system further confirming competition effects between metals in a binary sorption system with the species preferentially sorb being sequestered at a faster rate.

Metal Ion- Solution type	**K_{ads} ($x10^{-3}$) ($g/mgmin^{-1}$)**	**Correlation coefficient (r^2)**
Cd^{2+} - single	2.1	0.999
Cd^{2+} - binary	5.7	0.999
Zn^{2+} - single	1.2	0.950
Zn^{2+} - binary	1.0	0.820
Cu^{2+} - single	1.5	0.998
Cu^{2+} - binary	1.9	0.997
Ni^{2+} - single	7.0	0.994
Ni^{2+} - binary	5.0	0.989

Table 7.8 Pseudo second order adsorption constants for single and binary metal ion solutions.

7.1.8. Discussion and Summary of Binary Sorption Results

The sorption data obtained from the binary metal solutions show that metal competition for binding sites is evident within the sorption system. This observation is common within the literature with many researchers documenting significant competition effects in mixed element systems (McKay and Porter, 1997, Panayotova and Velikov, 2002).

A comparison of the percentage metal uptake in single and binary metal ion environments revealed the occurrence of binding competition in the binary

solutions In the Cd(II)-Zn(II) binary system the percentage uptake of Zn(II) was reduced by a approximately 33% as compared to that sorbed in a pure Zn environment. This decrease in uptake can be attributed to competition effects between the metal species in solution with cadmium being preferentially sorbed as a result of having a larger ionic radius and electronegativity,

Similarly in the Cu(II)-Ni(II) binary system a 75% decrease in the amount of Ni metal removed from solution was indicative of the prevalence of antagonistic effects in the Cu(II)-Ni(II) binary system. The similarity of copper and nickel ions in electronegativity (Table 7.5), suggests that they have similar binding potential, however the slightly larger ionic radius of copper (Table 7.5), would enable more interaction between the biomass and metal ions, thereby giving rise to more metal uptake.

It can therefore be concluded that the ion with the larger of the ionic radii in the metal ion pair, cadmium and copper, maintained a similar percentage uptake to that obtained in the single metal solution. This result is indicative of little variation in the affinity of the biomass for the metal ion species thus maintaining the high uptake in the presence of other metal ions. This however is contrary for the accompanying metal ions, zinc and nickel, which comparatively, have a smaller ionic radius and as a result have a lower affinity for the biomass which is readily compromised in the presence of the larger metal ion and results in their reduced uptake in the binary environment.

7.2. Metal Desorption

7.2.1. Experimental Results for Heavy Metal Desorption

As previously discussed desorption data for microbially generated sulphides is limited in the literature with only the use of a citrate salt buffer being documented (Watson *et al.*, 2001). An optimal desorbing eluant must be cost effective, non damaging to the biomass, highly efficient and non polluting (Vijayaraghavan *et al.*, 2004). The reusability of the microbial sulphide biomass as a biosorbent was determined using a selection of desorbing agents in repeated sorption-desorption batch experiments (Table 7.9).

It was observed that distilled water was a poor eluant for copper, zinc and cadmium with less than 1% of the metal sequestered by the biomass being released into solution and recovered (Figure 7.13). Approximately 30% of the sorbed nickel was released into solution using distilled water as the desorbing eluant indicating that the binding between the biomass and the metal ions is weak and easily broken.

Experimental Parameters	**Conditions**
Mass of Biomass	~18mg
Metal solutions ($100mgL^{-1}$)	Cd, Zn, Cu, Ni
Metal Solution Volume	40ml
Sorption Contact time	(1) 60 minutes, (2) 30 minutes
Desorption eluants	Distilled H_2O (pH 6.7), 0.1M Acetic acid (pH) Citrate buffer (pH5), EDTA (pH8)
Desorption eluant volume	20ml
Desorption Contact time	60 minutes
Temperature	20±2°C

Table 7.9 Experimental parameters used for metal desorption experiments

Application of 0.1M acetic acid as the desorbing agent resulted in the release of 35% and 75% of the sorbed zinc and nickel metal ions respectively back into solution. Copper and cadmium however showed almost no response to the acidic agent with less than <5% recovery of the metal ions.

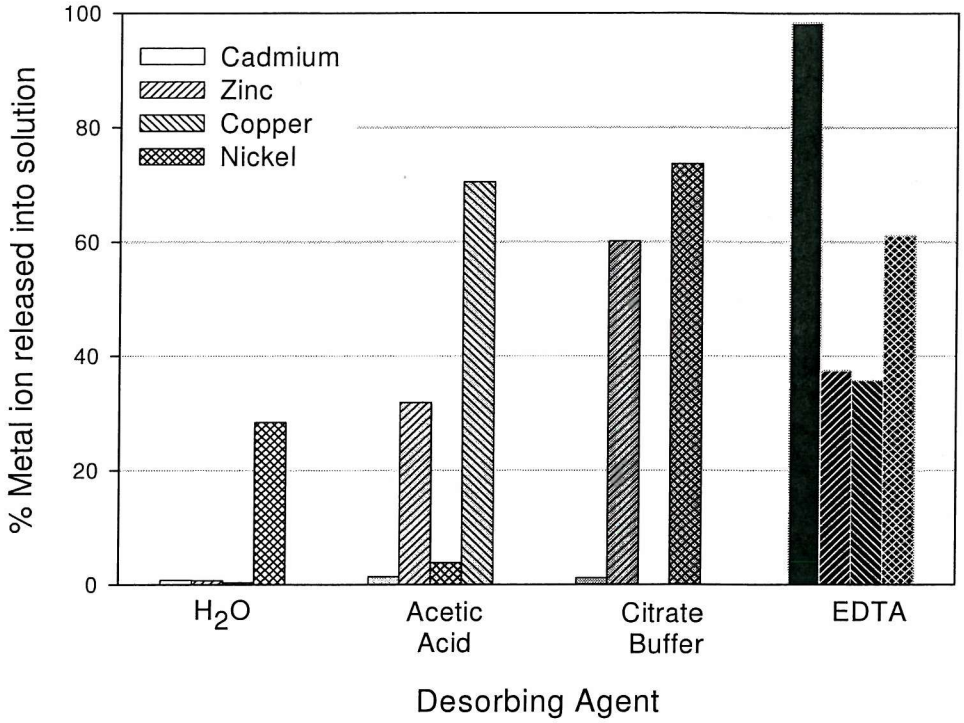

Figure 7.13 Effectiveness of desorbing agents in the recovery of various metal ion species bound to microbial sulphide biomass.

Nickel and zinc were also readily desorbed by the citrate buffer with 60 - 70% recovery within the 60 minute contact time (Figure 7.13). Similar to the results obtained for acetic acid, copper and cadmium showed almost no response (<2%) to the citrate desorbing solution. Poor recovery of cadmium using a citrate buffer were previously observed (Watson *et al.*, 2001) with the low cadmium recovery being attributed to the chemisorption of the metal ion to the biomass. It is therefore possible to assume that similar binding has occurred with copper hence the low recovery in the presence of citrate.

Significant metal recovery using EDTA as the desorbing agent was observed for all metal ion solutions with cadmium (~95%) and nickel (~60%), being most readily desorbed. Zinc and copper also recorded high levels of metal recovery (30-40%), in comparison to that attained using the other previously tested desorbing solutions.

Following the initial desorption procedure; the biomass was reapplied to a 100mgL^{-1} metal ion solution as detailed in section 4.13. Figure 7.14 to Figure

7.17 show a comparison of the amount of metal initially sorbed to that sorbed on the second application after desorption using each desorbing agent.

For all metal ion solutions, the amount of metal sorbed on the second application after desorption was significantly lower than the initial uptake using the fresh biomass. This is most noticeable in the cadmium application after desorption with EDTA where over 90% of the cadmium sorbed on the initial application is released into solution (Figure 7.14). This result, although dependant on the desorbing agent suggests the reversibility of the sorption process (Saeed and Iqbal, 2003) and should result in the unblocking of binding sites on the biomass. However, less than 20% of the metal ion in solution was sorbed in the second application (Figure 7.14) which is similar is magnitude to the amount sorb after the application of the other, less effective desorbing agents.

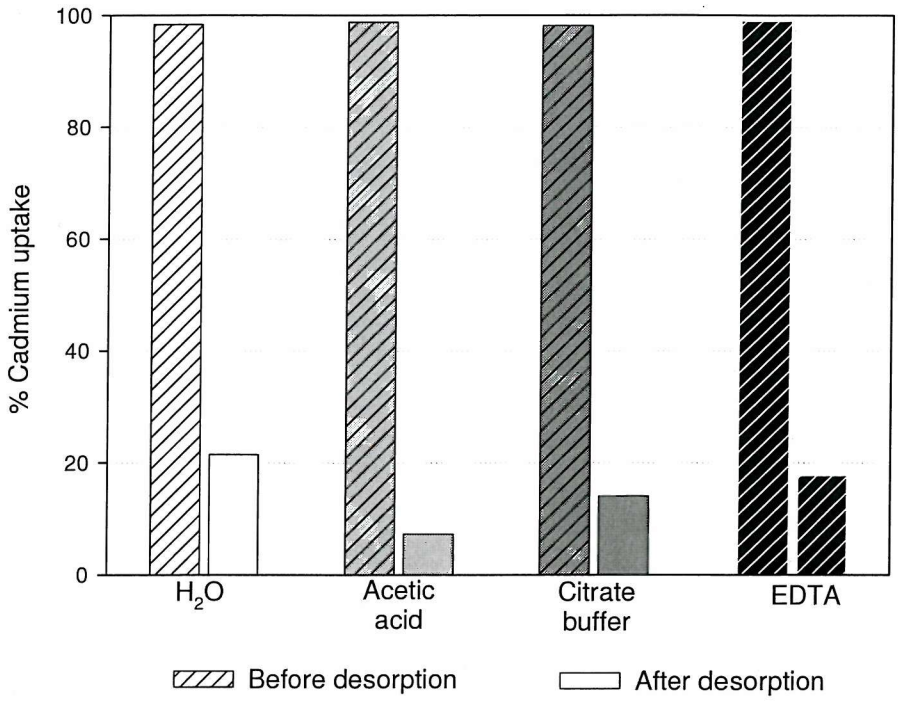

Figure 7.14 Uptake of cadmium metal ions from 100mgL^{-1} solution before (hatched) and after (plain) desorption using annotated desorbing agent.

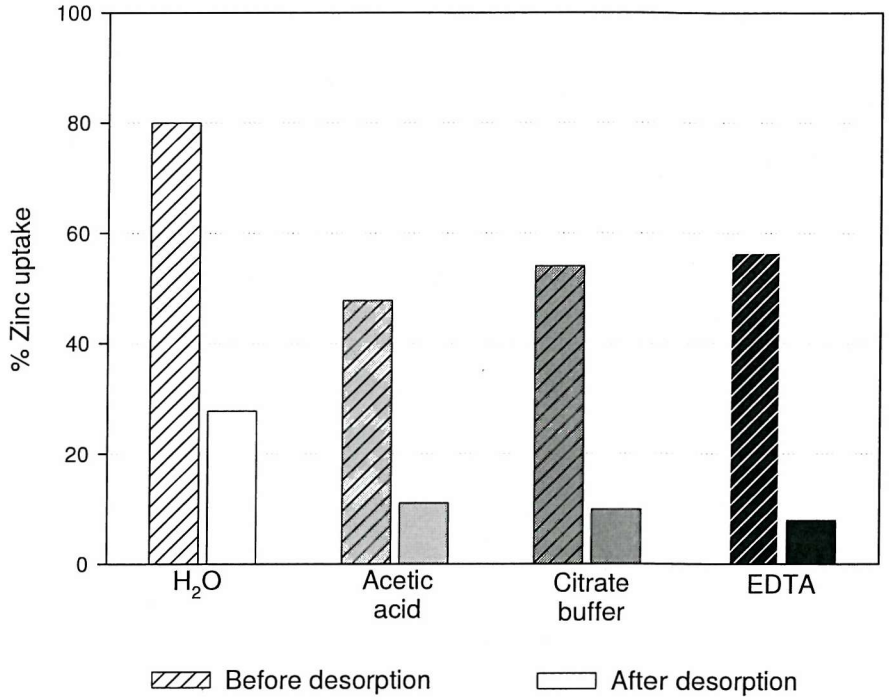

Figure 7.15 Uptake of zinc metal ions from 100mgL^{-1} solution before (hatched) and after (plain) desorption using the annotated desorbing agent.

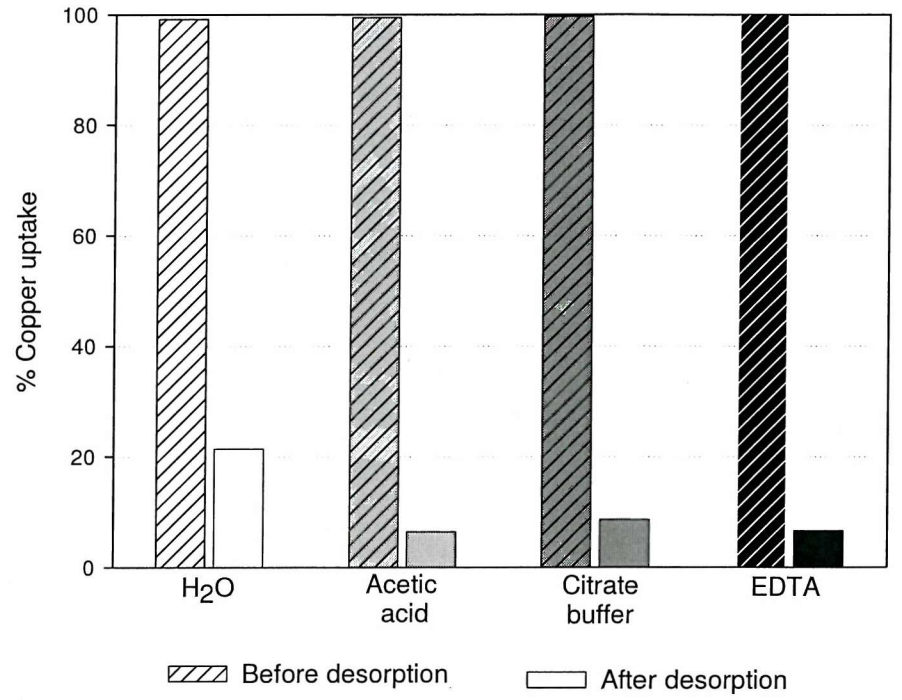

Figure 7.16 Uptake of copper metal ions from 100mgL^{-1} solution before (hatched) and after (plain) desorption using the annotated desorbing agent

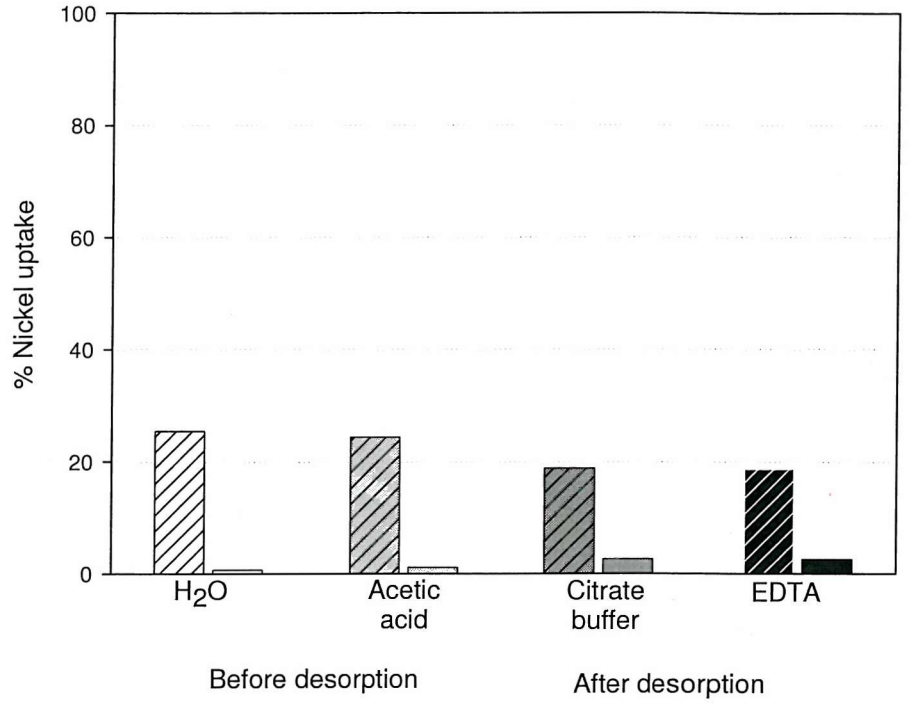

Figure 7.17 Uptake of nickel metal ions from 100mgL^{-1} solution before (hatched) and after (plain) desorption using the annotated desorbing agent.

A similar observation was made for zinc, copper and nickel, Figure 7.15, -Figure 7.17) whereby the amount of metal desorbed was not proportional to the amount of metal sorbed in the subsequent application.

7.2.2. Discussion and Summary of Desorption Results

Of the four desorbing agents tested, EDTA can be considered to be the most effective desorbing agent as it was the only eluant capable of releasing a significant proportion of each metal back into solution. This was particularly evident for cadmium and copper which were highly unresponsive to the other eluting agents. EDTA is well documented within the literature as an efficient desorbing agent for copper and cadmium (Holan *et al.*, 1993, Saeed and Iqbal, 2003).

Acetic acid and the citrate mineral salt although highly efficient, were limited to recovery of zinc and nickel. This high specificity of the desorbing agent would be favourable for target metal recovery.

The process of desorption serves primarily to return the biosorbent to its original status by the unblocking of sorption sites. Theoretically, this should enable the biomass to sorb an equivalent amount to that which was initially sorbed. Desorption however seldom returns the biomass to its original structure thereby resulting in the progressive degeneration of the biomass. The disproportional reduction in the sorption capacity of a biomass in relation to the amount of metal desorbed is very common in the literature and it indicates that the sorption-desorption process can show hysteretic characteristics (Gao *et al.*, 2003) depending on the desorbing agent used

The use of distilled water appears to have had the least effect on the uptake capacity with more cadmium, zinc and copper being sorbed in the second application than achieved after the use of any other chemical desorbing agent (Figure 7.14 to Figure 7.16). From this result it can be inferred that the biomass was not saturated by the initial application and available binding sites were still present. Also due to limited damaging effects to the biomass caused by oxidation, the biomass structure was not significantly altered and was able to continue to sequester aqueous metal ions.

The application of all desorbing agents, with the exception of distilled water appeared to have a negative effect on the integrity of the biomass. The biomass became discoloured changing from black to brown, which is usually associated with the possible oxidation of the iron present within the biomass. Changes in the mass of biosorbent were also noted with decreases of approximately 5% as a result of dissolution and possible ion exchange mechanisms.

This observation therefore suggests that although the binding sites were unblocked by efficient desorption, the biomass structure was altered and possible alterations in its chemical composition may have occurred, hence its reduced sorption capacity.

The microbial sulphide biosorbent appears to have a very short 'life-span' of only a single application before the biomass is sufficiently compromised. This characteristic is very unfavourable as most other biosorbent materials are readily

subjected to in excess of four recycling applications before the uptake capacity is reduced to less than 50% (Davis, 2000, Saeed and Iqbal, 2003). At first glance the lack of reusability of the microbial biomass may appear highly unfavourable, however on closer examination and quantification of the amount of metal sorbed in a single application of the microbial biomass is equivalent multiple applications (approximately 3-4) of other biomass types (Table 7.4).

From the perspective of efficiency and costs savings, the microbial biomass is significantly more efficient as in a single application metal concentration can be reduced to levels which would ordinarily require multiple treatments. This high recovery rate on a single application would also remove the need for significant effluent feedback thereby simplifying the system design requirements and costs.

7.3. SRB sulphide vs Synthetic FeS

7.3.1. Experimental Results for the Comparison of SRB sulphide vs Synthetic FeS

The high sorption capacity and affinity of iron mono-sulphide (FeS) for divalent metals is well documented within the literature (Morse and Arakaki, 1993, Wharton *et al.*, 2000, Wolthers *et al.*, 2003). The metal uptake capacity of synthetic iron sulphide was compared to microbially produced iron sulphide for two sorption cycles (sorption-desorption-sorption). The sorption results were used to determine whether synthetic iron sulphide could be used with comparable results as a chemical alternative for the microbial sulphide. Total sorption capacity results for both sulphide materials are shown in Figure 7.18 and Figure 7.20.

For both sorbing sulphide materials, the first sorption application using fresh material resulted in the binding of a significant amount of metal ion, greater than that referenced by other authors (Table 7.4). The microbially produced sulphide had a higher affinity approximately 25%, for cadmium, zinc and copper, than the synthetic sulphide. Nickel uptake however was significantly greater (>50%) for the synthetic sulphide.

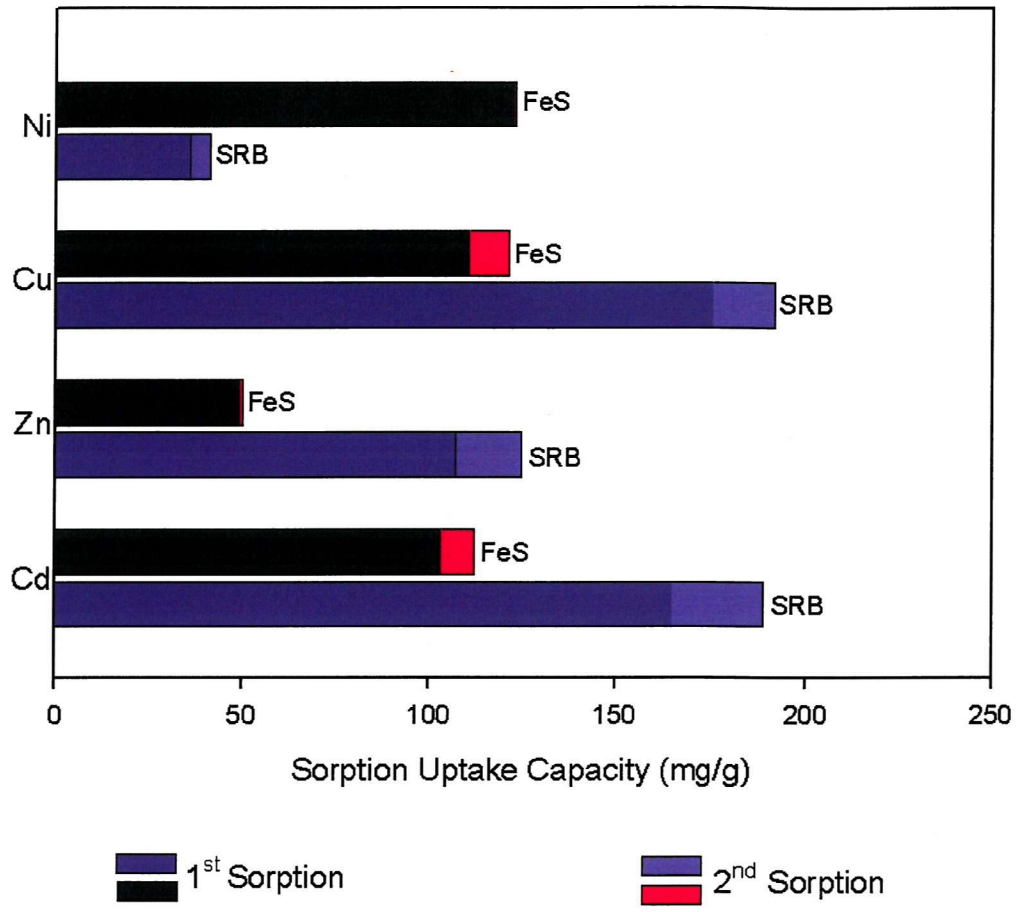

Figure 7.18 Comparison of cumulative metal uptake capacities for synthetic FeS and microbial iron sulphide for 2 consecutive sorption applications using a citrate desorbant.

After the initial sorption, both sulphides were treated with a desorbing agent for an hour then re-applied to fresh metal stock solutions. As shown in Figure 7.19 and consistent with other findings detailed herein (section 7.2), treatment with the citrate solution recovered a greater amount of zinc (70mg/g) and nickel (15mg/g) from the microbial sulphide. Recovery of cadmium and copper was less than 5%. Large quantities of copper (75mg/g), nickel (10mg/g) and zinc (35mg/g) were recovered from the synthetic sulphide using the citrate buffer. The chemical action of the desorbing agent on the sorbent material caused noticeable oxidation of the sulphides and the possible alteration in the structural nature of the material. As observed in previous experiments (section7.2) the sorption capacity of the material was expected to decline as a result of the desorption process.

Citrate desorption had a greater effect on the synthetic sulphide with the maximum metal sorbed on the second application being equivalent to 10mg Cu/g of the sorbing material. This represents an order of magnitude decrease in the amount of metal initially sorbed. The material reapplied to the zinc and nickel solutions removed no significant amount of metal ion from solution on the second sorption.

The microbially produced iron sulphide as shown in earlier studies had a reduced metal uptake during the second application; however the amount sorbed was uniformly greater than that sorbed by the synthetic sulphide (Figure 7.18). This overall result shows that the microbial sulphide is a better sorbent of cadmium zinc and copper and under citrate desorbing conditions the microbial sulphide has greater longevity than its synthetic counterpart.

Repeat sorption-desorption cycles using EDTA as the desorbing agent showed a similar total sorption uptake capacity for the synthetic sulphide (Figure 7.20). The effectiveness of EDTA on the synthetic sulphide was such that less than 7mg/g of metal was recovered during the desorption process (Figure 7.19). The material therefore maintained a high concentration of metal ions on its surface with few available sorption sites and was able to sorb small amounts of cadmium and nickel. No additional zinc and nickel was removed from solution on the second application (Figure 7.20).

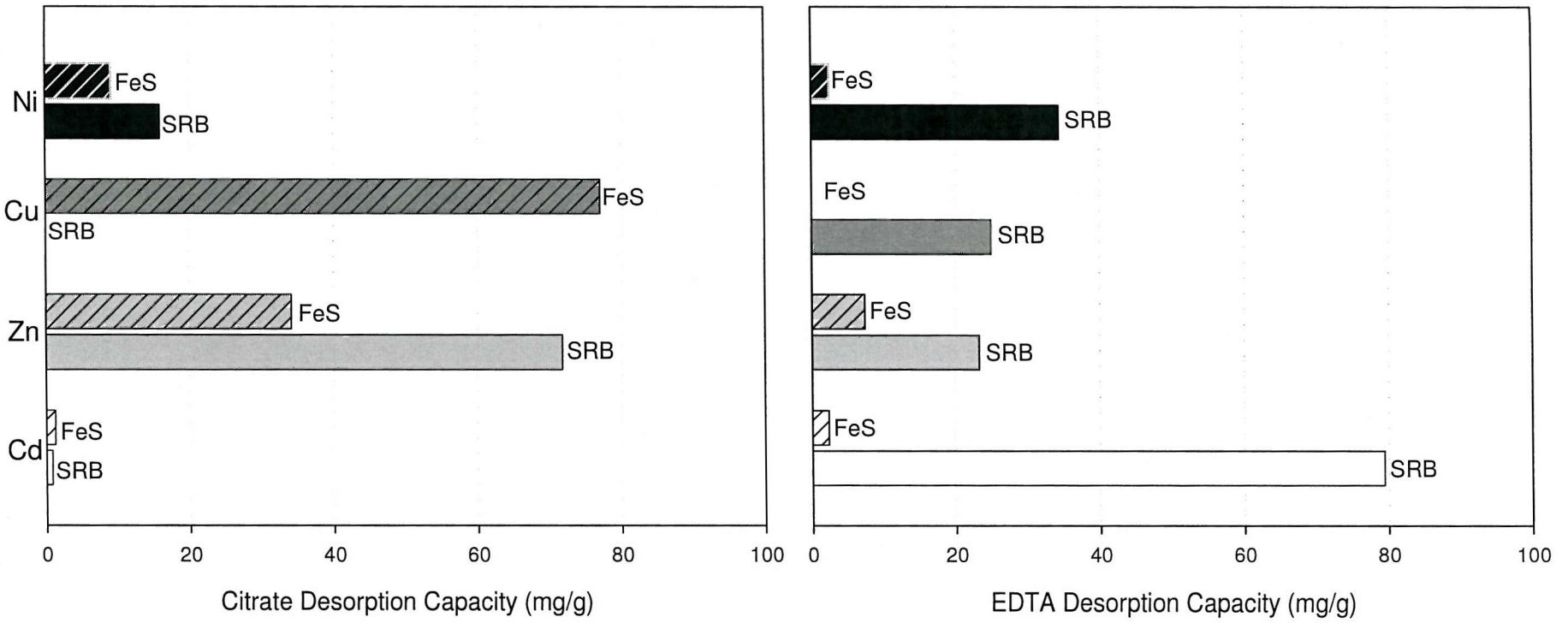

Figure 7.19 Metal desorption capacities for synthetic FeS and the microbial iron sulphide using a mineral citrate buffer solution and EDTA.

With the exception of cadmium, the amount of metal ion desorbed from the microbial biomass using EDTA was similar within the range of 20-35mg/g (Figure 7.19). Cadmium desorption using EDTA however was highly effective as documented by other authors (Saeed and Iqbal, 2003) with approximately 80mg/g of metal being recovered within 1 hour. Despite the significant metal recovery, less than 30mg/g was sorbed on the second application of the biomass (Figure 7.20).

These findings correlate with previous results (section 7.2) which showed that the sorption-desorption process is reversible; however the integrity of the biomass is often compromised in the process thereby reducing its reusability.

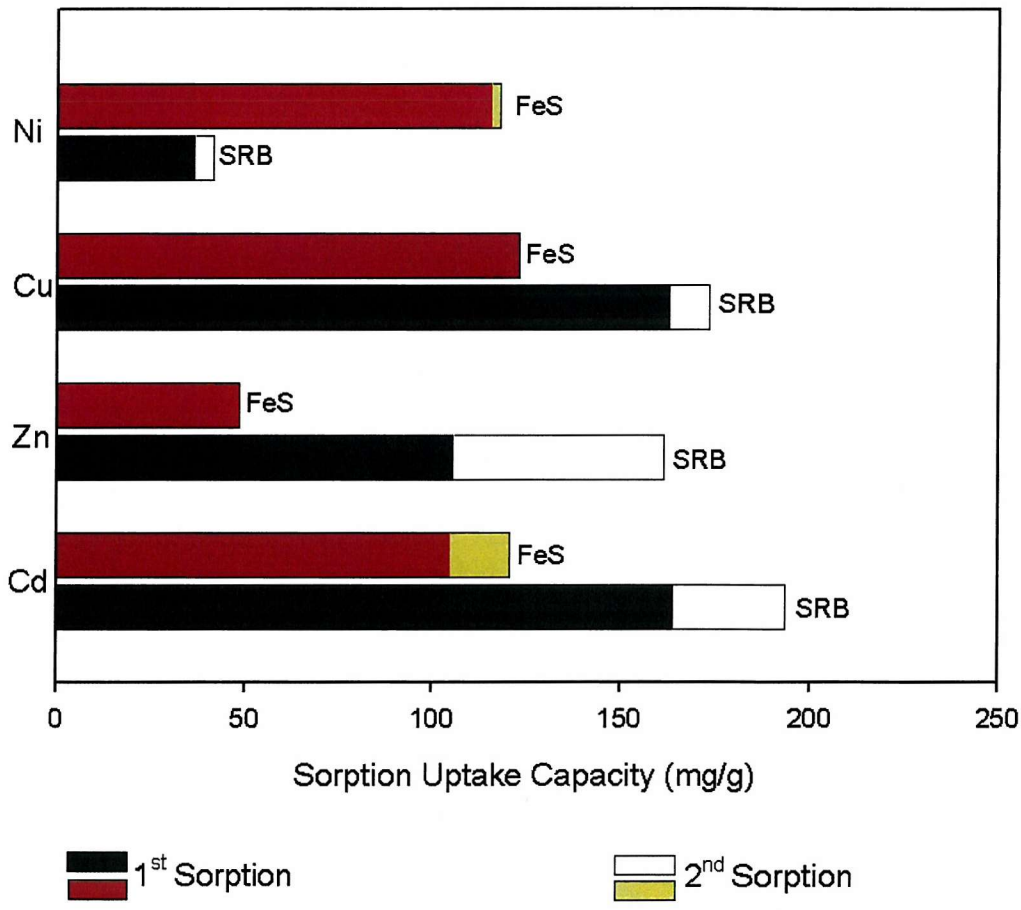

Figure 7.20 Comparison of cumulative metal uptake capacities for synthetic FeS and microbial iron sulphide for 2 consecutive sorption applications using EDTA as the desorbant.

7.3.2. Discussion and Summary of SRB sulphide vs Synthetic FeS Results

The experimental results confirm the high affinity of synthetic FeS for divalent metals with copper being the most readily sorbed from solution. When compared with the microbially produced iron sulphide, in general less metal ions (cadmium, nickel and zinc) were sorbed from the test solutions by the synthetic sulphide. This difference in sorption capacity could be as a result of the structure of the sulphide with greater binding in the microbial sulphide possibly attributed to the availability of more binding sites. Work by other authors (Watson *et al.*, 1995) suggested that the irregular structure of the iron sulphide and the similarity of the ironic radii of zinc (0.74Å), nickel (0.64 Å), copper(0.73 Å) and iron (0.75 Å) would facilitate easy iron replacement and substitution into the FeS compound matrix. Greater nickel metal uptake in the synthetic sulphide could therefore imply higher prevalence of small structural vacancies suitable for only nickel ion binding.

The metal loaded solids, when treated with a citrate buffer solution and EDTA, the two tested desorbing solutions, showed signs of permanent binding with an average of less than 20% of the metal being returned to solution. Once treated with the desorbing agent the synthetic material was significantly altered and its sorption capacity was significantly reduced.

Both sulphide materials show limited reusability with the desorption process causing significant reduction in the longevity of the material. However, the proportion of metal sequestered by the microbial sulphide is on average 25% more than that sorbed by the synthetic sulphide. The lower metal sorption uptake of the synthetically produced iron sulphide makes it less favourable for commercial use as it is effectiveness does not surpass that of the microbial sulphide.

7.4. *Metal Polluted Wastewater Biosorption*

7.4.1. Experimental Results for the Sorption of Metals from Polluted Wastewater

Laboratory sorption experiments using analytical grade chemical reagents and distilled water as the mobile phase seldom gives a true assessment of the effectiveness of a biomass. Laboratory tests serve primarily as a screening process through which the potential effectiveness; kinetics, and equilibrium isotherms can be determined.

'Real' heavy metal polluted wastewaters are rarely pure and often contain various ionic forms of a metal in addition to a mixture of other metals and impurities (Volesky, 2001). Company disclosure policies often make availability and access to raw industrial effluent difficult. A synthetic effluent which could be used to test the true effectiveness of the microbial biomass in the presence of a variety of impurities and multi-metal conditions was prepared using a raw municipal wastewater effluent spiked with metal ion solutions (Table 7.11). The effect of impurities on the sorption efficiency was determined in a parallel experiment using identical sample conditions and metal concentrations, but the wastewater mobile phase was replaced with distilled water.

Wastewater Characteristic	**Parameter**
pH	6.5
Carbon Content (DOC)	340-360mgL^{-1}
Dissolved metal concentration	Cd, Zn, Cu, Ni- below detection level

Table 7.10: Characteristics of wastewater used for preparation of synthetic effluent.

Experimental Parameters	Conditions
Mass of Biomass	~18mg
Metal solutions (12.5mgL^{-1})	Cd, Zn, Cu, Ni
Liquid Phase	(1) raw wastewater effluent (2) distilled water
Temperature	20±2°C
Metal Solution Volume	40ml
Contact time	60 minutes,

Table 7.11 Experimental parameters used for wastewater biosorption experiments

Control experiments conducted using the multi-metal solution prepared in raw effluent and distilled water, devoid of biomass and allowed to interact for 60 minutes to determine whether the mobile phase and presence of other metals had any effects on the individual metal ion concentrations. The sorption vials were placed on roller beds at 33rpm to ensure representative mixing of the solutions. shows the metal ion concentration in solution with time.

Metal concentrations prepared in distilled water (Figure 7.21a) showed no significant concentration decreases indicating that the interactions between the metal ion species were such that no binding or precipitation occurred. In agreement with previous control experiments using single metal solutions, the absence of significant metal losses also confirmed no losses as a result of interactions with the reaction vials. Losses of metal ion in the presence of biomass were therefore assumed to be equivalent to concentration sorbed by the biomass.

In the presence of raw wastewater as the liquid phase, the aqueous nickel ion concentration remained unchanged for the duration of the interaction period. This result indicates a lower reactivity of the metal ion in comparison to the other metal ions present. Concentrations of the other metal ions in solution showed decreases of 21% (Zn), 22% (Cd) and 48% (Cu) (Figure 7.21b). Given that no metal losses were recorded in the distilled water samples, the presence of impurities in the form of suspended solids were thought to be responsible for the significant metal losses.

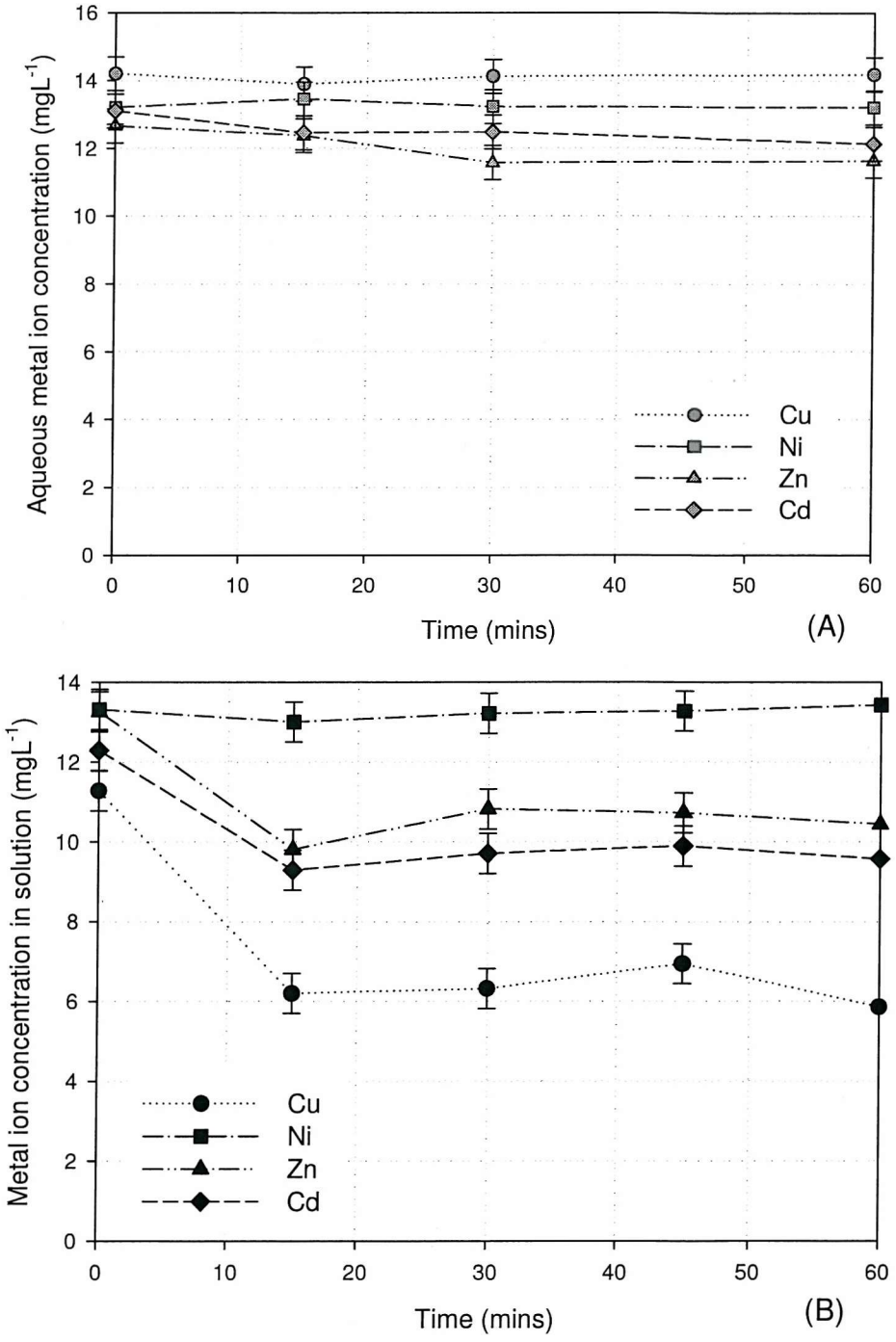

Figure 7.21 Metal ion concentration for control experiments devoid of biomass. (A) Distilled water (B) wastewater effluent used as liquid phase.

Measurement of the total suspended solids in a pure wastewater sample before and after rolling showed an increase in solid concentration from $0.1gL^{-1}$ - $0.5gL^{-1}$

in the wastewater sample. Agitation of the sample appeared to increase flocculation of the solids in solution resulting in an increase in solid concentration (Miyanami *et al.*, 1982). The presence of suspended solids had a synergistic effect on the sequestration of the metal ions in solution. Metal losses from solution in further experiments using biomass were therefore attributed to the joint effect of the biomass and the suspended solids

Figure 7.22 to Figure 7.25 show a comparison of the amount of metal sorbed from solution prepared using water and wastewater effluent. The copper, zinc and cadmium solutions prepared in water show little variation from the solvent prepared in effluent, however closer examination of the results show that the effluent prepared samples have a greater percentage of metal (1%) sorbed. The synergistic effect of the suspended solids and the biomass are most visible in the nickel solutions with 30% more metal being sequestered from solution.

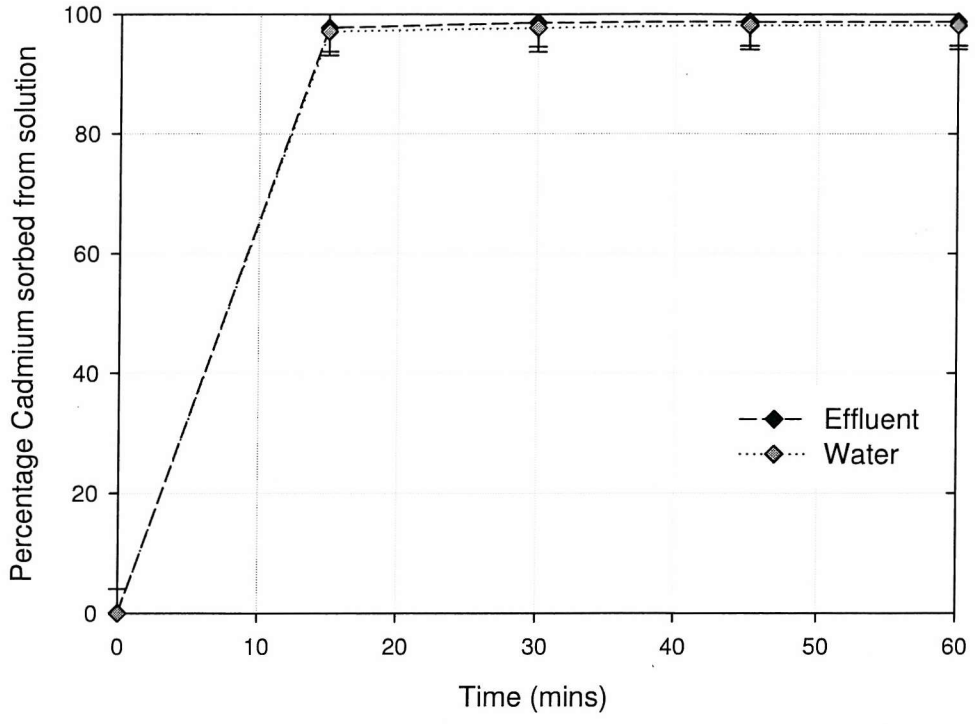

Figure 7.22 Comparison of percentage cadmium metal ion sorbed from solutions prepared with distilled water or raw wastewater effluent.

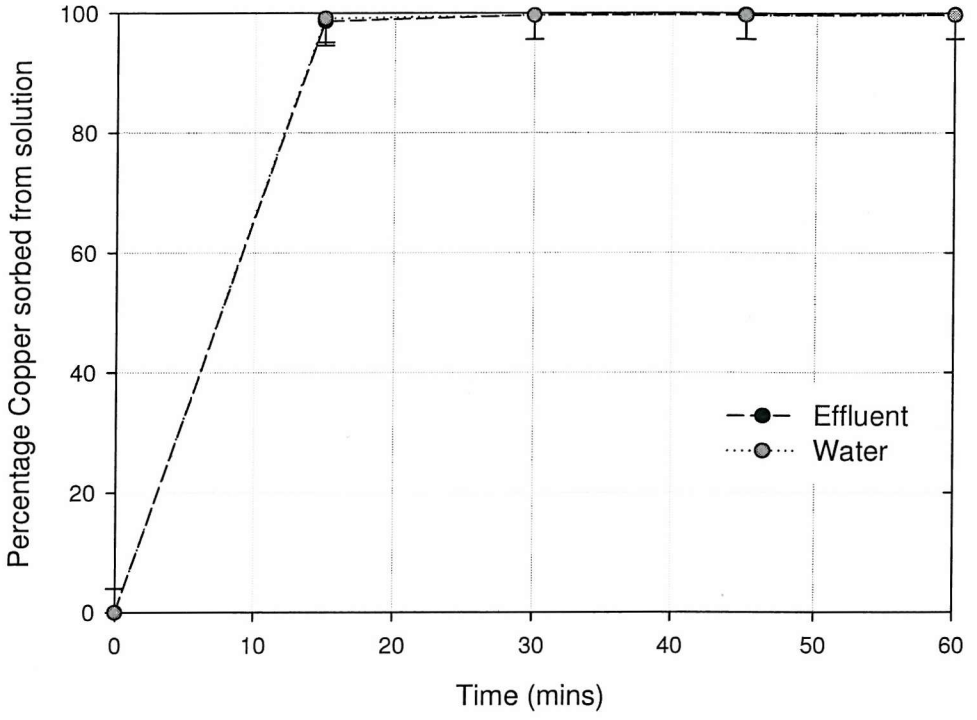

Figure 7.23 Comparison of percentage copper metal ion sorbed from solutions prepared with distilled water or raw wastewater effluent

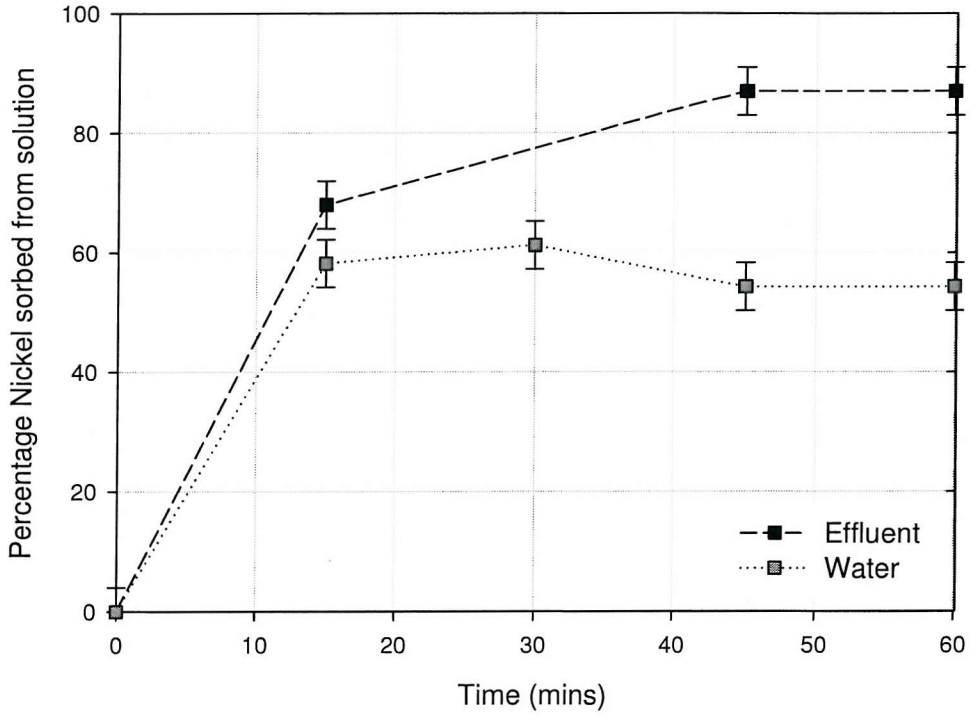

Figure 7.24 Comparison of percentage nickel metal ion sorbed from solutions prepared with distilled water or raw wastewater effluent

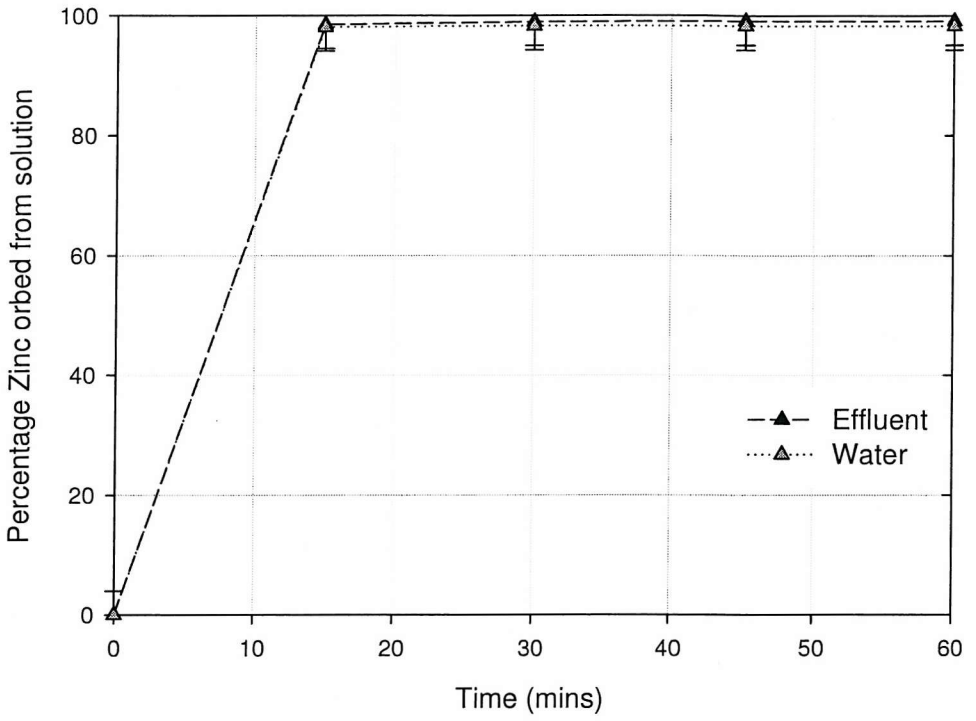

Figure 7.25 Comparison of percentage zinc metal ion sorbed from solutions prepared with distilled water or raw wastewater effluent

7.4.2. Discussion and Summary of Sorption Results for Metal Recovery from Polluted Wastewater

The results (Figure 7.22 to Figure 7.25) confirm that under mixed metal conditions and the presence of suspended impurities as would be found in real industrial effluent the sorption capacity of the SRB produced iron sulphide was not compromised. The suspended solids and biosorbent worked synergistically to reduce the overall metal concentration within the solvent; however this is more apparent for nickel which has consistently displayed a lower affinity for the biomass than the other metal ions.

Agitation of the solvent accelerated the flocculation of the suspended solids which sequestered a small proportion of some of the metal ions from solution. The remnant concentration was then sequestered by the applied biomass. The concentration of nickel ion in both control vials showed no sorption suggesting that presence of suspended solids had no effect on the amount of metal sorbed

and therefore in the test solutions all sorption was dependant entirely on the biomass. However as can be seen in Figure 7.24 there is a clear distinction between the effluent and distilled water sample. It can be proposed that the presence of the biomass promoted the agglomeration of solids which then worked synergistically to sequester the metal ions from solution.

The presence of a mixture of metal ions in solution would be expected to give rise to competition effects as was seen in previous studies (section 7.1.7) with the larger and more electronegative ions being preferentially sorbed, however all the metals, with the exception of nickel were almost completely removed from solution (>99%).

Chapter 8.

CONCLUSIONS AND RECOMMENDATIONS

8.1. Conclusions

Iron sulphide and the associated biomass and inorganic products generated by SRB have been studied as an alternative sorbent material for heavy metal recovery and biomagnetic separation. However, their commercial application has been limited. With enhanced magnetic properties these SRB generated sulphides could be poised as a new and innovative sorbent material in the ever dynamic market search for a truly innovative and efficient biosorbent.

Laboratory experiments performed during the course of this research programme focussed on developing a highly magnetic iron sulphide and evaluation of its sorption capacity and feasibility for application as a commercial sorbent. The following conclusions are derived from the experimental results, (chapters 5-7), and presented in accordance to the stated objectives detail in section 1.3.

1. The culturing mode experiments confirmed that continuous culture, although most widely used within the literature (Watson *et al.*, 1995, Watson *et al.*, 1996), does not produce a material with a sufficiently high magnetic susceptibility to allow recovery at low applied magnetic fields (<0.5T). Batch culture experiments produced a material which was approximately 3 times more magnetic than that produced during continuous culture. However due to the rapid depletion of the nutrients within the closed system, the longevity of the bacteria growth phase was restricted and similarly the amount of reactive sulphide produced which in

turn impacts on the amount and quality of magnetic sulphide produced. In the case of both batch only and continuous only culture (sections 0 and 0 respectively), the magnetic susceptibility of the sulphide was not sufficiently high to enable easy manipulation using a low magnetic field (<0.5T). This result indicates that the sulphide produced is unfavourable for cost effective separation using low field operated biomagnetic separator. The implementation of a semi-continuous growth cycle consistently yielded a highly magnetic iron sulphide during the batch culture phase (section 0). This magnetic material measured on average, 8 times more magnetic than that produced during continuous culture and an order of magnitude greater than that documented in the literature (Watson and Ellwood, 1994). This high magnetic susceptibility material was readily manipulated using a permanent magnet (0.5T) from which is can be concluded that it would be suitable for easy recovery with a low field magnetic separator .

2. The effect of the relative composition of Fe^{2+}: Fe^{3+} in the growth medium on the magnetic susceptibility of the produced microbial sulphide revealed that ferric iron (Fe^{3+}) is an essential constituent in the growth medium (section 0) . However when present in higher concentrations than ferrous iron (300:500mgL^{-1}) a negative effect on the measured magnetic susceptibility is also observed. The most magnetic material was produced when the ratio of Fe^{2+}: Fe^{3+} was 750:50mgL^{-1} (15:1 expressed empirically).

3. The literature indicates that there are 6 species of microbially produced iron sulphide compounds (Rickard, 1969), of which 3 are known to display magnetic characteristics. Characterisation of the microbial sulphide was inconclusive as the material revealed a mixed (impure) composition which included the identifiable presence of elemental sulphur (S^{O}) and vivianite ($Fe_3(PO_4)_2.8H_2O$). Amorphous (disordered) mackinawite was the only iron sulphide inferred from XRD data.

4. (a) Sorption of the test metal ions occurred rapidly with an apparent equilibrium being attained within 1-2 hours of sorbent-sorbate contact. The affinity of the sorbent biomass for the cadmium metal sorbate was found

to be related to the magnetic susceptibility (which is also related to the biomass structure) (section 7.1). The biomass with a lower magnetic susceptibility (~$7x10^{-4}$ SI units) consistently had a greater uptake of cadmium metal from solution (on average 10%) than its more magnetic counterpart (χ = ~$98x10^{-4}$SI units). However, for purposes of biomagnetic separation this difference in metal uptake is negligible in comparison to the difference in magnetic strength.

(b) Sorption isotherms showed a high degree of linearity and implied monolayer binding of the metal ions to the biomass surface (Langmuir model). Metal uptake capacity of the microbial biomass appeared to be influenced primarily by the ionic radii of the target metal ions, following the preferential order of Cd>Zn>Cu>Ni, for the metals studied. In mixed metal environments sorption competition was evident with the larger metal ion being preferentially sorbed. The rate at which the sorption reaction occurred appeared to be governed by the presence of metal ions at the surface of the biomass as well as the metal ion concentration in solution (pseudo-second order model).

5. (a) Desorption data showed the occurrence of hysteresis, with the integrity of the biomass being readily compromised after the first desorbing application and the amount of metal subsequently sorbed being reduced by over 60%. Distilled water was observed to have the least effect on the biomass structure; however it was also the least effective desorbing agent. Acetic acid and the citrate salt buffer acted as metal specific desorbing agents with good recovery of zinc and nickel (30-75%). EDTA was confirmed to be the best general elution agent as it was the only solution able to release between 35-95% of each metal ion back into solution. It appears therefore that the magnetic iron sulphide is only appropriate for single cycle usage. However, the observed sorption capacity is 3-4 times higher than that of other sorbents over a single application cycle. This high loading offsets the inability to reuse the magnetic material over multiple cycles.

In summary; this thesis has presented results showing the successful production of a highly magnetic microbial iron sulphide generated under laboratory conditions. The magnetic sulphide was achieved by applying a semi continuous growth cycle and altering the relative iron ratios within the growth medium. This work also confirmed that this magnetic sulphide can be used as an effective sorbent for tested divalent heavy metals. Commercial development of the biosorbent could benefit from additional research within the areas of characterisation of the magnetic structure of the material, upscale production processing and storage.

APPENDICES

Appendix. 1 Growth Medium Concentration

Table 1A-1 Composition of reference growth medium

	Chemical Reagent	Required concentration (gL^{-1})
Freke & Tate (Freke	Ferrous (II) Sulphate $[FeSO_4 \cdot 7H_2O]$	3.22 (650ppm Fe^{2+})
	Ferric (III) Sulphate $[Fe_2(SO_4)_3 \cdot 2H_2O]$	0.58 (150ppm Fe^{3+})
	Ammonium Sulphate $[(NH_4)_2SO_4]$	0.07
Postgate Medium C (Postgate,	Potassium Phosphate $[KH_2PO_4]$	0.5
	Sodium Sulphate $[Na_2SO_4]$	4.5
	Calcium Chloride $[CaCl_2 \cdot 2H_2O]$	0.06
	Magnesium Sulphate $[MgSO_4 \cdot 7H_2O]$	0.06
	Sodium Lactate	5ml @70%
Sodium hydroxide pellets were added as needed to raise pH to 6.7-7.0		

Table 1A-2 Iron Concentration modifications to reference medium

Iron Species	Mass of Reagent (g/L) required to attain Iron Ratio [Fe(II): Fe(III)]			
	800:0	750:50	700:100	500:300
Fe (II)	3.96	3.71	3.47	2.48
Fe(III)	-	0.19	0.39	1.17

Appendix. 2 Supporting Data for Growth medium Effect on Magnetic Susceptibility of Culture

Table A2-1: Magnetic susceptibility data for batch culture

Days	Wet Susceptibility [a] (χ_v)	Dry Weight Equivalent Mass Susceptibility [b] (χ_g) (x10^{-4}SI units)
0	0.048	5.03
3	0.046	4.82
5	0.06	6.28
7	0.066	6.91
9	0.064	6.70
11	0.062	6.49
13	0.061	6.39
15	0.06	6.28
17	0.064	6.70
19	0.064	6.70
21	0.054	6.28

Notes: [a]- Measurement taken using MSB-Auto

[b]- Calculate value correcting for moisture content

Table A2-2: Calculated susceptibility data for continuous culture experiment

	Dry Weight Equivalent Mass Susceptibility (χ_g) (x10^{-4}SI units	
Days	**Unrefined Culture**	**Magnetically Refined Culture**
0	6.28	13.28
1	4.85	15.98
2	4.31	12.93
3	5.92	10.59
4	6.28	12.03
5	7.00	13.64
6	4.67	11.85
7	-	7.72
8	4.13	6.28
9	3.77	5.21
10	3.41	6.28
11	3.41	6.28
12	1.97	3.05
13	1.97	3.23
14	1.97	2.87

Table A2-3: Calculated mass susceptibility and pH data for switch batch continuous (SBC) and continuous control (CC) bioreactor

	Switch-batch Continuous Culture (SBC) [a]		Continuous Culture (CC) [b]	
Days	pH	*Dry Weight Equivalent Mass Susceptibility (χ_g) (x10^{-4}SI units*		pH
-5	6.48	5.98	4.06	7.1
-4	6.71	3.42	2.56	7.01
-3	6.96	3.42	3.42	7.01
-2	7.11	3.63	3.42	6.5
-1	7.07	3.63	5.77	6.55
0	7.01	9.19	3.63	6.53
1	6.43	26.49	7.48	6.86
2	6.55	26.28	8.12	6.34
3	6.51	23.93	6.20	6.3
4	6.6	24.14	4.70	6.39
5	6.71	17.30	4.27	6.65
6	6.51	12.18	2.78	6.44
7	7.18	29.91	4.27	7.1
8	6.52	24.14	5.34	6.4
9	6.66	19.23	3.85	6.49
10	7.02	23.07	5.34	6.84
11	7.48	33.75	7.90	6.47
12	7.43	-	-	6.93
13	7.73	-	-	6.53
14	6.98	85.66	5.55	6.72
15	6.74	79.04	5.77	6.46
16	6.53	45.93	6.62	6.5
17	6.62	30.98	4.49	6.59
18	6.87	39.09	5.13	6.83
19	6.43	41.66	5.13	6.45
20	7.36	36.74	5.77	6.65
21	7.45	34.18	6.84	6.53
22	7.38	38.67	9.40	6.63
23	7.33	54.90	12.18	6.41
24	7.42	78.62	9.19	6.51
25	7.05	104.89	5.55	6.71
26	6.73	93.78	4.49	6.67
27	6.6	-	-	6.68
28	6.87	50.20	4.06	6.86
29	6.62	30.98	4.27	6.87
30	6.72	12.18	4.49	6.87
31	6.74	13.03	4.49	6.73
32	7.31	10.04	4.70	6.67
33	7.42	28.20	5.55	6.77
34	7.48	38.88	4.91	6.88
35	7.3	58.75	5.13	6.87
36	7.78	98.91	4.91	6.98
37	6.83	108.95	3.85	6.46
38		102.76	5.13	

39	6.96	88.01	4.70	6.52
40	6.8	-	-	6.47
41	6.7	52.55	4.49	6.82
42	6.6	33.75	7.26	6.64
43	7.3	34.18	8.12	6.83
44	7.48	27.77	8.76	6.67
45	7.54	30.12	10.04	6.66
46	7.7	34.61	9.83	6.86
47	7.29	66.22	8.33	6.69
48	7.03	79.90	8.12	6.85
49	7.1	58.53	7.05	6.82
50	6.77	48.07	11.11	6.72
51	6.84	37.81	9.19	6.76
52	6.81	25.21	7.48	6.69
53	6.84	20.08	7.05	6.81
54	-	14.31	5.77	-
55	7.47	14.10	5.98	6.9
56	7.49	-	-	6.74
57	7.53	20.94	5.98	6.84
58	7.76	22.86	6.41	6.76
59	6.97	26.06	7.48	6.81

Notes: [a]- SBC bioreactor: 5 days batch, 6 days continuous culture at dilution rate 0.028hr^{-1}. Average 11 day dilution rate = 0.015hr^{-1}

[b]- CC bioreactor: continues culture at a dilution rate of 0.028hr^{-1} until day 40. Dilution rate reduced to 0.015hr^{-1} there after.

Grey shaded area representing days in batch culture.

Appendix. 3 Supporting Data for Growth medium Effect on Magnetic Susceptibility of Culture

Table 3A-1 Calculated mass susceptibility data for phase 1 experiments

	Dry Weight Equivalent Mass Susceptibility (χ_g) (x10^{-4}SI units		
Day	**750:50[a]**	**500:300[b]**	**650:150[ca]**
-4	9.56	10.04	10.04
-3	5.84	6.20	6.69
-2	4.78	4.58	5.33
-1	3.51	3.47	4.50
0	4.67	3.35	3.35
1	3.40	3.47	7.22
2	4.46	4.71	6.59
3	4.78	5.82	7.32
4	4.14	5.95	9.20
5	4.36	5.33	5.96
6	4.04	8.67	7.32
7	4.78	6.94	7.01
8	3.82	5.33	4.08
9	2.87	3.97	1.78
10	3.40	3.47	3.03
11	3.19	2.97	4.39
12	7.54	4.71	9.10
13	12.11	4.34	8.89
14	26.66	5.33	17.99
15	62.25	6.69	29.70
16	52.58	6.69	31.58
17	51.20	3.59	27.19
18	33.35	3.10	23.53
19	23.48	2.97	22.59
20	13.38	2.35	18.09
21	14.45	2.23	14.95
22	15.40	3.97	16.52
23	22.31	4.83	17.46
24	34.95	6.07	18.61
25	47.38	6.57	22.07
26	54.28	7.06	26.77
27	34.63	5.33	20.91
28	29.95	3.72	15.90
29	15.83	2.73	14.12
30	14.23	2.97	13.49
31	11.37	2.60	11.71
32	7.54	1.86	8.16
33	7.75	1.98	10.35

Notes: [a, b,c]-: Ratio of Fe(II):Fe(III) (ppm) in growth medium

Grey shaded area representing days in batch culture

Table 3A-2: Calculated mass susceptibility data for phase 2 experiments

	Dry Weight Equivalent Mass Susceptibility (χ_g) (x10^{-4}SI units		
Day	**800:00[a]**	**700:100[b]**	**650:150[c]**
-6	14.92	14.77	17.53
-5	13.51	9.68	14.85
-4	10.81	7.26	13.71
-3	9.00	4.72	10.83
-3	8.23	3.90	9.28
-2	4.50	3.90	5.26
-1	3.73	3.63	3.71
0	3.86	3.99	4.05
1	3.73	3.99	4.74
2	3.47	4.36	5.05
3	3.73	4.24	5.46
4	3.73	4.72	7.42
5	3.34	3.63	7.01
6	2.96	2.90	6.19
7	2.83	2.66	4.12
8	2.83	2.66	3.51
9	2.32	1.94	2.99
10	2.57	2.42	3.09
11	2.57	2.54	3.51
12	2.44	2.66	3.81
13	2.70	2.90	5.46
14	2.96	3.15	7.42
15	2.70	2.90	7.63
16	2.70	2.54	6.19
17	2.83	2.30	5.77
18	2.57	2.18	5.16
19	2.19	2.18	4.33
20	-	-	-
21	1.93	1.82	3.71
22	1.67	1.82	3.51
23	1.67	2.06	4.02
24	1.93	2.18	4.33
25			
26	2.57	2.30	4.43
27	-	-	-
28	2.32	2.54	2.99
29	-	-	-
30	2.32	2.18	2.17
31	-	-	-
32	2.57	1.94	2.17
33	2.57	1.82	2.27

Notes: [a, b, c]- Ratio of Fe(II):Fe(III) (mgL^{-1}) in growth medium

Grey shaded area representing days in batch culture

Appendix. 4 Supporting Data for Sorption Experiments

Table 4A-1: Sorption data for magnetic susceptibility effects on sorption uptake

		High Magnetic Susceptibility		Low Magnetic Susceptibility	
Time	Initial Cd Conc. (mgL^{-1})	Aqueous Conc. (mgL^{-1})	% Sorbed[a]	Aqueous Conc. (mgL^{-1})	% Sorbed[a]
0	**50**	49.6	0.0	48.4	0.0
5		24.9	49.8	22.4	53.7
10		22.1	55.6	18.9	60.9
15		19.6	60.6	15.6	67.7
30		19.4	60.9	15.7	67.5
45		17.4	65.0	11.9	75.5
60		15.5	68.8	12.1	75.0
90		8.9	82.1	6.7	86.2
120		9.8	80.4	7.0	85.5
0	**150**	152.7	0.0	153.2	0.0
5		126.8	17.0	121.4	20.8
10		113.5	25.7	112.3	26.7
15		118.2	22.6	113.8	25.7
30		114.2	25.2	108.5	29.2
45		107.6	26.0	97.0	30.0
60		106.8	28.0	104.6	32.0
90		126.4	29.5	118.0	36.7
120		123.7	30.1	116.7	31.7
0	**500**	512.5	0.0	517.5	0.0
5		501.4	2.2	487.7	5.8
10		487.1	5.0	468.0	9.6
15		467.7	8.7	453.6	12.3
30		464.6	9.3	457.9	11.5
45		469.4	8.4	454.7	12.1
60		455.7	11.1	433.3	16.3
90		399.3	22.1	386.6	25.3
120		376.4	26.6	352.8	31.8

Notes [a]:- Calculated using equation 4.5

Table 4A-2: Sorption Isotherm data for microbial iron sulphide on test metals

Metal	Conc.	Initial Conc. (mgL^{-1})	Aqueous Conc. (mgL^{-1})	Conc. Sorbed (mgL^{-1})	M (g)
Cadmium	10	8.7	0.0	8.7	1.17E-02
		9.4	0.0	9.4	1.17E-02
	50	49.7	0.2	49.5	1.14E-02
		47.8	0.2	47.6	1.14E-02
	100	102.3	0.2	102.1	1.27E-02
		91.7	0.2	91.5	1.27E-02
	200	240.8	9.8	231.0	1.04E-02
		187.7	9.9	177.8	1.04E-02
	500	502.5	356.1	146.4	9.82E-03
		507.7	357.7	150.0	9.82E-03
Zinc	10	9.2	0.4	8.8	1.65E-02
		9.7	0.4	9.3	1.65E-02
	50	54.4	0.8	53.6	1.13E-02
		52.0	0.8	51.2	1.13E-02
	100	84.5	15.3	69.2	1.39E-02
		90.1	15.4	74.7	1.39E-02
	200	181.4	117.9	63.5	1.03E-02
		184.4	119.1	65.3	1.03E-02
	500	483.5	376.6	106.9	1.38E-02
		481.4	377.4	104.1	1.38E-02
Copper	10	8.2	0.4	7.8	6.80E-03
		8.2	0.5	7.7	6.80E-03
	50	46.4	0.9	45.5	2.03E-02
		48.0	0.9	47.0	2.03E-02
	100	99.0	2.6	96.4	2.06E-02
		94.5	2.8	91.7	2.06E-02
	200	196.3	1.4	194.8	2.01E-02
		198.3	1.5	196.8	2.01E-02
	500	488.0	247.2	240.8	6.52E-02
		481.0	221.9	259.1	6.52E-02
Nickel	10	8.2	2.1	6.1	2.20E-02
		9.7	2.6	7.1	2.20E-02
	50	48.7	18.1	30.6	1.91E-02
		49.6	18.7	30.9	1.91E-02
	100	96.9	63.5	33.4	1.99E-02
		99.0	67.3	31.7	1.99E-02
	200	190.3	136.1	54.2	2.42E-02
		194.3	136.5	57.8	2.42E-02
	500	484.0	411.4	72.6	2.24E-02
		486.2	426.9	59.3	2.24E-02

Table 4A-3: Soprtion Kinetics data for single and binary metal solutions

		Single metal Solution		Binary metal solution[a]	
Cadmium	Time	Conc in solution	% sorbed[c]	Conc in solution	% sorbed[c]
	0	125.00	0.00	125.00	0.00
	5	37.25	70.20	8.97	92.82
	15	12.07	90.34	5.99	95.21
	30	1.48	98.82	1.18	99.06
	45	0.97	99.22	0.10	99.99
	60	0.14	99.89	0.10	99.99

		Single metal Solution		Binary metal solution[a]	
Zinc	Time	Conc in solution	% sorbed[c]	Conc in solution	% sorbed[c]
	0	125.00	0.00	125.00	0.00
	5	72.92	41.66	118.57	5.15
	15	72.00	42.40	115.18	7.86
	30	76.72	38.63	108.37	13.31
	45	64.20	48.64	103.77	16.99
	60	53.73	57.02	100.42	19.66

		Single metal Solution		Binary metal solution[b]	
Copper	Time	Conc in solution	% sorbed[c]	Conc in solution	% sorbed[c]
	0	125.00	0.00	125.00	0.00
	5	55.96	55.23	55.52	55.58
	15	24.31	80.55	35.26	71.79
	30	18.56	85.15	33.88	72.90
	45	15.10	87.92	32.57	73.94
	60	14.44	88.45	31.78	74.58

		Single metal Solution		Binary metal solution[b]	
Nickel	Time	Conc in solution	% sorbed[c]	Conc in solution	% sorbed[c]
	0	138.00	0.00	142.00	0.00
	5	118.28	14.29	134.71	5.13
	15	114.85	16.78	136.70	3.73
	30	110.00	20.29	139.63	1.67
	45	110.74	19.75	136.13	4.13
	60	111.43	19.25	135.40	4.65

Notes [a]- Cd-Zn binary metal solution

[b]- Cu-Ni binary metal solution

[c]:- Calculated using equation 4.5

Appendix. 5 Supporting Data for desorption results

Table 5A-1 Cadmium desorption data for reusability of microbial biomass

		1st Sorption		1st Desorption		2nd Soprtion	
	C_O	C_{sorbed}	% sorb	C_{desorb}	% desorb	C_{sorb}	% sorbed
	100.25	98.56	98.31	0.79	0.80	21.53	21.48
Water	100.45	99.29	98.84	0.93	0.94	21.35	21.25
Acetic	104.6	102.42	97.91	1.42	1.39	7.55	7.22
Acid	105.44	104.14	98.77	1.43	1.37	7.64	7.24
						0	
Citrate	106.51	104.51	98.12	1.06	1.01	14.76	13.86
Buffer	107.78	104.38	96.84	1.26	1.21	15.14	14.05
						0	
	104.78	103.67	98.94	100.33	96.78	18.59	17.74
EDTA	101.73	100.7	98.99	98.95	98.26	16.38	16.10

Table 5A-2 Zinc desorption data for reusability of microbial biomass

		1st Sorption		1st Desorption		2nd Soprtion	
	C_O	C_{sorbed}	% sorb	C_{desorb}	% desorb	C_{sorb}	% sorbed
	110.94	105.54	95.131	0.71	0.673	30.80	27.77
Water	103.49	98.28	94.97	0.521	0.53	19.34	18.69
Acetic	102.45	48.58	47.42	30.29	62.35	11.01	10.74
Acid	101.39	48.44	47.77	31.9	65.86	11.23	11.08
Citrate	101.82	62.48	61.36	60.16	96.29	10.07	9.89
Buffer	84.31	45.55	54.02	58.6	128.65	4.90	79.72
	109.05	61.54	56.44	35.07	56.98	8.62	7.90
EDTA	126.68	88.98	70.24	37.43	42.06	32.72	25.83

Table 5A-3 Copper desorption data for reusability of microbial biomass

		1st Sorption		1st Desorption		2nd Soprtion	
	C_O	C_{sorbed}	% sorb	C_{desorb}	% desorb	C_{sorb}	% sorb
	102.43	101.59	99.18	0.39	0.38	20.47	19.98
Water	104.49	102.77	98.35	0.39	0.38	22.39	21.43
Acetic	109.28	108.04	98.86	2.09	1.93	7.02	6.43
Acid	107.22	106.61	99.43	3.86	3.62	2.12	1.98
Citrate	128.13	126.29	98.56	0.08	0.06	11.06	8.63
Buffer	126.97	126.55	99.67	0.08	0.06	126.97	
	117.06	116.98	99.93	35.81	30.61	7.75	6.62
EDTA	111.36	111.28	99.93	31.88	28.65		

Table 5A-4 Nickel desorption data for reusability of microbial biomass

		1st Sorption		1st Desorption		2nd Soprtion	
	C_O	C_{sorbed}	% sorb	C_{desorb}	% desorb	C_{sorb}	% sorb
	108.41	26.98	24.89	7.68	28.46	0.64	0.59
Water	110.76	28.21	25.47	7.85	27.83	0.76	0.68
Acetic	117.80	28.706	24.37	20.23	70.47	1.39	1.18
Acid	114.59	24.48	21.363	48.72	199.02	0.28	0.24
						0	
Citrate	120.93	22.79	18.84	58.05	254.72	0.05	0.04
Buffer	124.19	27.54	22.17	20.28	73.64	3.31	2.66
	123.9	23.15	18.68	43.69	188.72	3.18	2.56
EDTA	123.23	29.66	24.07	18.11	61.06	3.03	2.46

Appendix. 6 Supporting Data for sorption/desorption cycle of synthetic iron sulphide

Table 6A-1 Cadmium sorption/desorption/sorption data for synthetic iron sulphide

		1st Sorption		1st Desorption		2nd Sorption	
	C_o	C_{sorb}	% sorb	C_{desorb}	% desorb	C_{sorb}	% sorb
Citrate Buffer	102.26	98.05	95.88	2.43	2.48	8.37	8.19
	101.98	99.63	97.69	2.23	2.24	8.09	7.94
						0	
EDTA	104.33	100.02	95.87	2.19	2.19	0.09	0.09
	104.89	102.1	97.34	2.01	1.97	0.35	0.33

Table 6A-2 Zinc sorption/desorption/sorption data for synthetic iron sulphide

		1st Sorption		1st Desorption		2nd Sorption	
	C_o	C_{sorb}	% sorb	C_{desorb}	% desorb	C_{sorb}	% sorb
Citrate Buffer	111.319	48.70	43.75	33.68	69.15	0.63	0.56
	111.31	50.33	45.22	28.33	56.29	0.63	0.56
						0	
EDTA	118.18	45.76	38.72	6.93	15.14	7.71	6.52
	118.18	51.39	43.48	6.78	13.20	7.71	6.52

Table 6A-3 Copper sorption/desorption/sorption data for synthetic iron sulphide

		1st Sorption		1st Desorption		2nd Sorption	
	C_o	C_{sorb}	% sorb	C_{desorb}	% desorb	C_{sorb}	% sorb
Citrate Buffer	106.36	100.27	94.27	69.81	69.62	9.55	8.98
	105.78	101.45	95.91	62.92	62.02	8.97	8.48
EDTA	109.18	105.42	96.56	0.003	0.003	12.36	11.32
	110.23	108.3	98.25	0.003	0.0037	1.1	1.00

Table 6A-4 Nickel sorption/desorption/sorption data for synthetic iron sulphide

		1st Sorption		1st Desorption		2nd Sorption	
	C_o	C_{sorb}	% sorb	C_{desorb}	% desorb	C_{sorb}	% sorb
Citrate Buffer	122.38	106.75	87.23	7.97	7.472	0.38	0.31
	125.01	12.1	9.68	8.09	66.86	0.01	0.08
						0	
EDTA	104.33	100.02	95.87	2.19	2.19	0.09	0.09
	104.89	102.1	97.34	2.01	1.97	0.35	0.33

Appendix. 7 Supporting data for metal sorption from wastewater environment

Table 7A-1 Cadmium sorption data for microbial sulphide biomass from multimetal environment

	H_2O medium		Effluent medium	
time	C_{sorbed}	% sorbed	C_{sorbed}	% sorbed
0	0.00	0.00	0.00	0.00
15	12.11	97.08	12.01	97.71
30	12.18	97.68	12.11	98.54
45	12.24	98.16	12.14	98.73
60	12.24	98.16	12.14	98.73

Table 7A-2 Zinc sorption data for microbial sulphide biomass from multimetal environment

	H_2O medium		Effluent medium	
time	C_{sorbed}	% sorbed	C_{sorbed}	% sorbed
0	0.00	0.00	0.00	0.00
15	11.27	98.12	13.06	98.53
30	11.29	98.29	13.12	98.98
45	11.29	98.30	13.14	99.10
60	11.29	98.30	13.14	99.10

Table 7A-3 Copper sorption data for microbial sulphide biomass from multimetal environment

	H_2O medium		Effluent medium	
time	C_{sorbed}	% sorbed	C_{sorbed}	% sorbed
0	0.00	0.00	0.00	0.00
15	14.37	99.10	11.13	98.63
30	14.44	99.60	11.24	99.63
45	14.45	99.66	11.25	99.73
60	14.45	99.66	11.25	99.73

Table 7A-4 Nickel sorption data for microbial sulphide biomass from multimetal environment

	H_2O medium		Effluent medium	
time	C_{sorbed}	% sorbed	C_{sorbed}	% sorbed
0	0.00	0.00	0.00	0.00
15	7.55	58.20	9.05	67.97
30	7.95	61.23		
45	7.04	54.26	11.58	86.97
60	7.04	54.26	11.58	86.97

REFERENCES

AHALYA, N., RAMACHANDRA, T. V. & KANAMADI, R. D. (2003) Biosorption of Heavy Metals. *Research Journal of Chemistry and Environment,* 7, 71-79.

ALI, A. A., COOPER, D. G. & NEUFELD, R. J. (1987) Uptake of Metal-Ions by Sulfonated Pulp. *Journal Water Pollution Control Federation,* 59, 109-114.

AMORIM, W. B., HAYASHI, A. M., PIMENTEL, P. F. & DA SILVA, M. G. C. (2003) A study of the process of desorption of hexavalent chromium. *Brazilian Journal of Chemical Engineering,* 20, 283-289.

ARFIN, B., BONO, A. & JANAUN, J. (2006) The Transformation of Chicken Manure into Mineralised Organic Fertilizer *Journal of Sustainability Science and Management,* 1, 58-63.

ATKINSON, B. W., BUX, F. & KASAN, H. C. (1998) Considerations for application of biosorption technology to remediate metal-contaminated industrial effluents. *Water Sa,* 24, 129-135.

BAHAJ, A. S., CROUDANCE, I. W., JAMES, P. A. B., MOESCHLER, F. D. & WARWICK, P. E. (1998a) Continuous Radionuclide Recovery From Wastewater Using Magnetotactic Bacteria. *Journal of Magnetism and Magnetic Materials,* 184, 241-244.

BAHAJ, A. S., ELLWOOD, D. C. & WATSON, J. H. P. (1991) Extraction of Heavy-Metals Using Microorganisms and High-Gradient Magnetic Separation. *IEEE Transactions on Magnetics,* 27, 5371-5374.

BAHAJ, A. S. & JAMES, P. A. B. (1994) Metal Uptake and Separation Using Magnetotactic Bacteria. *IEE Transactions on Magnetics,* 30, 4707-4709.

BAHAJ, A. S., JAMES, P. A. B. & MOESCHLER, F. D. (1996) High Gradient Magnetic Separation of Motile and Non-Motile Bacteria. *IEE Transactions on Magnetics,* 32, 5106-5108.

BAHAJ, A. S,, JAMES, P. A. B. & MOESCHLER, F. D. (1998b) A Comparative Study of the Magnetic Separation Characteristics of Magnetotactic and Sulphate Reducing Bacteria. *Journal of Applied Physics,* 83, 6444-6446.

BAHAJ, A. S., JAMES, P. A. B. & MOESCHLER, F. D. (1998c) Low Magnetic Field Separation System for Metal Loaded Magnetotactic Bacteria. *Journal of Magnetism and Magnetic Materials,* 177-181, 1453-1454.

BAHAJ, A. S., WATSON, J. H. P. & ELLWOOD, D. C. (1989) Determination of Magnetic Susceptibility of Load Mirco-Organisms in Bio-Magnetic Separation. *IEE Transactions on Magnetics,* 25, 3809-3811.

BASU, S. K., MINO, T. & OLESZKIEWICZ, J. A. (1995) Novel Application of Sulphur Metabolism in Domestic Wastewater Treatment. *Canadian Journal of Civil Engineering,* 22, 1217-1223.

BEIJERINCK, W. M. (1895) Ueber Spirillum desulfuricans als Ursache von Sulfatreduction. *Centralbl Bakteriol II,* Abt.1, 1-9, 49-59, 104-114.

BENNING, L. G., WILKIN, R. T. & BARNES, H. L. (2000) Reaction pathways in the Fe-S system below 100 degrees C. *Chemical Geology,* 167, 25-51.

BLAKEMORE, R. (1975) Magnetotactic Bacteria. *Science,* 190, 377-379.

BRAIDA, W. J., PIGNATELLO, J. J., LU, Y. F., RAVIKOVITCH, P. I., NEIMARK, A. V. & XING, B. S. (2003) Sorption hysteresis of benzene in charcoal particles. *Environmental Science & Technology,* 37, 409-417.

BSI (1990) Part 2 Classification Tests. IN BSI (Ed.) *Methods of Tests for Soils for Civil Engineering Purposes.*

BSI (2005) Determination of Suspended Solids: Method by filtration through glass fibre filters. IN BSI (Ed.) *Water Quality.*

CASTRO, H. F., WILLIAMS, N. H. & OGRAM, A. (2000) Phylogeny of sulfate-reducing bacteria^1. *Fems Microbiology Ecology,* 31, 1-9.

CELIK, A. & DEMIRBAS, A. (2005) Removal of heavy metal ions from aqueous solutions via adsorption onto modified lignin from pulping wastes. *Energy Sources,* 27, 1167-1177.

CHEN, B. Y., UTGIKAR, V. P., HARMON, S. M., TABAK, H. H., BISHOP, D. F. & GOVIND, R. (2000) Studies on biosorption of zinc(II) and copper(II) on Desulfovibrio desulfuricans. *International Biodeterioration & Biodegradation,* 46, 11-18.

CHEUNG, C. W., PORTER, J. F. & MCKAY, G. (2001) Sorption kinetic analysis for the removal of cadmium ions from effluents using bone char. *Water Research,* 35, 605-612.

CHRISTENSEN, B., LAAKE, M. & LIEN, T. (1996) Treatment of Acid Mine Water by Sulfate Reducing Bacteria; Results from a Bench Scale Experiment. *Water Research,* 30, 1617-1624.

CHU, K. H., HASHIM, M. A., PHANG, S. M. & SAMUEL, V. B. (1997) Biosorption of cadmium by algal biomass: Adsorption and desorption characteristics. *Water Science and Technology,* 35, 115-122.

CIMINO, G., PASSERINI, A. & TOSCANO, G. (2000) Removal of toxic cations and Cr(VI) from aqueous solution by hazelnut shell. *Water Research,* 34, 2955-2962.

CLINE, J. D. (1969) Spectrophotometric Determination of Hydrogen Sulfide in Natural Waters. *Limnology and Oceanography,* 14, 454-458.

COE, B. T., GERBER, R. & WITTS, D. (1998) High Gradient Magnetic Separation of a Biologically Produced FeS Adsorbent using Sulphate Reducing Bacteria. *IEE Transactions on Magnetics,* 34, 2126-2128.

COLEMAN, M. L., HEDRICK, D. B., LOVLEY, D. R., WHITE, D. C. & PYE, K. (1993) Reduction of Fe(Iii) in Sediments by Sulfate-Reducing Bacteria. *Nature,* 361, 436-438.

CORDERO, B., LODEIRO, P., HERRERO, R. & DE VICENTE, M. E. S. (2004) Biosorption of Cadmium by Fucus spiralis. *Environmental Chemistry,* 1, 180-187.

DALEY, R. J. & HOBBIE, J. E. (1975) Direct Counts of Aquatic Bacteria by a Modified Epi-fluorescent Technique. *Liminology and Oceanography,* 20, 875-882.

DAVIS, J. E. (2000) Geochemical Controls on Arsenic and Phosphorus In Natural and Engineered Systems. *Civil Engineering.* Virginia, Virginia Technical.

DAVIS, T. A., VOLESKY, B. & VIEIRA, R. H. S. F. (2000) *Sargassum* Seaweed as Biosorbent for Heavy Metals. *Water Research,* 34, 4270-4278.

DUFFUS, J. H. (2002) "Heavy metals" - A meaningless term? (IUPAC technical report). *Pure and Applied Chemistry,* 74, 793-807.

EHRLICH, H. L. (1997) Microbes and Metals. *Applied Microbiology and Biotechnology,* 48, 687-692.

EPA (1999a) Volume I: The K_d Model, Methods of Measurement, and Applicaiton of Chemical Reaction Codes. IN EPA (Ed.) *Understanding Variation in Partition Coefficient, K_d, Values.*

EPA (1999b) Volume II: Review of Geochemistry and Available K_d Values for Cadmium, Chromium, Lead, Plutonium, Radon, Strontium, thorium, Tritium (^3H) and Uranium. IN EPA (Ed.) *Understanding Variation in Partition Coefficient, K_d, Values.*

EPA (2000) Chemical Precipitation. IN EPA, U. S. (Ed.) *Wastewater Technology Fact Sheet.* Washington, D.C.

FOSSING, H. & JORGENSEN, B. B. (1989) Measurement of Bacterial Sulfate Reduction in Sediments - Evaluation of a Single-Step Chromium Reduction Method. *Biogeochemistry,* 8, 205-222.

FOUCHER, S., BATTAGLIA-BRUNET, F., IGNATIADIS, I. & MORIN, D. (2001) Treatment by sulfate-reducing bacteria of Chessy acid-mine drainage and metals recovery. *Chemical Engineering Science,* 56, 1639-1645.

FRANKEL, R. B., BLAKEMORE, R. P. & WOLFE, R. S. (1979) Magnetite in Freshwater Magnetotactic Bacteria. *Science,* 203, 1355-1356.

FREKE, A. M. & TATE, D. (1961) The Formation of Magnetic Iron Sulphide by Bacterial Reduction of Iron Solutions. *Journal of Biochemical and Microbiological Technology and Engineering,* 3, 29-39.

FU, T. T. (2005) Influence of Sulfate Reducing Bacteria and Spartina Alterniflora on Mercury Methylation in Simulated Salt Marsh Systems. *School of Civil and Environmental Engineering.* Georgia, Georgia Institute of Technology.

GAO, Y., KAN, A. T. & TOMSON, M. B. (2003) Critical evaluation of desorption phenomena of heavy metals from natural sediments. *Environmental Science & Technology,* 37, 5566-5573.

GARCIA, C., MORENO, D. A., BALLESTER, A., BLAZQUEZ, M. L. & GONZALEZ, F. (2001) Bioremediation of an industrial acid mine water by metal-tolerant sulphate-reducing bacteria. *Minerals Engineering,* 14, 997-1008.

GULNAZ, O., SAYGIDEGER, S. & KUSVURAN, E. (2005) Study of Cu(II) biosorption by dried activated sludge: effect of physico-chemical environment and kinetics study. *Journal of Hazardous Materials,* 120, 193-200.

HAN, J. S., PARK, J. K. & MIN, S. H. (2000) Removal of Toxic Heavy Metal Ions in Runoffs by Modified Alfalfa and Juniper. IN COMMITTEE, I. P. C. A. H. O. (Ed.) *1st World Congress of the International Water Association.* Paris, France.

HERBERT, R. B., BENNER, S. G., PRATT, A. R. & BLOWES, D. W. (1998) Surface chemistry and morphology of poorly crystalline iron sulfides precipitated in media containing sulfate-reducing bacteria. *Chemical Geology,* 144, 87-97.

HO, Y. S. (2003) Removal of copper ions from aqueous solution by tree fern. *Water Research,* 37, 2323-2330.

HO, Y. S. & MCKAY, G. (1999) Pseudo-second order model for sorption processes. *Process Biochemistry,* 34, 451-465.

HO, Y. S. & MCKAY, G. (2000) The kinetics of sorption of divalent metal ions onto sphagnum moss peat. *Water Research,* 34, 735-742.

HO, Y. S., NG, J. C. Y. & MCKAY, G. (2000) Kinetics of Pollutant Sorption by Biosorbents: Review. *Separation and Purification Methods,* 29, 189-232.

HOBBIE, J. E., DALEY, R. J. & JASPER, S. (1977) Use of Nuclepore Filters for Counting Bacteria by Fluorescence Microscopy. *Applied and Environmental Microbiology,* 33, 1225-1228.

HOLAN, Z. R., VOLESKY, B. & PRASETYO, I. (1993) Biosorption of Cadmium by Biomass of Marine-Algae. *Biotechnology and Bioengineering,* 41, 819-825.

HORSFALL, M. & SPIFF, A. I. (2005) Sorption of lead, cadmium, and zinc on sulfur-containing chemically modified wastes of fluted pumpkin (Telfairia occidentalis HOOK f.). *Chemistry & Biodiversity,* 2, 373-385.

HUGGINS, M. L. (1922) The Crystal Structures of Marcasite (FeS_{2}), Arsenopyrite (FeAsS) and Loellingite (FeAs_{2}). *Physical Review,* 19, 369.

HURTGEN, M. T., LYONS, T. W., INGALL, E. D. & CRUSE, A. M. (1999) Anomalous enrichments of iron monosulfide in euxinic marine sediments and the role of H2S in iron sulfide transformations: Examples from Effingham Inlet, Orca Basin, and the Black Sea. *American Journal of Science,* 299, 556-588.

JALALI, K. & BALDWIN, S. A. (2000) The Role of Sulphate Reducing Bacteria in Copper Removal From Aqueous Sulphate Solutions. *Water Research,* 34, 797-806.

JEFFREY, R. & MELCHERS, R. E. (2003) Bacteriological influence in the development of iron sulphide species in marine immersion environments. *Corrosion Science,* 45, 693-714.

JONG, T. & PARRY, D. L. (2004) Adsorption of Pb(II), Cu(II), Zn(II), Ni(II), Fe(II), and As(V) on bacterially produced metal sulphides. *Journal of Colloid and Interface Science,* 275, 61-71.

KAWAGUCHI, R., BURGESS, J. G., SAKAGUCHI, T., TAKEYAMA, H., THORNHILL, R. & MATSUNAGA, T. (1995) Phylogenetic Analysis of a Novel Sulphate Reducing Magnetic Bacterium, RS-1, Demonstrates its Membership of the δ-Proteobacteria. *FEMS Microbiology Letters,* 126, 277-282.

KOTRBA, P., DOLECKOVA, L., DE LORENZO, V. & RUML, T. (1999) Enhanced Bioaccumulation of Heavy Metal Ions by Bacterial Cells Due to Surface Display of Short Metal Binding Peptides. *Applied and Environmental Microbiology,* 65, 1092-1098.

KRATOCHVIL, D. & VOLESKY, B. (1998) Advances in the Biosorption of Heavy Metals. *Trends in Biotechnology,* 16, 291-300.

LANGMUIR, I. (1918) The Adsorption of Gases on Plane Surfaces of Glass, Mica and Platinum. *Journal of the American Chemical Society,* 40, 1361-1403.

LENNIE, A. R., REDFERN, S. A. T., CHAMPNESS, P. E., STODDART, C. P., SCHOFIELD, P. F. & VAUGHAN, D. J. (1997) Transformation of mackinawite to greigite: An in situ X-ray powder diffraction and transmission electron microscope study. *American Mineralogist,* 82, 302-309.

LIDE, D. R. (1996) *CRC Handbook of Chemistry and Physics: A Ready Reference Book of Chemical and Physical Data,* Boca Raton, CRC Press.

LLOYD, J. R. (2002) Bioremediation of Metals; The Application of Micro-organisms That Make and Break Minerals. *Microbiology Today,* 29, 67-69.

LLOYD, J. R. & MACASKIE, L. E. (1996) A Novel PhosphorImager-Based Technique for Monitoring the Microbial Reduction of Technetium. *Applied and Environmental Microbiology,* 62, 578-582.

LOUBINOUX, J., BRONOWICKI, J.-P., PEREIRA, I. A. C., MOUGENEL, J.-L. & FAOU, A. E. (2002) Sulfate-Reducing Bacteria in Human Feces and Their Association with Inflammatory Bowel Diseases. *FEMS Microbiology Ecology,* 40, 107-112.

LUPTAKOVA, A. & KUSNIEROVA, M. (2005) Bioremediation of Acid Mine Drainage Contaminated by SRB. *Hydrometallurgy,* 77, 97-102.

MACMILLAN, B. (2000) The Possible Use of Bacterially Produced Iron Sulphide in the Clean-up of Land and Water Resources Contaminated by Heavy Metals and or by Organic Pollution. *Centre for Environmental Sciences.* Southampton, University of Southampton.

MAHVI, A. H., NAGHIPOUR, D., VAEZI, F. & NAZMARA, S. (2005) Teawaste as an Adsorbent for Heavy Metal Removal from Industrial Wastewaters. *American Journal of Applied Sciences,* 2, 372-375.

MARIUS, M. S., JAMES, P. A. B., BAHAJ, A. S. & SMALLMAN, D. J. (2005) Development of a Highly Magnetic Iron Sulphide for Metal Uptake and Magnetic Separation. *Journal of Magnetism and Magnetic Materials,* 293, 567-571.

MATIAS, P. M., PEREIRA, I. A. C., SOARES, C. M. & CARRONDO, M. A. (2005) Sulphate Respiration from Hydrogen in Desulfovibrio Bacteria: A Structural Biology Overview. *Progress in Biophysics & Molecular Biology,* 89, 292-329.

MCKAY, G. & PORTER, J. F. (1997) Equilibrium Parameters for the Sorption of Copper, Cadmium and Zinc Ions onto Peat. *Journal of Chemical Technology and Biotechnology,* 69, 309-320.

MERROUN, M. L. & SELENSKA-POBELL, S. (2001) Interactions of three eco-types of Acidithiobacillus ferrooxidans with U(VI). *Biometals,* 14, 171-179.

MIN, S. H., HAN, J. S., SHIN, E. W. & PARK, J. K. (2004) Improvement of cadmium ion removal by base treatment of juniper fiber. *Water Research,* 38, 1289-1295.

MIYANAMI, K., TOJO, K., YOKOTA, M., FUJIWARA, Y. & ARATANI, T. (1982) Effect of Mixing on Flocculation. *Industrial and Engineering Chemistry Fundamentals,* 21, 132-135.

MORICE, J. A., REES, L. V. C. & RICKARD, D. T. (1969) Mossbauer Studies of Iron Sulphides. *Journal of Inorganic and Nuclear Chemistry,* 31, 3797-3802.

MORSE, J. W. & ARAKAKI, T. (1993) Adsorption and coprecipitation of divalent metals with mackinawite (FeS). *Geochimica et Cosmochimica Acta,* 57, 3635-3640.

NAMASIVAYAM, C. & KADIRVELU, K. (1997) Agricultural solid wastes for the removal of heavy metals: adsorption of Cu(II) by coirpith carbon. *Chemosphere,* 34, 377-399.

NOVICK, A. & SZILARD, L. (1950) Description of the Chemostat. *Science,* 112, 715-716.

OBERTEUFFER, J. A. (1974) Magnetic Separation: A Review of Principles, Devices and Applications. *IEE Transactions on Magnetics,* Mag. 10, 223-238.

OKABE, S., NIELSEN, P. H., JONES, W. L. & CHARACKLIS, W. G. (1995) Sulfide Product Inhibition of Desulfovibrio Desulfuricans in Batch and Continuous Cultures. *Water Research,* 29, 571-578.

PAGNANELLI, F., MAINELLI, S. & TORO, L. (2005) Optimisation and validation of mechanistic models for heavy metal bio-sorption onto a natural biomass. *Hydrometallurgy,* 80, 107-125.

PAGNANELLI, F., PAPINI, M. P., TORO, L., TRIFONI, M. & VEGLIO, F. (2000) Biosorption of metal ions on Arthrobacter sp.: Biomass characterization and biosorption modeling. *Environmental Science & Technology,* 34, 2773-2778.

PANAYOTOVA, M. & VELIKOV, B. (2002) Kinetics of heavy metal ions removal by use of natural zeolite. *Journal of Environmental Science and Health Part a-Toxic/Hazardous Substances & Environmental Engineering,* 37, 139-147.

PATZAK, M., DOSTALEK, P., FOGARTY, R. V., SAFARIK, I. & TOBIN, J. M. (1997) Development of magnetic biosorbents for metal uptake. *Biotechnology Techniques,* 11, 483-487.

PAUL, F., MELVILLE, D. & ROATH, S. (1979) Axial Particle Trajectory Measurements in High Gradient Magnetic Separation. *IEE Transactions on Magnetics,* Mag.15, 989-991.

POSTGATE, J. R. (1979) *The Sulphate Reducing Bacteria,* Cambridge, Cambridge Univeristy Press.

QUEK, S. Y., WASE, D. A. J. & FORSTER, C. F. (1998) The use of sago waste for the sorption of lead and copper. *Water Sa,* 24, 251-256.

RICKARD, D. (1995) Kinetics of FeS Precipitation: Part 1. Competing Reaction Mechanisms. *Geochimica et Cosmochimica Acta,* 59, 4367-4379.

RICKARD, D. & LUTHER, G. W. (1997) Kinetics of pyrite formation by the H2S oxidation of iron(II) monosulfide in aqueous solutions between 25 and 125 degrees C: The mechanism. *Geochimica Et Cosmochimica Acta,* 61, 135-147.

RICKARD, D. & MORSE, J. W. (2005) Acid volatile sulfide (AVS). *Marine Chemistry,* 97, 141-197.

RICKARD, D. T. (1969) The Microbiological Formation of Iron Sulphides. *Stockholm Contributions in Geology,* 20, 55-66.

RIETMEIJER, F. J. M. (2002) Thermal Modifications of Silicate Materials on Flash-Heated Sulphide IDPs: The First Clues for Chemically Controlled, Early Silicate Mineral Evolution. *Lunar and Planetary Science XXXIII.* Houston, Texas, Lunar and Planetary Institute.

SAEED, A. & IQBAL, M. (2003) Bioremoval of cadmium from aqueous solution by black gram husk (Cicer arientinum). *Water Research,* 37, 3472-3480.

SAKAGUCHI, T., BURGESS, J. G. & MATSUNAGA, T. (1993) Magnetite Formation by a Sulphate Reducing Bacterium. *Nature,* 365, 47-49.

SANDER, M., LU, Y. F. & PIGNATELLO, J. J. (2005) A Thermodynamically Based Method to Quantify True Sorption Hysteresis. *Journal of Environmental Quality,* 34, 1063-1072.

SCHNEIDER, I. A. H., RUBIO, J. & SMITH, R. W. (2001) Biosorption of Metals onto Plant Biomass: Exchange Adsorption or Surface Precipitation? *International Journal of Mineral Processing,* 62, 111-120.

SCHOONEN, M. A. A. & BARNES, H. L. (1991a) Reactions Forming Pyrite and Marcasite from Solution: I. Nucleation of FeS_2 below 100[deg]C. *Geochimica et Cosmochimica Acta,* 55, 1495-1504.

SCHOONEN, M. A. A. & BARNES, H. L. (1991b) Reactions Forming Pyrite and Marcasite from Solution: II. Via FeS Precursors Below 100[deg]C. *Geochimica et Cosmochimica Acta,* 55, 1505-1514.

SCHULTZELAM, S., FORTIN, D., DAVIS, B. S. & BEVERIDGE, T. J. (1996) Mineralization of Bacterial Surfaces. *Chemical Geology,* 132, 171-181.

SCHWARTZ, T., HOFFMANN, S. & OBST, U. (1998) Formation and Bacterial Composition of Young, Natural Biofilms Obtained from Public Bank-filtered Drinking Water Systems. *Water Research,* 32, 2787-2797.

SCIBAN, M., KLASNJA, M. & SKRBIC, B. (2006) Modified Hardwood Sawdust as Adsorbent of Heavy Metal Ions from Water. *Wood Science and Technology,* 40, 217-227.

SMITH, W. L. & GADD, G. M. (2000) Reduction and Precipitation of Chromate by Mixed Culture Sulphate Reducing Bacterial Biofilms. *Journal of Applied Microbiology,* 88, 983-991.

SPARKS, D. L. (1995) *Environmental Soil Chemistry,* Academic Press Inc.

SPEAR, J. R., FIGUEROA, L. A. & HONEYMAN, B. D. (1999) Modeling the Removal of Uranium U(VI) from Aqueous Solutions in the Presence of Sulphate Reducing Bacteria. *Environmental Science and Technology,* 33, 2667-2675.

SPEAR, J. R., FIGUEROA, L. A. & HONEYMAN, B. D. (2000) Modeling Reduction of Uranium U(VI) Under Variable Sulphate Concentrations by Sulphate Reducing Bacteria. *Applied and Environmental Microbiology,* 66, 3711-3721.

TAUXE, L. (2002) *Paleomagnetic Principles and Practice,* Boston, Kluwer Academic Publishers.

THOMAS, R. A. P. & MACASKIE, L. E. (1996) Biodegradation of Tributyl Phosphate by Naturally Occurring Microbial Isolates and Coupling to the Removal of Uranium from Aqueous Solution. *Environmental Science and Technology,* 30, 2371-2375.

ULRICH, G. A., KRUMHOLZ, L. R. & SULFITA, J. M. (1997) A Rapid and Simple Method of Estimating Sulfate REduction Activity and Quantifying Inorganic Sulfides. *Applied and Environmental Microbiology,* 63, 1627-1630.

UTGIKAR, V. P., HARMON, S. M., CHAUDHARY, N., TABAK, H. H., GOVIND, R. & HAINES, J. R. (2002) Inhibition of sulfate-reducing bacteria by metal sulfide formation in bioremediation of acid mine drainage. *Environmental Toxicology,* 17, 40-48.

VALLENTYNE, J. R. (1963) Isolation of Pyrite Spherules from Recent Sediments. *Limnology and Oceanography,* 8, 16-30.

VAN DEUREN, J., LLOYD, T., CHHETRY, S., LIOU, R. & PECK, J. (2002) Remediation Technologies Screening Matrix and Reference Guide. 4th Edition ed.

VAN HULLEBUSCH, E. D., PEERBOLTE, A., ZANDVOORT, M. H. & LENS, P. N. L. (2005) Sorption of Cobalt and Nickel on Anaerobic Granular Sludges: Isotherms and Sequential Extraction. *Chemosphere,* 58, 493-505.

VAN HULLEBUSCH, E. D., ZANDVOORT, M. H. & LENS, P. N. L. (2004) Nickel and Cobalt Sorption on Anaerobic Granular Sludges: Kinetic and Equilibrium Studies. *Journal of Chemical Technology and Biotechnology,* 79, 1219-1227.

VEGLIO, F. & BEOLCHINI, F. (1997) Removal of metals by biosorption: A review. *Hydrometallurgy,* 44, 301-316.

VIEIRA, R. H. S. F. & VOLESKY, B. (2000) Biosorption: a solution to pollution? *International Microbiology,* 3, 17-24.

VIJAYARAGHAVAN, K., JEGAN, J. R., PALANIVELU, K. & VELAN, M. (2004) Copper Removal From Aqueous Solution by Marine Green Alga *Ulva Reticulata. Electronic Journal of Biotechnology (online),* 7.

VIJAYARAGHAVAN, K., JEGAN, J. R., PALANIVELU, K. & VELAN, M. (2005) Nickel Recovery from Aqueous Solution Using Crab Shell Particles. *Adsorption Science & Technology,* 23, 303-311.

VILLAESCUSA, I., FIOL, N., MARTINEZ, M., MIRALLES, N., POCH, J. & SERAROLS, J. (2004) Removal of Copper and Nickel Ions from Aqueous Solutions by Grape Stalks Wastes. *Water Research,* 38, 992-1002.

VOLESKY, B. (2001) Detoxification of Metal Bearing Effluents: Biosorption for the Next Century. *Hydrometallurgy,* 59, 201-216.

VOLESKY, B. (2003) Biosorption Process Simulation Tools. *Hydrometallurgy,* 71, 179-190.

WATSON, J. H. P., CRESSEY, B. A., ROBERTS, A. P., ELLWOOD, D. C., CHARNOCK, J. M. & SOPER, A. K. (2000) Structural and Magnetic Studies on Heavy-Metal-Adsorbing Iron Sulphide Nanoparticles Produced by Sulphate-Reducing Bacteria. *Journal of Magnetism and Magnetic Materials,* 214, 13-30.

WATSON, J. H. P., CROUDACE, I. W., WARWICK, P. E., JAMES, P. A. B., CHARNOCK, J. M. & ELLWOOD, D. C. (2001) Adsorption of Radioactive Metals by Strongly Magnetic Iron Sulfide Nanoparticles Produced by Sulfate-Reducing Bacteria. *Separation Science and Technology,* 36, 2571-2607.

WATSON, J. H. P. & ELLWOOD, D. C. (1994) Biomagnetic Separation and Extraction Process For Heavy Metals From Solution. *Minerals Engineering,* 7, 1017-1028.

WATSON, J. H. P. & ELLWOOD, D. C. (2003) The Removal of the Pertechnetate Ion and Actinides From Radioactive Waste Streams at Hanford, Washington, USA and Sellafield, Cumbria, UK: The Role of Iron-Sulfide-Containing Adsorbent Materials. *Nuclear Engineering and Design,* 226, 375-385.

WATSON, J. H. P., ELLWOOD, D. C., CRESSEY, B. A. & LIDZEY, R. A. (2005) The Adsorption of Heavy Metals by Tochilinite, an Iron Sulfide Material Produced by Chemical Precipitation: Analysis Using a Simple Theory of Chemisorption. *Separation Science and Technology,* 40, 959-990.

WATSON, J. H. P., ELLWOOD, D. C., DENG, Q. X., MIKHALOVSKY, S., HAYTER, C. E. & EVANS, J. (1995) Heavy-Metal Adsorption on Bacterially Produced FeS. *Minerals Engineering,* 8, 1097-1108.

WATSON, J. H. P., ELLWOOD, D. C. & DUGGLEBY, C. J. (1996) A Chemostat with Magnetic Feedback for the Growth of Sulphate Reducing Bacteria and Its Application to the Removal and Recovery of Heavy Metals from Solution. *Minerals Engineering,* 9, 973-983.

WATSON, J. H. P., ELLWOOD, D. C., SOPER, A. K. & CHAROCK, J. M. (1999) Nanosized Strongly Magnetic Bacterially Produced Iron Sulphide Materials. *Journal of Magnetism and Magnetic Materials,* 203, 69-72.

WEST, I. (2003) Geology of Fawley Power Station, Southampton Water. *Geology of the Central South Coast of England.* http://www.soton.ac.uk/~imw/Fawley-Power-Station-geology.htm.

WHARTON, M. J., ATKINS, B., CHAROCK, J. M., LIVENS, F. R., PATTRICK, R. A. D. & COLLISON, D. (2000) An X-ray Absortpion Spectroscopy Study of the Coprecipitation of Tc and Re with Mackinawite (FeS). *Applied Geochemistry,* 15, 347-354.

WHITE, C. & GADD, G. M. (1996) Mixed Sulphate Reducing Bacterial Cultures for Bioprecipitation of Toxic Metals: Factorial and Response-Surface Analysis of the Effects of Dilution Rate, Sulphate and Substrate Concentration. *Microbiology,* 142, 2197-2205.

WHITE, C. & GADD, G. M. (2000) Copper Accumulation by Sulphate Reducing Bacterial Biofilms. *FEMS Microbiology Letters,* 183, 313-318.

WHITE, C., WILKINSON, S. C. & GADD, G. M. (1995) The Role of Microorganisms in Biosorption of Toxic Metals and Radionuclides. *International Biodeterioration and Biodegradation*, 17-40.

WIDDEL, F. (1988) Microbiology and Ecology of Sulfate- and Sulfur-Reducing Bacteria. IN ZEHNDER, A. J. B. (Ed.) *Biology of Anaerobic Microorganisms.* New York, John Wiley and Sons.

WILKIN, R. T. & BARNES, H. L. (1996) Pyrite Formation by Reactions of Iron Monosulfides with Dissolved Inorganic and Organic Sulfur Species. *Geochimica Et Cosmochimica Acta,* 60, 4167-4179.

WOLTHERS, M., VAN DER GAAST, S. J. & RICKARD, D. (2003) The Structure of Disordered Mackinawite. *American Mineralogist,* 88, 2007-2015.

YANG, C. H. (1998) Statistical Mechanical Study on the Freundlich Isotherm Equation. *Journal of Colloid and Interface Science,* 208, 379-387.

YOON, W. E. & ROSSON, R. A. (1990) Improved Method of Enumeration of Attached Bacteria of Study of Fluctuation in the Abundance and Free-Living Bacteria in Response to Diel Variation in Seawater Turbidity. *Applied and Environmental Microbiology,* 56, 595-600.